



National Library  
of Canada

Bibliothèque nationale  
du Canada

Canadian Theses Service

Services des thèses canadiennes

Ottawa, Canada  
K1A 0N4

## CANADIAN THESES

## THÈSES CANADIENNES

### NOTICE

The quality of this microfiche is heavily dependent upon the quality of the original thesis submitted for microfilming. Every effort has been made to ensure the highest quality of reproduction possible.

If pages are missing, contact the university which granted the degree.

Some pages may have indistinct print especially if the original pages were typed with a poor typewriter ribbon or if the university sent us an inferior photocopy.

Previously copyrighted materials (journal articles, published tests, etc.) are not filmed.

Reproduction in full or in part of this film is governed by the Canadian Copyright Act, R.S.C. 1970, c. C-30. Please read the authorization forms which accompany this thesis.

**THIS DISSERTATION  
HAS BEEN MICROFILMED  
EXACTLY AS RECEIVED**

### AVIS

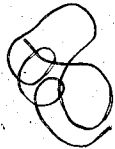
La qualité de cette microfiche dépend grandement de la qualité de la thèse soumise au microfilmage. Nous avons tout fait pour assurer une qualité supérieure de reproduction.

S'il manque des pages, veuillez communiquer avec l'université qui a conféré le grade.

La qualité d'impression de certaines pages peut laisser à désirer, surtout si les pages originales ont été dactylographiées à l'aide d'un ruban usé ou si l'université nous a fait parvenir une photocopie de qualité inférieure.

Les documents qui font déjà l'objet d'un droit d'auteur (articles de revue, examens publiés, etc.) ne sont pas microfilmés.

La reproduction, même partielle, de ce microfilm est soumise à la Loi canadienne sur le droit d'auteur, SRC 1970, c. C-30. Veuillez prendre connaissance des formules d'autorisation qui accompagnent cette thèse.

  
**LA THÈSE A ÉTÉ  
MICROFILMÉE TELLE QUE  
NOUS L'AVONS REÇUE**

THE UNIVERSITY OF ALBERTA

FINITE ELEMENT MODELLING OF BURIED STRUCTURES

by

C

DAVID KENNETH PLAYDON

A THESIS

SUBMITTED TO THE FACULTY OF GRADUATE STUDIES AND RESEARCH  
IN PARTIAL FULFILMENT OF THE REQUIREMENTS FOR THE DEGREE  
OF MASTER OF SCIENCE

DEPARTMENT OF CIVIL ENGINEERING

EDMONTON, ALBERTA

FALL 1985

## ABSTRACT

The primary objective of this thesis is to evaluate the finite element program ADINA of use in analyzing soil-structure interaction problems. This evaluation consists of three stages:

1) an overview of the element types, material models, formulations and other features in ADINA that are useful when analysing soil-structure interaction problems.

2) a disucssion of the application of ADINA and general modelling considerations to soil-structure problems. Methods for modelling various stages of construction were also developed.

3) the application of the modelling methods and and other considerations to the arch-beam culvert structure. This structure involves a combination of three materials: soil, steel and concrete. In addition the soil cover and the structure's stiffness were varied. The predicted responce of this structure was compared to field test data.

The material models and modelling techniques used in the analyses are evaluated and changes in the test and design procedures for arch beam culverts are suggested.

## ACKNOWLEDGEMENTS

The author is thankful to Dr. S. H. Simmonds for suggesting the topic of this thesis, for providing the financial funding required and his continued emotional support.

The co-operation of Alberta Transportation and the Alberta Research Council and their making available the test results from the Blairmore Creek Culvert is sincerely appreciated.

The finite element analysis was conducted using the University of Alberta's Amdahl 5860 mainframe with funding provided by the Department of Civil Engineering.

Dr. A. E. Elwi provided valuable comments and advice on the direction of the analyses. The advice and time spent are both appreciated.

The author also wishes to thank both Dr. A. E. Elwi and Dr. D. R. Budney for accepting to serve on the oral examination committee.

## Table of Contents

Chapter		Page
1.	INTRODUCTION .....	1
1.1	Soil-Structure Interaction .....	1
1.2	Object and Scope .....	4
2.	ADINA .....	6
2.1	General Description .....	6
2.1.1	A Finite Element Program for Automatic Dynamic Incremental Nonlinear Analysis .....	6
2.1.2	Ancillary Programs .....	7
2.2	ADINA Features .....	8
2.2.1	Element Types .....	8
2.2.2	Formulations .....	11
2.2.3	Material Models .....	11
2.2.4	Other Capabilities .....	29
2.2.4.1	Element Birth and Death Options .....	29
2.2.4.2	Restart Option .....	31
2.2.4.3	Substructuring .....	31
2.2.4.4	Dynamic Analysis .....	32
3.	FINITE ELEMENT MODELLING OF BURIED STRUCTURES .....	33
3.1	General Comments .....	33
3.2	General Procedure .....	33
3.3	Modelling of Construction .....	34
3.3.1	Excavation .....	34
3.3.2	Modelling of Soil Compaction .....	35
3.4	Mesh Development Considerations .....	41
3.4.1	Boundary Conditions .....	41
3.4.2	Mesh Progression .....	42

3.4.3	Compatibility .....	43
3.4.4	Aspect Ratio's and Order of Integration ..	46
3.4.5	Methods of Formulation .....	49
3.5	Summary .....	56
4.	ARCH-BEAM CULVERTS .....	57
4.1	General Description .....	57
4.1.1	Description of an Arch-Beam Culvert .....	57
4.1.2	Other Culvert Modifications .....	60
4.2	Preliminary Design Considerations .....	62
4.2.1	Corrugated Steel Culvert Design Considerations .....	62
4.2.2	Arch-Beam Culvert Design Considerations ..	64
4.3	Prototype Geometry .....	68
4.4	Construction of Prototype .....	68
4.5	Instrumentation .....	73
4.6	Testing Program .....	74
4.7	Summary .....	76
5.	MODELLING OF ARCH-BEAM CULVERTS .....	78
5.1	Definition of Problem .....	78
5.2	Structure Nomenclature .....	79
5.3	Developement of the Mesh .....	82
5.4	Determination of Material Parameters .....	86
5.5	The Triaxial Concrete Cracking Model .....	92
5.6	Method of Analysis .....	93
5.6.1	Modelling of Construction .....	93
5.7	Live Loadings .....	101
5.8	Results of Analysis Using ADINA .....	103
5.8.1	Elastic Analysis .....	103

5.8.2	Nonlinear Analysis .....	104
5.8.3	Nonlinear Analysis with Elastic Soil ....	121
5.8.4	Reduced Soil Cover .....	126
5.8.5	Summary of Analyses .....	130
5.9	Effect of not Modelling Construction .....	131
5.10	Comparision of Analysis and Test Results .....	132
6.	CONCLUSIONS, AND RECOMMENDATIONS .....	134
6.1	Conclusions .....	134
6.1.1	Evaluation of ADINA .....	134
6.1.2	Recommendations for Arch-beam Culverts ..	136
6.2	Recommendations for Ancillary Programs .....	137
	BIBLIOGRAPHY .....	139
	APPENDIX A .....	146
	APPENDIX B .....	149
	APPENDIX C .....	151
	APPENDIX D .....	155

## List of Figures

Figure		Page
1.1	A Typical Arch-Beam Culvert in Use .....	3
2.1	Collapsed Rectagular Element .....	10
2.2	Axes of Orthotropy .....	14
2.3	Input to Curve Description Model .....	15
2.4	Isotropic and Kinematic Strain Hardening .....	19
2.5	Drucker Prager Yield Surface .....	21
2.6	Stress-Strain Behaviour with Cap Hardening .....	23
2.7	Uniaxial Compression Stress-Strain Curve .....	26
2.8	Triaxial Failure Surface as Input to ADINA .....	27
3.1	Preload Method Test Structure .....	37
3.2	Zones of Yielding when No Preload was Used .....	39
3.3	The Three Preload Variations .....	40
3.4	Examples of Discontinuity Between Elements .....	44
3.5	High Shear Caused by the Order of the Shape Function .....	47
3.6	Advantage of using Reduced Integration .....	48
3.7	Disadvantage of using Reduced Integration .....	50
3.8	A Clamped Continuous Plate .....	51
3.9	Behaviour of a Continuous Plate (detail) .....	53
3.10	Behaviour of a Continuous Plate .....	54
4.1	Cutaway View of a Circular Arch-Beam Culvert .....	58
4.2	Blairmore Creek Arch-Beam Culvert .....	59
4.3	Compaction Beside the Prototype Arch-Beam Culvert .....	59
4.4	Soil Steel Culvert Modifications .....	61



Figure	Page
4.5 Wellington County Culvert .....	63
4.6 Compression Ring Culvert Design .....	65
4.7 Simplified Design Procedure .....	67
4.8 Prototype Arch-Beam Culvert Geometry .....	69
4.9 Corrugated Culvert Profile .....	70
4.10 Cross-section Through the Composite Culvert .....	70
4.11 Construction Sequence of Prototype .....	71
4.12 Construction Sequence continued .....	72
4.13 Longitudinal Cross-section .....	75
5.1 Composite Cross-sections used in the Analyses .....	80
5.2 The Geometry used for Analyses .....	81
5.3 A Typical Finite Element Mesh .....	83
5.4 Discontinuities in the Finite Element Mesh .....	85
5.5 Grain Size Distribution for Backfill Material .....	88
5.6 Drucker Prager Yield Surface for Concrete .....	91
5.7 Mesh Progression During Construction .....	95
5.8 Description of the Time Steps used in Modelling .....	96
5.9 Distribution of Lateral Preload Pressure .....	98
5.10 Preload used to Place Concrete .....	99
5.11 Vertical Deflection of Steel Culvert During Construction .....	105
5.12 Axial Forces and Bending Moments in the Steel Culvert (470D - 1250D) .....	107
5.13 Bending Moment Diagram for Mesh (470D - 1250D) .....	110

Figure	Page
5.14 Axial Force Diagram for Mesh (470D - 1250D) .....	111
5.15 Bending Moment Diagram for Mesh (270D - 1250D) .....	112
5.16 Axial Force Diagram for Mesh (270D - 1250D) .....	113
5.17 Distribution of Vertical Stresses on the Concrete Structure (470D - 1250D) .....	115
5.18 Simplified Design Under Dead Load (470 - 1250) .....	117
5.19 Simplified Design Under Live Load (470 - 1250) .....	118
5.20 Progression of Yielding in the Soil (470D - 1250D) .....	120
5.21 Axial Force Diagram for Mesh (270T - 1250E) .....	123
5.22 Bending Moment Diagram for Mesh (270T - 1250E) .....	124
5.23 Deflection of Soil at the Culvert Crown .....	125
5.24 Axial Force Diagram for Mesh (270T - 450E) .....	127
5.25 Bending Moment Diagram for Mesh (270T - 450E) .....	128
5.26 Internal Concrete Deflections .....	129

## List of Symbols

$a, b, c$	Principal axes of Orthotropy. (Orthotropic linear elastic model)
$A_t$	Truss element area.
$C$	Radial compressive force per millimeter in a corrugated steel culvert.
$d_s$	Soil cover at the crown of an arch-beam culvert.
$D$	Total volumetric strain rate. (Drucker Prager model)
$e_c$	Uniaxial strain corresponding to the maximum compressive stress for concrete. (Triaxial Concrete Cracking model)
$e_u$	Ultimate uniaxial strain of concrete. (Triaxial Concrete Cracking model)
$e_v$	Volumetric strain.
$e_v^p$	Plastic volumetric strain.
$E$	Young's modulus.
$\bar{E}_o$	Initial tangent Young's modulus of concrete. (Triaxial Concrete Cracking model)
$f'_c$	Specified compressive strength of concrete, MPa.
$f_r$	Modulus of rupture of concrete, MPa.
$G_{LD}$	Shear modulus while loading. (Curve Description model)
$h_i$	Element interpolation function for node $i$ .
$I$	Moment of inertia.
$I_1$	First invariant of stress.
$o_{I_1}$	Initial position of hardening cap. (Drucker Prager model)

$K_{LD}$	Bulk modulus while loading. (Curve Description model)
$K_o$	Coefficient of earth pressure at rest.
$K_{UN}$	Bulk modulus while unloading. (Curve Description model)
$P_L$	Magnitude of the applied live load.
$r, s, t$	Local coordinate system for an element.
$s_{ij}$	Deviator stress.
$W$	Maximum volumetric strain. (Drucker Prager model)
$x, y, z$	Global coordinate system of the finite element mesh.
$z_i$	Z-coordinate of node number $i$ .
$\alpha$	One third the slope of the Drucker Prager yield surface in the $\bar{\sigma}, \sigma_m$ stress space. (Drucker Prager model)
$\beta$	Angle of orientation for axes of orthotropy. (Orthotropic linear elastic model) <sup>a</sup>
$\Delta$	Relative deflection of the crown and support slab for an arch-beam culvert.
$\gamma_s$	Density of soil.
$K$	$\bar{\sigma}$ axis intercept of the Drucker Prager yield surface in the $\bar{\sigma}, \sigma_m$ stress space. (Drucker Prager model)
$\nu$	Poisson's ratio.
$\sigma_c$	Maximum uniaxial stress for concrete. (Triaxial Concrete Cracking model)
$\sigma_u$	Ultimate uniaxial stress for concrete. (Triaxial Concrete Cracking model)
$\sigma_{ij}$	Stress-component on plane $i$ in the $j$ direction.
$\sigma_m$	Mean of the principal stresses.

$\sigma_{p1}, \sigma_{p2}, \sigma_{p3}$

Principal stresses.

$\sigma_y$

Uniaxial yield stress.

$\bar{\sigma}$

Square-root of the second invariant of stress deviation.

$\phi$

Internal angle of friction.

$\phi_r$

Curvature.

$\phi_y$

Curvature at the time of first yielding.

## 1. INTRODUCTION

### 1.1 Soil-Structure Interaction

Soil-structure interaction problems can be considered to include any structure that is either resting on or in soil; however in this study this term is restricted to include only those structures whose strength and stiffness are dependent upon interaction with the soil. These problems are not in the direct realm of responsibility of either the geotechnical or structural engineer and therefore are some of the least understood and most ignored problems. Modelling of the nonlinear behaviour of the soil is, in most cases, essential to understanding the true interaction between the structure and the soil on which it is dependent. Therefore, in any problem where soil is involved, a linear analysis is of questionable value because the engineer must depend upon the plasticity of the soil to have a practical design.

Soil-structure interaction problems are frequently highly indeterminate and construction dependent and therefore, difficult to analyze. The soil is usually considered to be a two- or three-dimensional solid with defined or assumed boundary conditions. In the past, many empirical methods have been developed to analyze the interaction between soil and certain types of structures. These methods are limited in their application and rarely represent the true behaviour of the structure. The finite element method is able to analyze structures that are both

nonlinear and indeterminate. Therefore, it is ideally suited to the solution of these problems.

In recent years, with an increase in the computing capability available and a large reduction in cost, it has become more common to use a nonlinear finite element program to analyze soil structure interaction problems. ADINA, one such finite element program, is described in Chapter 2. Although ADINA is a general purpose, nonlinear finite element program, it was written primarily for structurally oriented problems. Research was undertaken at the University of Alberta to investigate the possible use of ADINA to solve soil-structure interaction problems and construction dependent problems in general. ADINA has a number of features that can be used to model soil-structure interaction problems. These features include a variety of linear and nonlinear material models, formulations and element types. The procedures and techniques presented in Chapters 3 and 5 were developed for use in the modelling of soil-structure problems where the construction process affects the final stresses or where the stresses during construction are of interest.

It was decided that an actual application would be useful in understanding the problems that can be encountered in modelling a soil-structure interaction. The application chosen was the arch-beam culvert, an example of which is shown in Figure 1.1. A particular arch-beam culvert structure as constructed by Alberta Transportation at

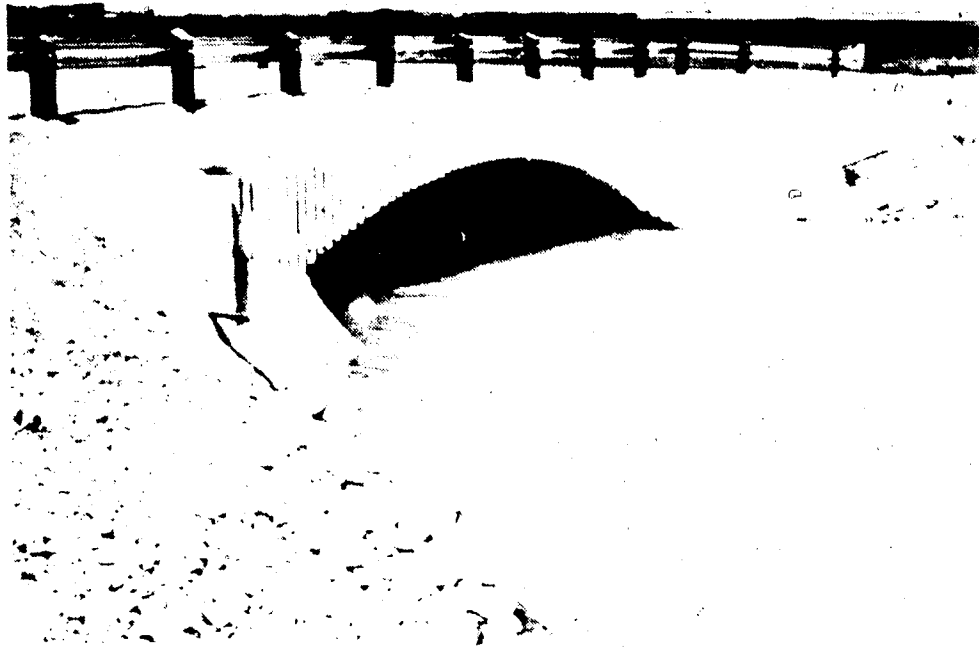


Figure 1.1 A Typical Arch-Beam Culvert in Use



Blairmore, Alberta was modelled in detail. An advantage of considering this structure was that it was instrumented by the Alberta Research Council. Measurements of strains and displacements were taken both during construction and during two subsequent static load tests. This allowed the analysis to be compared to the actual test results. This comparison, given in Chapter 5, brought to light a number of modelling considerations that would have been overlooked if an arbitrary structure had been chosen. A description of design and construction considerations for large span culverts and arch-beam culverts is given in Chapter 4.

## 1.2 Object and Scope

The primary objective of the research was to gain familiarity with ADINA and to evaluate its application to soil-structure interaction problems. To achieve this goal a series of analyses were done to evaluate ADINA's ability to model a structure's nonlinear response and its ability to model the interaction between a structure and the surrounding soil.

A secondary objective was to evaluate the structural response of the arch-beam culvert. This included its response during construction and under a static live load. This required the evaluation of the structural adequacy of the prototype culvert and an evaluation of the possible failure modes. From this evaluation it should be possible to determine the aspects of the design that could prove to be

critical. It also illustrated the aspects of the structure which required special attention during the analysis. ▶

The scope of the analysis was greatly influenced by the results of the preliminary analyses. The analysis was limited to a two-dimensional plane strain model using only those features that were already included in ADINA. A preliminary nonlinear elastic analysis was followed by a material nonlinear analysis. The material nonlinear analysis included a partial parametric study of the example structure. The parameters considered include the soil cover and the thickness of the concrete section, and method of construction.

## 2. ADINA

### 2.1 General Description

#### 2.1.1 A Finite Element Program for Automatic Dynamic Incremental Nonlinear Analysis

ADINA is a computer program for the static and dynamic displacement and stress analysis of solids, structures and fluid-structure systems. It is capable of solving many structural engineering problems including those that involve nonlinearities due to large displacements and strains and/or nonlinear material properties. ADINA has a large variety of element types and material models to choose from. These can be combined to provide more realistic models.

This program was developed at the Acoustics and Vibration Laboratory in the Mechanical Engineering Department of the Massachusetts Institute of Technology under the direction of K. J. Bathe. It is presently controlled by ADINA Engineering Inc. and is in a constant state of development. At the University of Alberta two versions of ADINA have been used, the first being ADINA78, which does not include all of the features of the present version ADINA81. ADINA81 includes features such as new material models, element types, and information on convergence for each solution step. It is also able to be used with the version of ADINA-PLOT, a post-processing program, available at the University of Alberta. At this

time ADINA84 is in its final stages of development, but is not yet available at the University of Alberta. Therefore all references to ADINA, except where explicitly stated to the contrary, are to ADINA81.

### 2.1.2 Ancillary Programs

There are three ancillary programs available from ADINA Engineering Inc.. These programs are described briefly below and their complete abstracts are included in Appendix A.

ADINA-PLOT is a post-processing program for ADINA. It can be used to produce plots and list results directly from the ADINA porthole file using a command language. It was used to produce the finite element mesh plots; however, because of problems with the program installation it was not used to produce the other plots or the tables of results. This program is expensive to use because of the large amounts of data that must be stored on magnetic tape and in temporary files.

ADINA-IN, a pre-processor, uses a command language to generate a finite element mesh and the complete ADINA input file. It also includes plotting and listing facilities to check the ADINA model. It is not available at the University of Alberta at this time; however with the complex geometry involved in the example problem described in Chapters 4 and 5, ADINA-IN would have been a great asset. It required one or two weeks to manually produce and correctly enter a new mesh for the example problem.

ADINAT, "A Finite Element Program for Automatic Dynamic Incremental Nonlinear Analysis of Temperatures" is a self-contained finite element program, which is available for use at the University of Alberta. It can be used on its own to solve steady-state and transient temperature and field problems, or with ADINA to analyze structures that include temperature dependent materials.

## 2.2 ADINA Features

### 2.2.1 Element Types

The finite element program ADINA includes a large variety of element types. These element types include a truss element, two- and three-dimensional isoparametric solid elements, a two-node beam element, an isoparametric beam element, plate/shell element and an isoparametric thin shell element. All of these element types can be combined into a single analysis. This simplifies the creation of a mesh that models the problem realistically. These element types can be used in conjunction with a series of linear and nonlinear material models. A complete list of material models that may be used with each type of element is presented in Appendix B.

Four element types were considered for use in the two-dimensional example analysis. The truss element is a one-dimensional member that has three translational degrees-of-freedom at each node and can only transmit axial

force. The element can have two to four nodes and is mapped isoparametrically in three dimensions.

The two-dimensional solid elements may have between four and eight nodes and each node has two translational degrees-of-freedom. The element is mapped isoparametrically onto the structure. The two-dimensional solid element can be formulated as either a plane-strain or a plane-stress element. The nodes of plane-strain elements must lie within the  $y-z$  plane while the nodes of plane-stress elements may lie in any arbitrary plane. A triangular element can be formed by collapsing the side with local node numbers one, four and eight, as shown in Figure 2.1.

The Two-Node Beam element has three translational and three rotational degrees-of-freedom at each node and can transmit axial forces, shear forces and moments. The element is a straight beam with an arbitrary orientation in three dimensions. The orientation of the beams local  $r, s, t$  coordinate system is defined using an auxiliary node in the local  $r, s$  plane. The element has two cross-sections that can be used in conjunction with a nonlinear material model, a rectangular section and a pipe section.

The Isoparametric Beam element, like the Two-Node Beam element, has three translational and three rotational degrees-of-freedom at each node. The element can have between two and four nodes and is mapped isoparametrically into three dimensions but all of the nodes used to define the beam and its orientation must lie on a single plane.

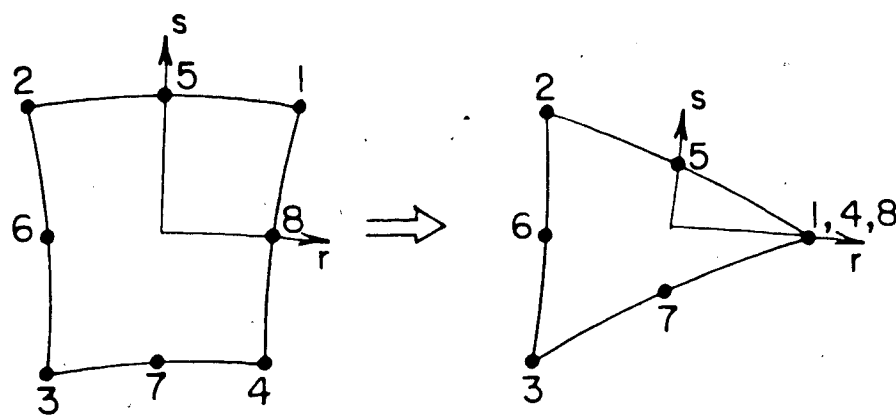
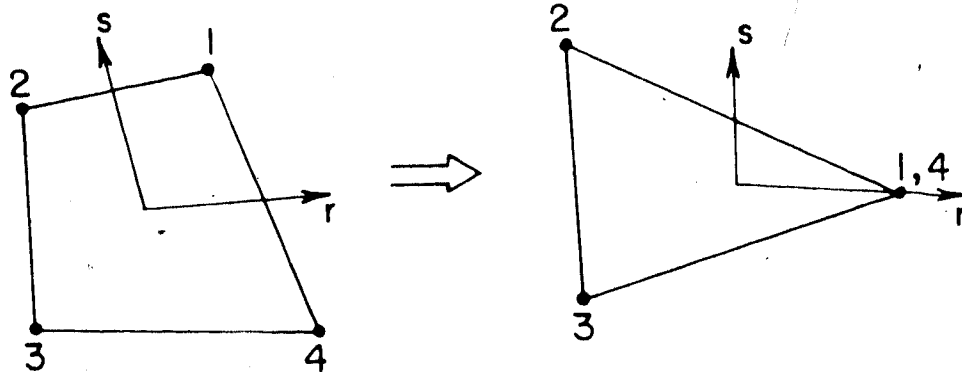


Figure 2.1 Collapsed Rectangular Element

### 2.2.2 Formulations

ADINA offers four different analysis formulations. The first is the linear elastic analysis which does not allow for any type of nonlinear behaviour and is limited to linear material types. The second type of analysis is the materially nonlinear only analysis. In this type of analysis only the nonlinearities of the material stress-strain description are considered. The last two formulations are the Total Lagrangian and the Updated Lagrangian which include the nonlinear behaviour due to large displacements as well as the nonlinear material stress-strain description. With the Updated Lagrangian formulation the effects of large strains are included by updating the mesh at the end of each time step.

### 2.2.3 Material Models

A number of material models are available in ADINA but only those which are considered most useful in soil-structure interaction problems are reviewed. Sources containing a development of the model and constitutive relationships are referenced.

The first two material models considered for use with the truss elements are the Linear Elastic model and the Nonlinear Elastic model [3,8]. The Linear Elastic model requires a single material parameter, Young's modulus, to define its behaviour. The Nonlinear Elastic model is identical in concept to the Linear Elastic model except that



it uses a nonlinear stress-strain relationship that is described by a piece-wise linear curve. These models, being elastic models, follow the same stress-strain curve during unloading and loading.

The Elastic-Plastic material model is defined by means of an initial Young's modulus, which is used up to the specified uniaxial yield stress, and a strain hardening modulus [3]. With this model either isotropic or kinematic strain hardening can be modelled. With isotropic strain hardening the yield stress after strain hardening is increased equally in tension and compression. Kinematic strain hardening causes the stress difference, between yielding in tension and compression, to be constant at twice the initial yield stress. All three of these models, used with the Updated Lagrangian formulation, can accommodate large displacements but only strains less than two per cent.

The material models considered for use with the two-dimensional element type are much more varied than those considered for the truss element. This is because three different materials, steel, concrete and soil, were to be modelled. In this chapter only their input parameters and general behaviour will be discussed. Their application to these materials is presented in Chapter 3.

The first two material models are the Isotropic and Orthotropic Linear Elastic models. The material parameters for these models are constant Young's moduli and Poisson's ratios. The Isotropic model has a single Young's modulus and

Poisson's ratio and the Orthotropic model has three principal Young's moduli and their corresponding Poisson's ratios. With the Orthotropic model one axis of orthotropy must lie perpendicular to the plane of the element. The other two axes are defined on an element by element basis, as shown in Figure 2.2.

The curve description model is a nonlinear model with no explicit yield surface [3]. The nonlinear behaviour is defined by the input of a piece-wise instantaneous bulk and shear moduli curves. The instantaneous bulk modulus curve is input both for loading and unloading, as shown in Figure 2.3. From the ratio of the loading and unloading bulk moduli curves and the shear modulus curve an unloading shear modulus curve is calculated. The determination of whether the material is being loaded or unloaded is based totally on the change in volumetric strain.

This model also allows either a tension cut-off or a tension failure to be included in the analysis. With the tension cut-off option, when a tension plane forms, the stresses across the plane are not released but the normal and shear stiffnesses are reduced by user supplied factors. With the tension failure option, the tension stress across the tension plane is released but the shear stress on the tension plane is not released unless the shear stiffness reduction factor is less than 0.001, the normal stiffness is reduced to zero and the shear stiffness is reduced by the shear stiffness reduction factor. With both the tension

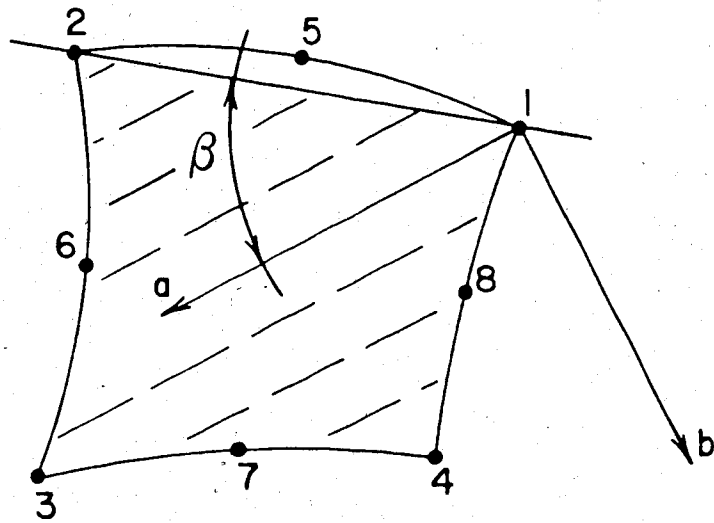


Figure 2.2 Axes of Orthotropy

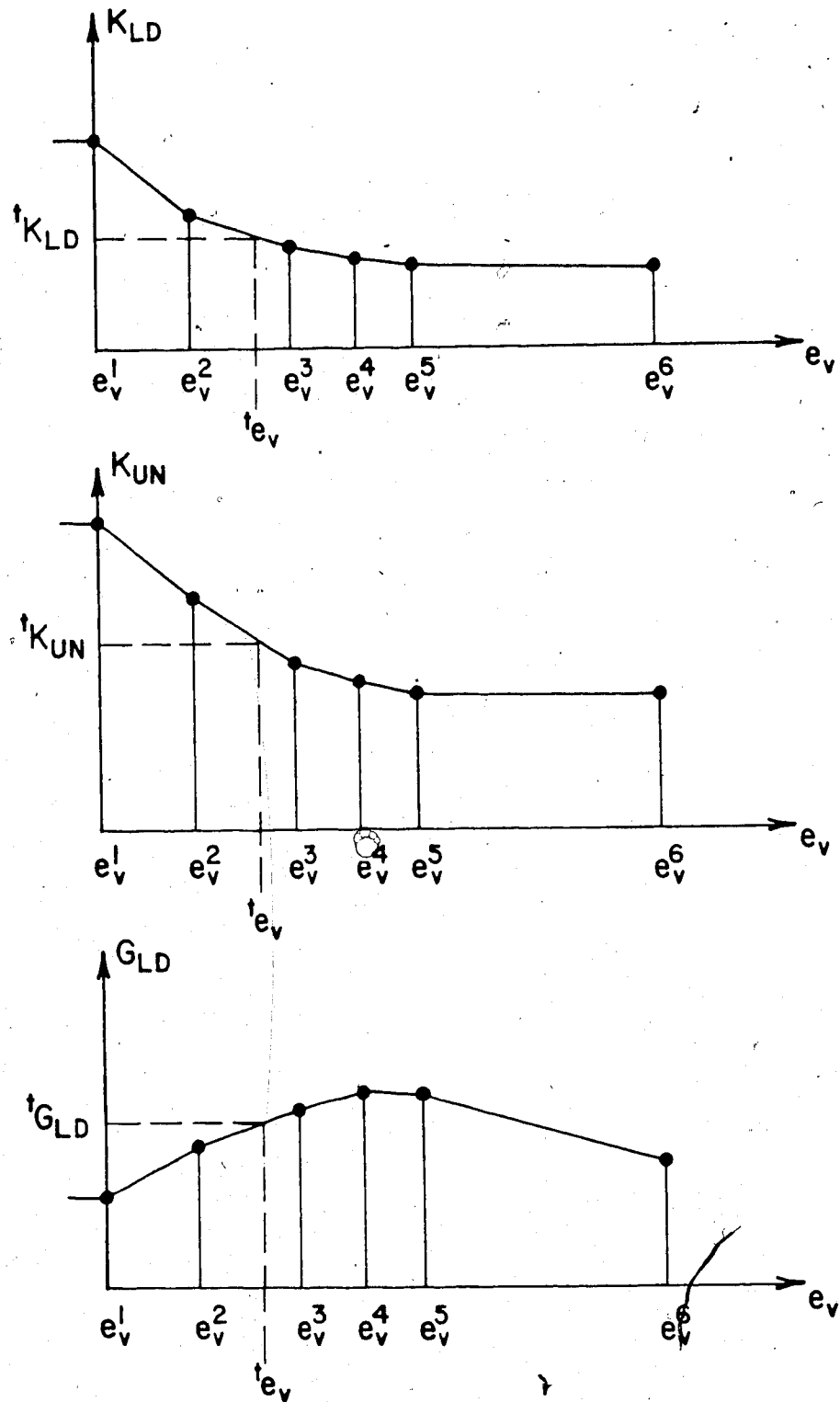


Figure 2.3 Input to Curve Description Model

failure and tension cut-off options, a tension plane once it has been defined, can become inactive upon unloading and then become active again on reloading. However, once a tension plane has been defined it can only have the same orientation or one perpendicular to it.

A tension failure or tension cut-off occurs when the principal stress exceeds the in-situ gravity pressure. With the curve description model the surface of the soil must have a z-coordinate of 0.0 because of the method used to calculate the gravity pressure. This causes problems when performing an analysis in which the soil surface changes either because of excavation or backfilling. The in-situ gravity pressure  $p$ , is determined by assuming that there is a hydrostatic pressure distribution within the material. The gravity pressure is calculated by the following formula.

$$p = \sum_{i=1}^N h_i p_i \quad (2.1)$$

In the formula  $h_i$  is the element interpolation function, and  $N$  is the total number of nodes belonging to the element. The value of  $p_i$  is calculated using the formula  $p_i = \gamma_s z_i$  where  $z_i$  is the z-coordinate of node  $i$  and  $\gamma_s$  is the material density. The stresses calculated in the analysis do not include the gravity in-situ stress unless a mass proportional loading is applied separately. Therefore, if

the Curve Description model is being considered, the coordinated system for the mesh must take into account the method used to calculate the gravity pressure.

This allows the formulation of the soil stiffness while removing the need to model the true in-situ stresses in the soil. A method that can be used, is to model the soil with a mass proportional loading with the true material density and the density in the curve description model set to zero. This would have the effect of setting the allowable tension stress in the soil to zero and the stresses in the soil would be the stress due to gravity and the other loads.

The Elastic-plastic, von Mises yield criterion is one of the most commonly implemented material models in nonlinear finite element programs; however the implementation of this criterion in ADINA has a number of features not normally available. This model can take two forms, the bilinear elastic-plastic and the multi-linear elastic-plastic [3,8,10]. The bilinear elastic-plastic model uses an initial Young's modulus in the elastic region and a strain hardening modulus thereafter. The cylindrical yield surface is defined by the input of the uniaxial yield stress and the resulting yield function is of the form shown in equation 2.2.

$$t_F = \frac{1}{2} t_{s_{ij}} t_{s_{ij}} - t_k \quad (2.2)$$

where

$$t_{s_{ij}} = t_{\sigma_{ij}} - \frac{t_{\sigma_{mm}}}{3}$$

$$t_k = \frac{1}{3} t_{\sigma_y}^2$$

The multi-linear elastic-plastic model also uses an initial Young's modulus and Poisson's ratio in the elastic region but in the inelastic region the behaviour is defined by up to seven points on the uniaxial stress-strain curve. For both the bilinear and multi-linear models, either isotropic or kinematic strain hardening can be assumed. The differences between these two types of strain hardening is shown in Figure 2.4. These two models, with either type of strain hardening, can be used in material nonlinear only analysis or with the Total Lagrangian formulation in a small strain, large displacement analysis. However, only isotropic strain hardening can be used when the Updated Lagrangian formulation is used.

The Drucker-Prager yield model, as implemented in ADINA, assumes elastic perfectly plastic behaviour in the material and can include cap hardening in compression and a stress cut-off in tension [10]. The Drucker Prager yield criterion uses a linear-conical yield surface as shown in

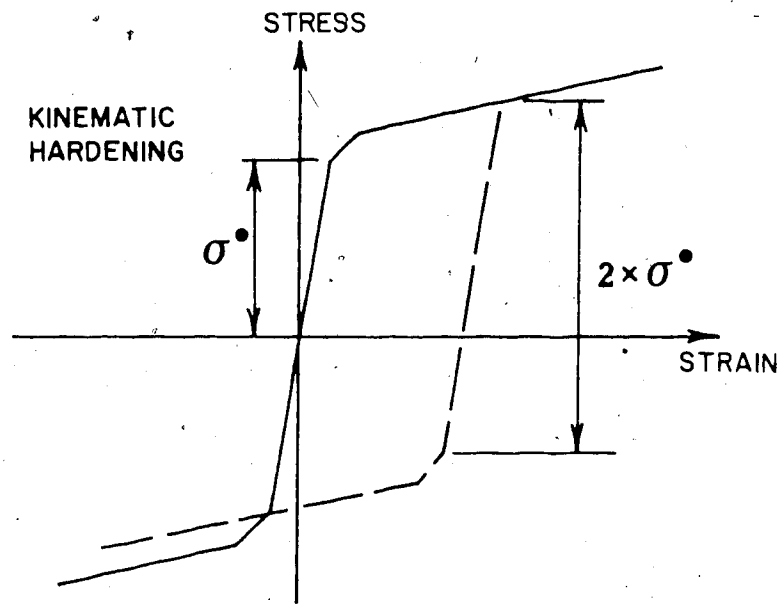
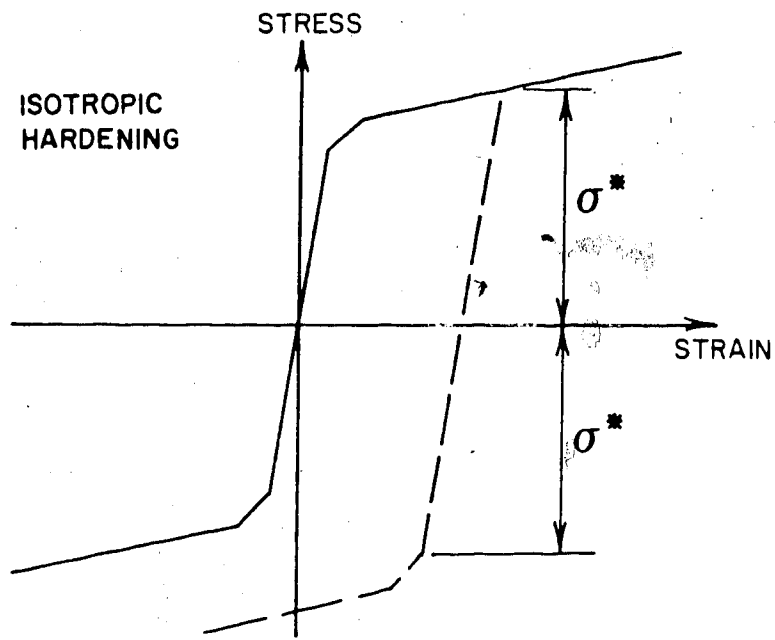


Figure 2.4 Isotropic and Kinematic Strain Hardening



Figure 2.5 and the yield function has the following form.

$$t_F = 3\alpha t_{\sigma_m} + t_{\sigma} - K \quad (2.3)$$

The values of  $\alpha$  and  $K$  are material parameters and can be determined experimentally in a triaxial compression test. The following formulæ are used to calculate  $\alpha$  and  $K$ , where  $\theta$  is the internal angle of friction and  $c$  is the cohesion.

$$\alpha = \frac{2 \sin \theta}{(3 - \sin \theta) \sqrt{3}} \quad (2.4)$$

$$K = \frac{6c \cos \theta}{(3 - \sin \theta) \sqrt{3}} \quad (2.5)$$

The material is linear elastic until it encounters the yield surface, the hardening cap or the tension cut-off. The elastic behaviour is defined by an initial Young's modulus and Poisson's ratio. The cap hardening behaviour is governed by the following formula.

$$t_{I_1}^a = \frac{-1}{D} \ln \left[ 1 - \frac{t_{e^p}}{W} \right] + {}^o I_1^a \quad (2.6)$$

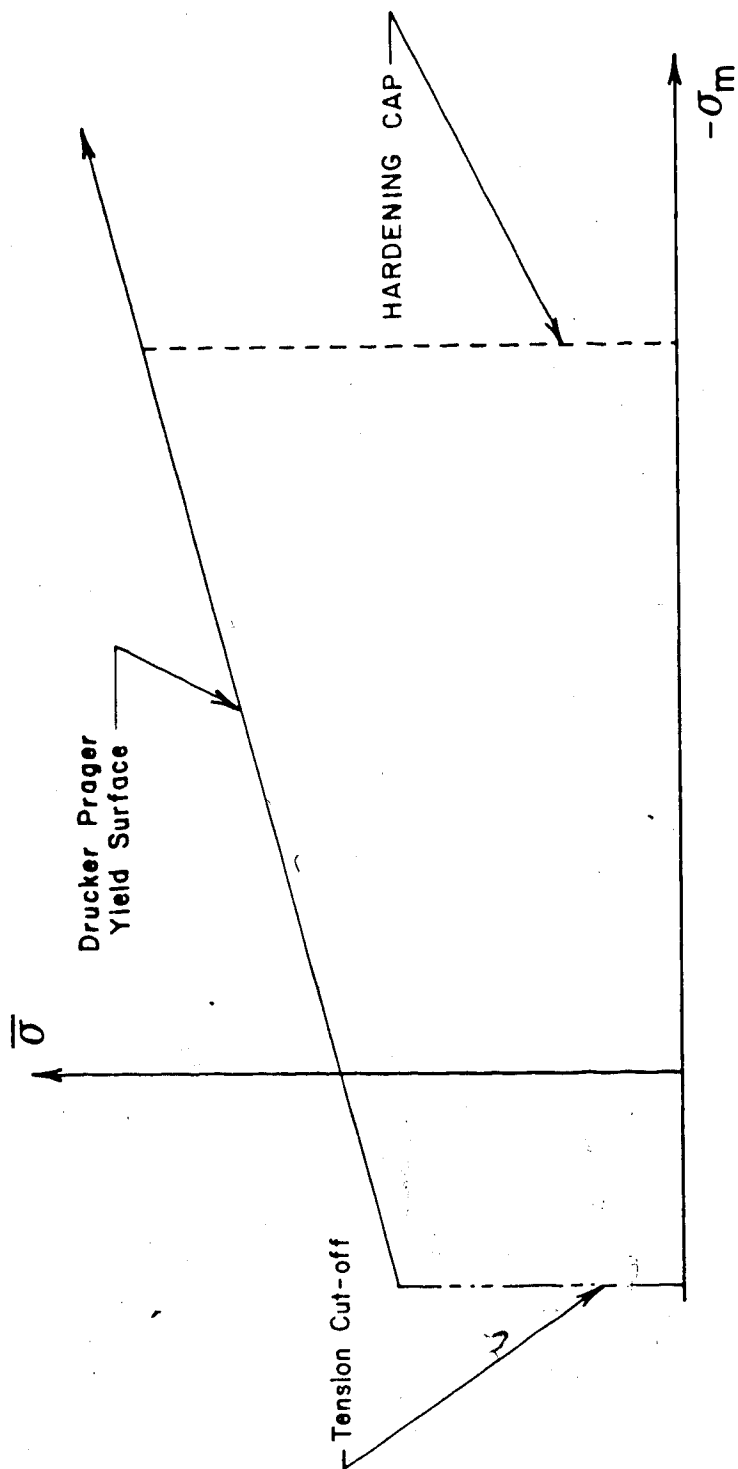


Figure 2.5 Drucker Prager Yield Surface

Where  $t_{I_1}^a$  is the current cap position,  ${}^oI_1^a$  is the initial cap position and  $t_{e_v}^p$  is the current volumetric plastic strain. The values of D and W are cap hardening parameters, D is the total volumetric plastic strain rate and W is the maximum plastic volumetric strain. The linear cap hardening surface in ADINA is defined by the following formula.

$$t_{F_c} = -t_{I_1} + t_{I_1}^a \quad (2.7)$$

The cap hardening surface changes the stress-strain behaviour of the material by reducing the effective Young's modulus and Poisson's ratio when the stress state is on the cap hardening surface. The effective Young's modulus approaches the values input as the total volumetric plastic strain approach the maximum plastic volumetric strain, W. The effective Poisson's ratio, in the usual application of this model, is negative over a large portion of the model's range. When the material is unloading, the values of Young's modulus and Poisson's ratio are those input (Figure 2.6).

The tension cut-off in the Drucker Prager model is not as sophisticated as in the Curve Description model or the Triaxial Concrete model. The tension cut-off occurs when a principal stress exceeds the input tensile strength of the material. All of the principal stresses at the point where the tension cut-off occurs, are reduced to one-third of

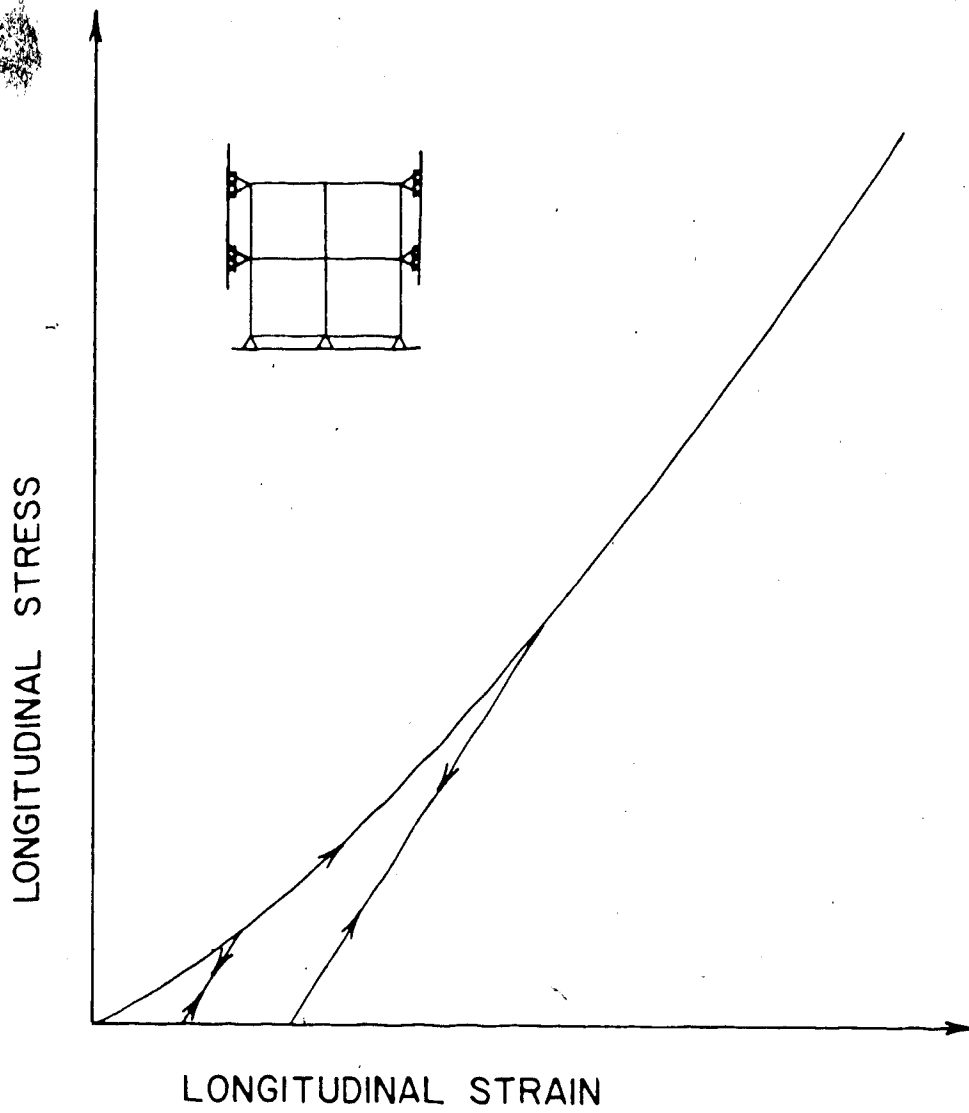


Figure 2.6 Stress-Strain Behaviour with Cap Hardening

the tensile strength. This reduction in stress leads to instability when a large area fails in tension. This is because the stiffness in all directions is reduced and not just the stiffness across the tension plane.

The Concrete Cracking model is a very complex model specifically developed to model concrete [3,9]. The input to define the uniaxial compression stress-strain curve, shown in Figure 2.7, include the initial tangent Young's modulus, the maximum uniaxial stress and corresponding strain, and the ultimate stress and corresponding strain. The tangential Young's modulus is given by the following formula.

$$t_{\tilde{E}} = \frac{\tilde{E}_O \left[ 1 - B(t_{\tilde{e}}/\tilde{e}_c)^2 - 2C(t_{\tilde{e}}/\tilde{e}_c)^3 \right]}{\left[ 1 + A(t_{\tilde{e}}/\tilde{e}_c) + B(t_{\tilde{e}}/\tilde{e}_c)^2 + C(t_{\tilde{e}}/\tilde{e}_c)^3 \right]^2} \quad (2.8)$$

where

$$A = \frac{\left[ \frac{\tilde{E}_O}{\tilde{E}_U} + (p^3 - 2p^2) \frac{\tilde{E}_O}{\tilde{E}_S} - (2p^3 - 3p^2 + 1) \right]}{[(p - 2p + 1)p]}$$

$$B = [(2 - \tilde{E}_O/\tilde{E}_S) + 2A]$$

$$C = [(2 - \tilde{E}_O/\tilde{E}_S) + A]$$

$\tilde{E}_O$  is the initial tangent modulus

$$\tilde{E}_S = \sigma_c/e_c, \quad \tilde{E}_U = \sigma_u/e_u, \quad p = e_u/e_c$$

$\sigma_c$  is the maximum compressive stress and

$e_c$  is the corresponding strain

$\sigma_u$  is the ultimate compressive stress and

$e_u$  is the corresponding strain

In the tensile region a linear stress strain relationship is used with a slope equal to the initial tangent modulus. The compressive stress-strain curve is adjusted for the triaxial containment by multiplying the stresses and strains, used to determine the stress-strain curve, by  $\gamma$  (Figure 2.7). The value of  $\gamma$ , the increase in compressive strength, is determined by linear interpolation between the eighteen points input by the user that define the triaxial failure surface. Figure 2.8 shows the failure surface as defined by the eighteen points and an example of triaxial test results. During unloading the stress-strain behaviour follows a straight line with the slope equal to the initial Young's modulus. Upon reloading the straight line is followed up to the original stress-strain curve and then follows the original curve.

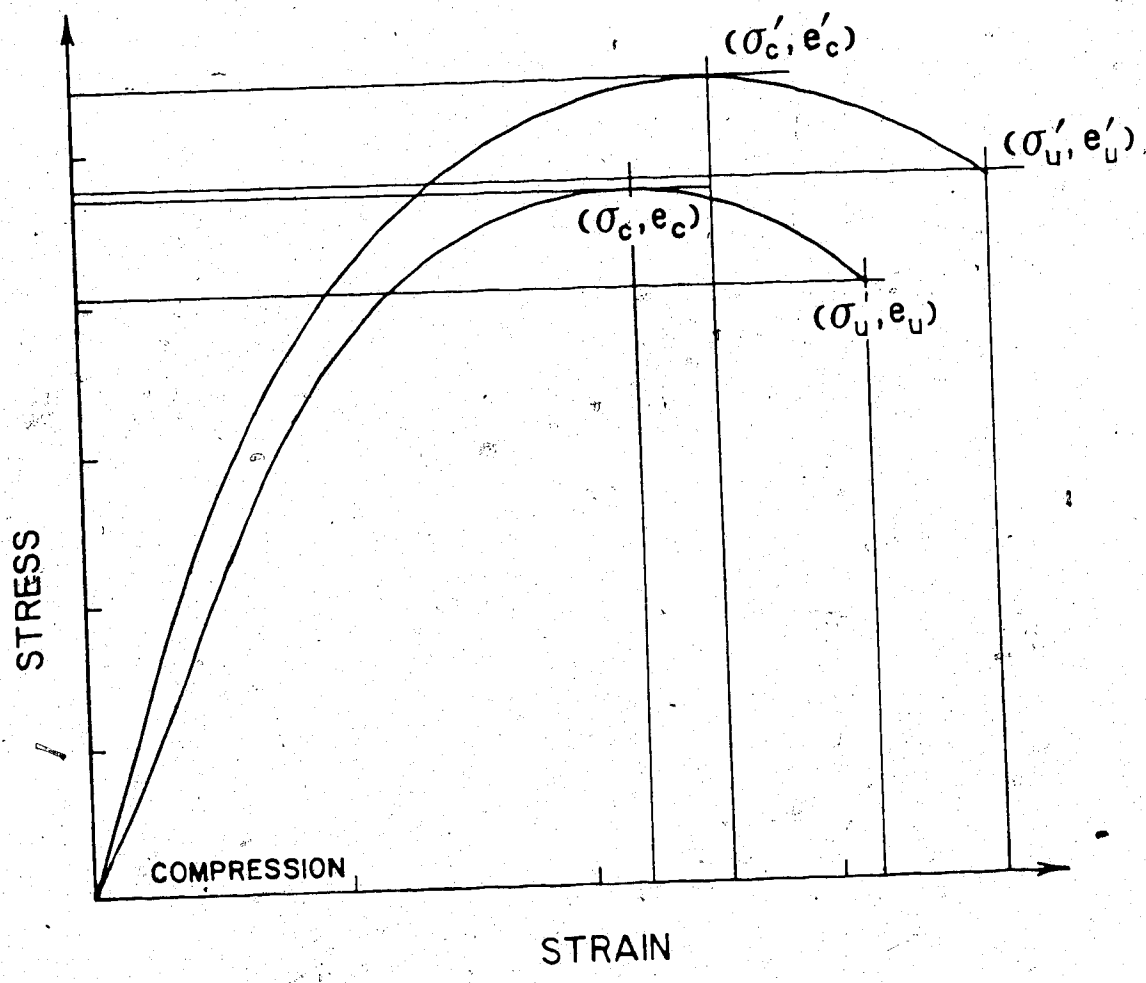


Figure 2.7 Uniaxial Compression Stress-Strain Curve

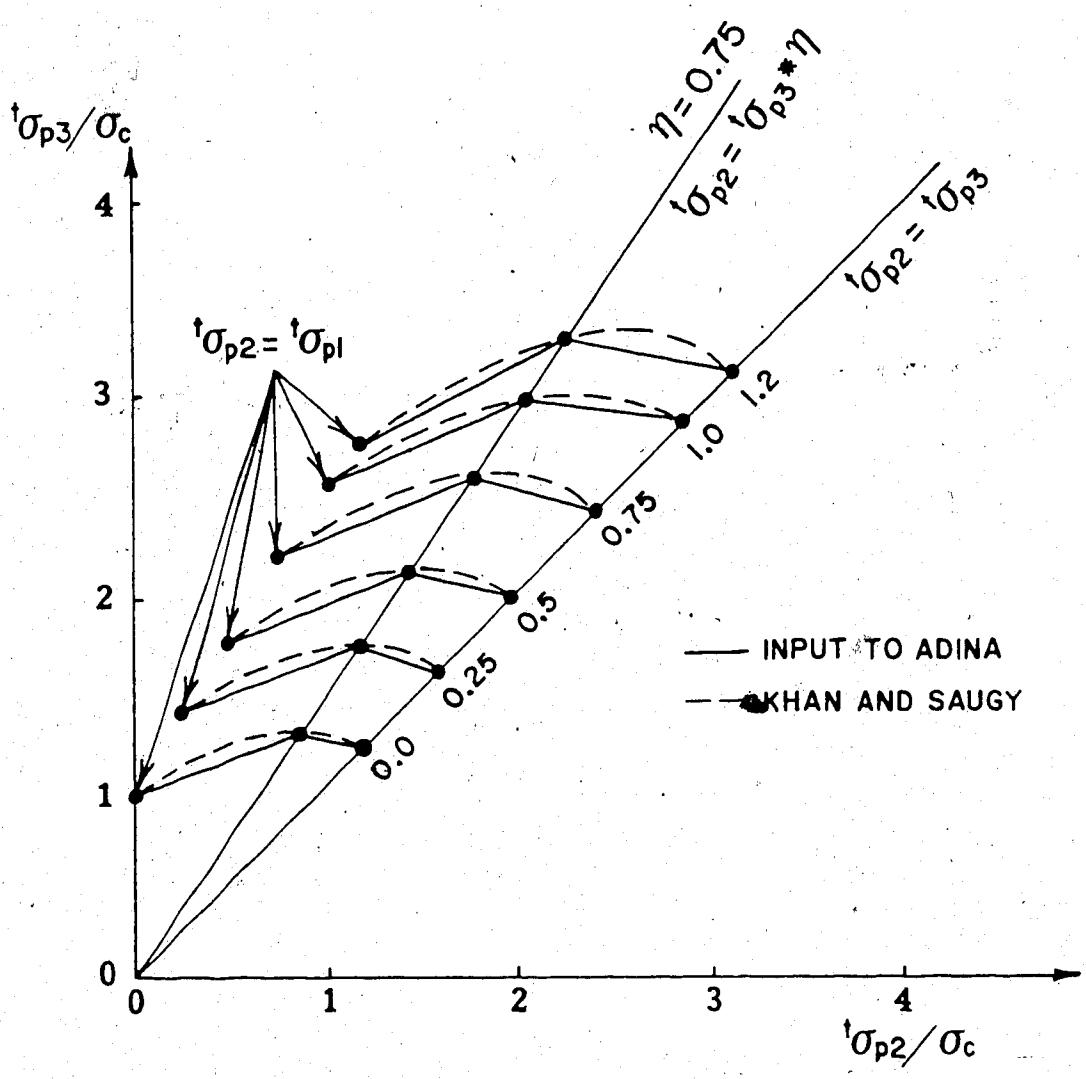


Figure 2.8 Triaxial Failure Surface as Input to ADINA



The function that determines whether the material is loading or unloading is shown below.

$$t_F = t_{\bar{\sigma}} + 3\alpha t_{\sigma_m} \quad (2.9)$$

where

$$t_{\bar{\sigma}} = \left[ \frac{1}{2} t_{s_{ij}} t_{s_{ij}} \right]^{\frac{1}{2}}$$

$$t_{\sigma_m} = \frac{1}{3} \sigma_{ii}$$

The value of  $\alpha$  is a constant equal to one third the slope of the failure surface in the  $\bar{\sigma}$  and  $\sigma_m$  stress space. The material is loading if  $t_F \geq F_{\max}$  and unloading is  $t_F < F_{\max}$ , where  $F_{\max}$  is the maximum value of  $t_F$  reached during the solution.

The Concrete Cracking model also includes a tension failure option. The uniaxial tensile failure stress is input to the program. This tensile strength is reduced linearly as the other principal stresses increase in compression. When a principal stress exceeds the tensile strength the stress across the failure plane is released and the normal and shear stiffnesses are reduced by the factors supplied by the user. The failure plane, having been formed, is allowed to become inactive upon unloading and active again on reloading. Once a failure plane has formed, its orientation is fixed and a second crack can only form perpendicular to

the original. It should be noted that to have the nonlinear behaviour due to cracking recognized, equilibrium iterations must be included. This is because the constitutive matrix is always reset to the initial elastic matrix after a crack has formed. The stiffness is only reduced by the equilibrium iterations. In all cases, even after cracking, Poisson's ratio is kept constant.

#### 2.2.4 Other Capabilities

##### 2.2.4.1 Element Birth and Death Options

The most important feature when using ADINA to model construction is the element Birth and Death option. This option allows the user to specify for each element in an element group where the Birth or Death option has been chosen, to specify the time step at which the element becomes active or ceases to be active. All degrees of freedom not active have their deflections set to zero and are eliminated from the stiffness matrix. The elements along the boundary where some of the nodes have deflected previous to the element being added, have all previous deflections subtracted in the calculation of their strains. The stiffness matrix must be reformulated whenever an element is added or removed. This option is available for all of the element types available in ADINA; however the following discussion concentrates on the two-dimensional solid elements. It should be noted that at this time ADINA does not allow

for an element to be both added and then later removed.

An important point of clarification on what is stated in the ADINA users manual is that if an element is given a birth time of 10.0 it becomes active at 10.0. If an element is given a death time of 10.0 it becomes inactive after 10.0, therefore if the element is to be inactive at time 10.0 and the time step increment is 1.0 a death time of 9.0 must be specified.

A major limitation with the element Birth and Death option is the way in which gravity loads are applied. In ADINA the gravity loads are applied using a lumped mass matrix rather than a consistent mass matrix. This method is used to reduce the amount of computation time required to calculate what part of an element's load is applied to each of its nodes. In the consistent mass method the load is divided according to each nodes ability to carry that load or in other words the load is proportional to the stiffness. The lumped mass matrix method divides the load evenly between the nodes irrespective of their stiffness. This method requires the calculation of the load vector only once at the beginning of the analysis.

A global node having more than one element contributing to its stiffness also has a portion of each element's mass contribute to the gravity load at the node. The mass of the surrounding elements is therefore attributed to the node and not the element, and has the

effect of having the mass from all of the elements that have ever or will ever contribute to the nodes whether or not the element is present at the time.

#### 2.2.4.2 Restart Option

To make the best use of this feature it should be decided at what points in the analysis that changes in the modelling of construction could occur or where different load cases are applied. The information to restart the analysis can then be stored for these time steps. This allows the analysis to continue from this point without rerunning the first part of the analysis. It should be noted that the information saved includes all material properties and the element birth and death times, therefore these values cannot be altered. If they are changed in the input to a restart run, ADINA echoes the input but uses the original values. ADINA does not save the solution time with the restart information and no error message is printed if the restart file for the wrong solution time is used.

#### 2.2.4.3 Substructuring

ADINA is capable of a limited form of substructuring. A substructure in ADINA can consist of a number of linear element groups and can be used as a "super element" a number of times to form a complete structure. The limitation that only linear element groups can be used in substructures limits their use.

Their major advantage is to statically condense out the majority of the degrees of freedom that are expected to perform linearly in an incremental nonlinear analysis.

#### 2.2.4.4 Dynamic Analysis

The program was developed to be a linear and nonlinear dynamic analysis program and allows the several types of dynamic analysis. In a linear dynamic analysis the mass matrix may be diagonal (lumped mass analysis) or banded (consistent mass analysis). The solution of the equilibrium equations can be carried out using mode superposition, implicit time integration (Newmark or Wilson method), or an explicit technique (central difference method) with a lumped mass matrix. Nonlinear dynamic analyses can use either the implicit or explicit time integration method.

### 3. FINITE ELEMENT MODELLING OF BURIED STRUCTURES

#### 3.1 General Comments

This chapter discusses the general modelling procedures used in finite element modelling of soil-structure interaction problems. This includes the decision making process used to pick the best method of analysis to obtaining the desired results, while not using unrequired options that increase the cost of the analysis. The methods presented in this chapter are those used in the analysis of the example structure, presented in Chapter 5.

#### 3.2 General Procedure

The first step in modelling a soil-structure interaction problem is to define the problem in terms of what is expected from the model. There are two basic reasons to carry out an analysis; to predict the behaviour of a particular structure or to evaluate the validity of a less complicated analysis. In either case, the features of the structure that are critical to its behaviour must be identified. These can be the geometric properties, construction procedure and the material properties. It must also be decided if the analysis is to be valid only at service load levels or is it expected to perform correctly near the ultimate load level.

If the analysis is to predict the behaviour of a structure, the actual geometry and material properties must

be determined. The parameters required for some material models are not easily determined. In these cases the literature may provide the information required.

If the objective is to evaluate an analytical procedure, two sets of analyses should be conducted; the first set to test the assumptions that are made in the simplified analysis, such as to assume an elasto-plastic material behaviour compared to the behaviour of the structure with strain hardening, and the second set should model a series of structures to determine a range of applicability for the simplified analysis.

### 3.3 Modelling of Construction

#### 3.3.1 Excavation

Before beginning excavation of the soil in which the structure will be constructed, the soil mass must be formed with its in-situ stresses and initial material properties. This is usually a simple process if the original surface of the soil is level and the soil properties are known. The soil mass can be placed in a single time step either with its compacted soil properties or have a load applied to the surface of the soil equal to the preconsolidation pressure. The self weight of the soil can also be applied at this time step.

Once the soil mass has been constructed, the excavation can be conducted by removing layers of soil elements. This

must proceed in a realistic manner because there is a possibility of slope failure. Depending upon the soil model being used there can be problems with convergence because a large portion of the structure changes from loading to unloading. The top layer of soil elements has a small net compressive stress and can develop tensile stresses that the nonlinear soil model cannot carry. The removal of soil also reduces the total weight and can cause the model to exhibit a large amount of rebound that may not be recognized in the field.

### 3.3.2 Modelling of Soil Compaction

The simplest method that can be used to model compacted soil is to give the properties of soil that has already been compacted. This is often used where a linear soil model is used and changes in the stress history have no effect, or where the construction procedure is not being explicitly being modelled as in a "Gravity on Analysis". In a Gravity on Analysis is where the structure is given its final geometry before gravity is applied. This can be used with good results in elastic soil-structure analyses if the structure is not construction dependent.

The second method is one used the most often in analyses where only soil is involved at the time of compaction [22]. With this method, the soil elements are added in layers to simulate "lifts" of soil being placed. A distributed load is then applied and removed to simulate the



compaction equipment compacting the soil. This load is calculated to give the same compactive effort as the compaction equipment used in the field. To be of use, this method must be used with a nonlinear material model that is dependent upon the stress history to determine the instantaneous response.

The major disadvantage of this method is that the distributed load used is, in most cases, greater in total magnitude than that of the weight of the compaction equipment being modelled. This is because the compaction equipment delivers a very concentrated load rather than a distributed load. If only soil is being modelled in a contained boundary and where the structure will not fail under the load, this method can be used; however if the structure is flexible, such as a steel culvert, the load will cause unrealistically large deflections or failure.

To model this type of problem the "Preload" method was developed. This method is a combination of the previous two methods in which the soil is placed in layers but the material is given initial properties of compacted soil and a load is applied to the existing structure prior to the addition of the layer of elements.

The preload is applied to reduce the effects of the differential settlements in the underlying layers. The differential settlements can cause unrealistic stresses in the soil being placed. This is demonstrated using the example mesh shown in Figure 3.1. When the soil in this

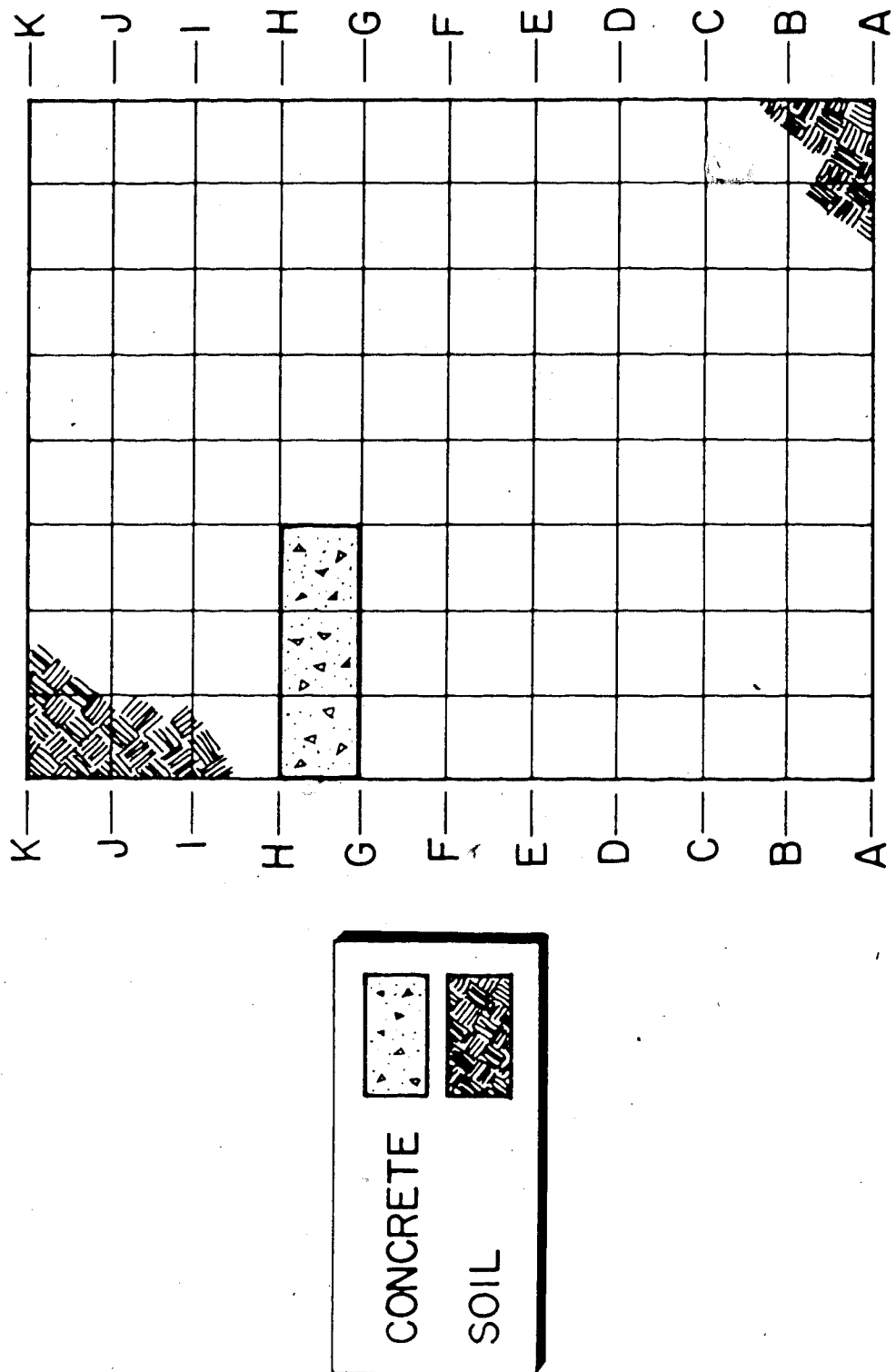


Figure 3.1 Preload Method Test Structure

structure is added without using the preload method the top layer of elements yield and areas of small tensile principal stresses appear (Figure 3.2). This is not realistic because the compaction process would remold the soil in this region.

The preload is equal to the weight of soil to be added in the next layer or total soil to be added. When the layer is placed, with its self weight, the preload is reduced and moved to the new surface. This allows the new layer of elements to be formed after the existing structure has deflected. These deflections can be ignored because when these deformations are taking place the actual soil is still being reformed by the compaction process.

There are three methods of preloading that can be used depending upon the structure and the intermediate results wanted (Figure 3.3). The first preloading method has the preload equal to weight of all remaining soil elements. The preload is applied to the structure, a single layer of soil elements is added and in the same time step the load is reduced by the weight of the elements added and is moved to the new soil surface. The problem with this method is that the structure may require the stiffness of the soil yet to be placed to carry the load of the soil represented by the preload. It also does not solve for intermediate construction steps.

Another method which does solve for intermediate steps has the preload equal to the weight of the next layer of soil elements. The preload is applied to the existing

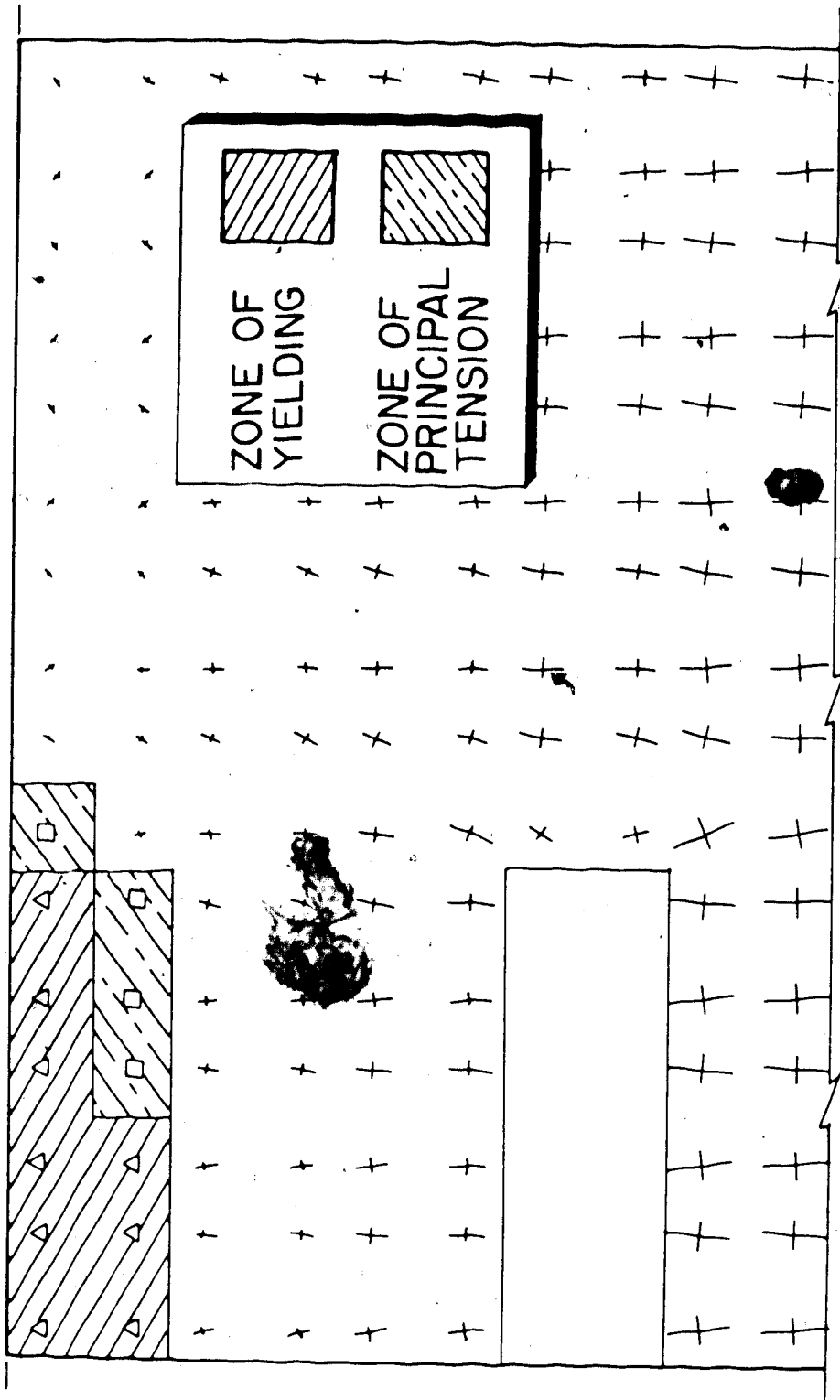
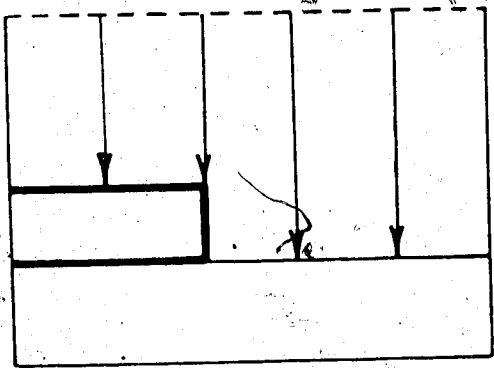
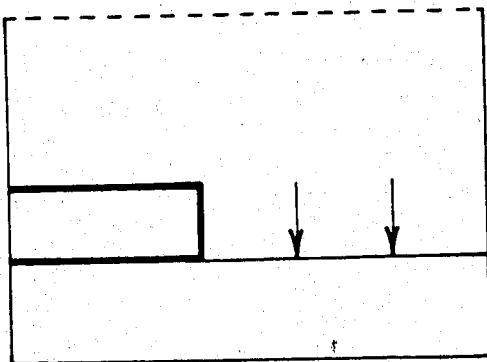
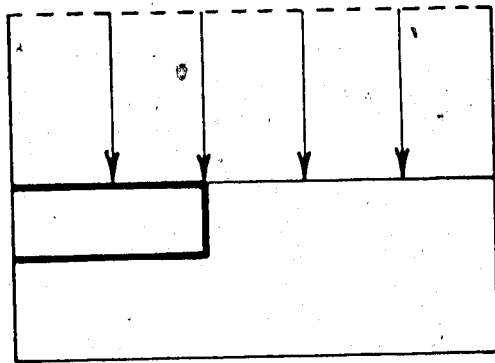


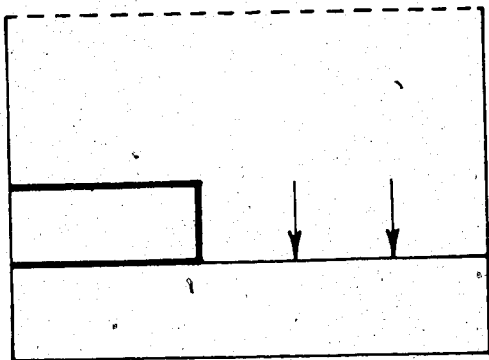
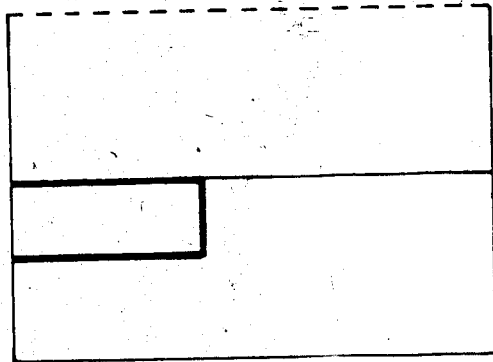
Figure 3.2 Zones of Yielding when No Preload was Used



METHOD 1



METHOD 2



METHOD 3

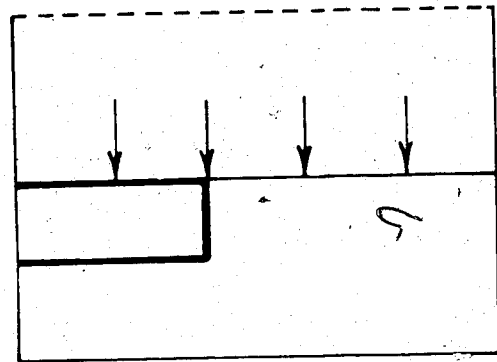


Figure 3.3 The Three Preload Variations

structure in one time step, the preload is then removed and the soil elements with their self weight are added in the next time step. The top layer of elements is without a net compressive stress when this method is used. This can cause zones of tension failure to occur when a structure in the soil causes differential settlements. These zones of tension failure can lead to numerical instabilities when a nonlinear material model is used.

The third variation of the preload method is very similar to the second. The preload is equal to the weight of the next layer of elements. The preload is applied, then the layer of elements is added and at the same time the preload is moved to the new surface. This keeps a small net compressive stress and reduces the possibility of a small tensile stress forming, while allowing the solution at intermediate construction steps.

### **3.4 Mesh Development Considerations**

#### **3.4.1 Boundary Conditions**

The extent of soil to be considered in a finite element analysis was suggested to have the vertical boundaries three times the span away from the centerline of the structure and the horizontal boundary one and a half time the rise below the base of the structure (ABDEL-SAYED and BAKHT 1981) [1]. The vertical boundaries are rollered to allow movement in the vertical direction and the horizontal base of the soil

mass is fully fixed. These boundaries were found by Abdel-Sayed et al to be sufficiently distant so that any further increase in the distance had no substantial affect on the structure. These are by no means the only boundary that can be used and a reduction in the distance to the boundary can be worthwhile if a large number of analyses are to be done. Any reduction would require investigation while the boundaries given above generally give good results.

It has been suggested that a radial boundary can be used, thereby reducing the amount of soil that need be modelled (ABEL, MARK and RICHARDS 1973) [2]. This is where the boundary of the soil mass is modelled as a circular arc that is perpendicular at the soil surface and radial movement is fixed while circumferential movement is allowed to occur. This possibility was investigated and found to give very unrealistic results in the soil. At the base of the soil mass, when a radial boundary is used, the lateral pressure under self weight is larger than the pressure on the horizontal plane. This is not a realistic stress field when the soil is assumed to have a Poisson's ratio of 0.3. This boundary condition was therefore abandoned.

#### 3.4.2 Mesh Progression

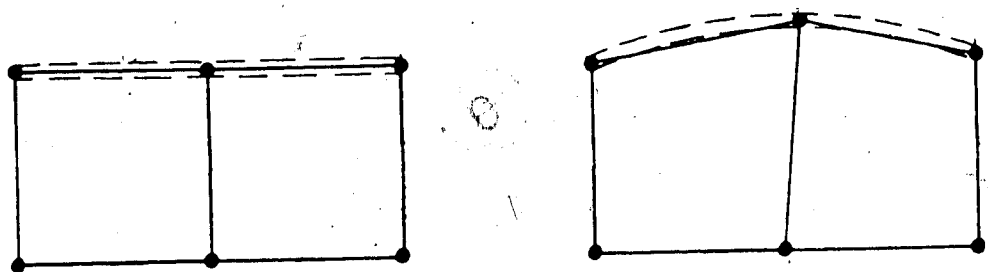
The progression of the finite element mesh is governed by the construction process used in the field. When the construction process includes both excavation and backfilling there must be areas of the mesh where two sets

of elements cover the same volume of soil, one to be removed during excavation and one to be added during the backfilling. This is required because of the limitation within the element Birth and Death option that an element can only be added or removed but not removed and later added. This overlapping of the mesh can have the same geometry; however this is not required and is usually not the best solution because of the different procedures used while modelling the excavation and backfilling operations. In either case a second set of nodes should be used to define the overlapping mesh geometry so that the original mesh geometry is maintained.

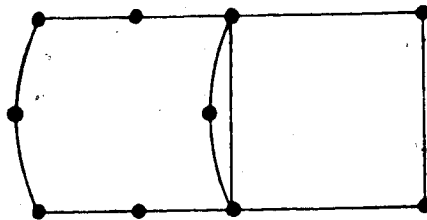
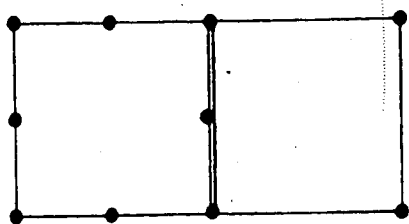
### 3.4.3 Compatibility

When the finite element mesh is being developed it is desirable to use elements that have the same order of displacement function. This ensures that the displacement field is continuous through the structure. Convergence as the mesh is refined will only occur monotonically if compatibility is maintained between elements. Three examples of incompatibility between elements are shown in Figure 3.4. In Figure 3.4a, the two-dimensional solid elements have a linear shape function while the two-node beam element has a cubic shape function. While the two-dimensional elements are compatible in their x and y translational displacements the beam element also maintains compatibility of slopes between elements. In the second example (Figure 3.4b) the node at

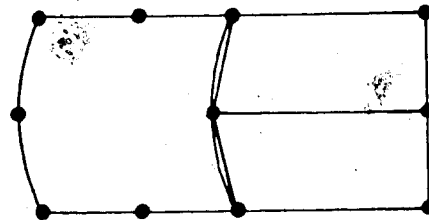
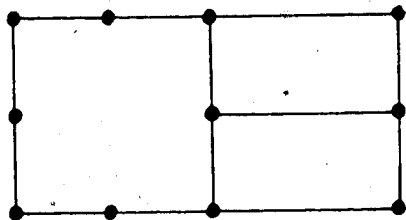




(a)



(b)



(c)

Figure 3.4 Examples of Discontinuity Between Elements

the midpoint of the common side is only connected to the quadratic element and not to the linear element. This allows the two elements to separate along their boundary as shown. In the example shown in Figure 3.4c, the two linear elements are connected to the single quadratic element. While this ensures continuity at the nodes other points along the sides of the elements are not connected because the quadratic element deflects into a parabolic shape while the two linear elements approximate this with two linear segments.

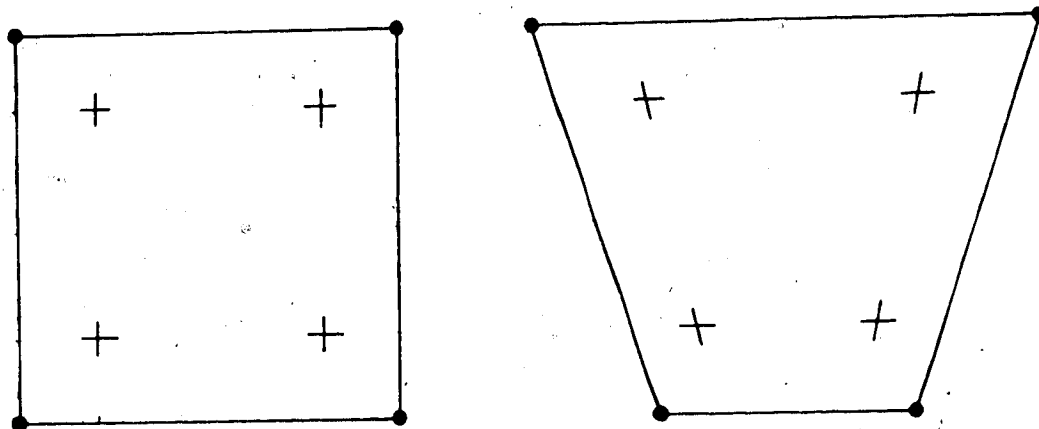
Incompatibility within a mesh can make the transition from a fine mesh, where it is needed, to a coarse mesh easier to construct. This is a possible alternative to keeping the mesh fine and maintaining compatibility if the negative effects can be accommodated, such as discontinuities in the stress field at the point of the displacement discontinuity, and possibly a slower rate of convergence.

Another form of discontinuity is introduced by using the element Birth and Death option in ADINA to model construction. In this case the discontinuity is caused by the existing mesh deflecting under loading before the new section of the mesh is added. This discontinuity is realistic if the modelling procedure follows the construction in the field.

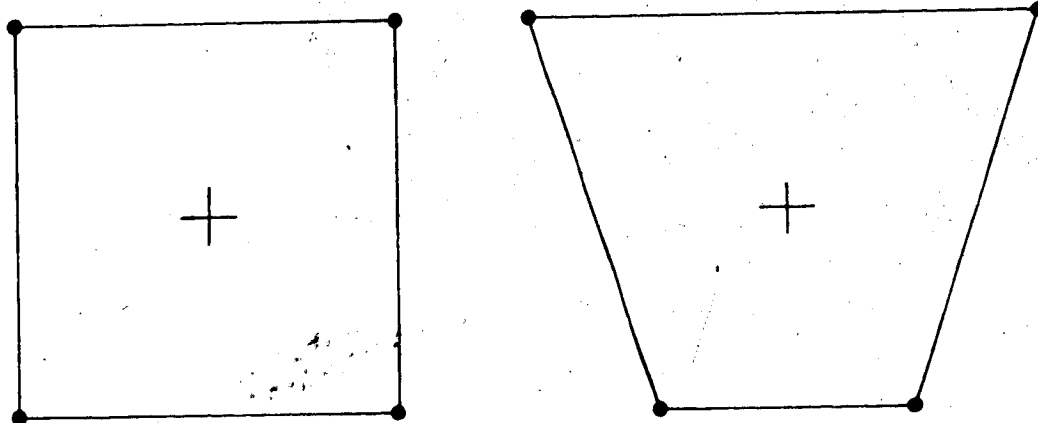
#### 3.4.4 Aspect Ratio's and Order of Integration

With isoparametric two- and three-dimensional elements the shape into which the element is mapped can have a great effect upon its stiffness. There are many recommendations as to the limits on aspect ratios in two and three dimensional solid elements but the recommended maximum of 2.5 and the absolute maximum of 5.0 are generally considered reasonable. These limits are placed assuming that exact integration is used. When the aspect ratio exceeds these limits the element may not perform as expected because of shear lock. Shear lock is when an element, because of its shape function, must undergo large shear deformations in order to assume the true deflected shape due to bending. This is demonstrated in Figure 3.5 using a linear two-dimensional solid element. Using 2x2 gaussian integration, the shear strains at the gauss points are large though no shear force is applied.

Using a four element cantilever beam modelled using quadratic elements with aspect ratios of 5.0, the average shear stress through the cross-section is shown in Figure 3.6. If 3x3 integration is used to sample the strains in the model of the beam the stresses would be either far larger or smaller than the theoretical value or even of the incorrect sign. This is because the average shear stress in the model has a parabolic shape and the 3x3 integration scheme samples at the peaks. If the reduced order of integration, 2x2, is used, the location of the gauss points correspond to the points where the theoretical average shear



(2x2) Exact Integration



(1x1) Reduced Integration

Figure 3.5 High Shear Caused by the Order of the Shape Function

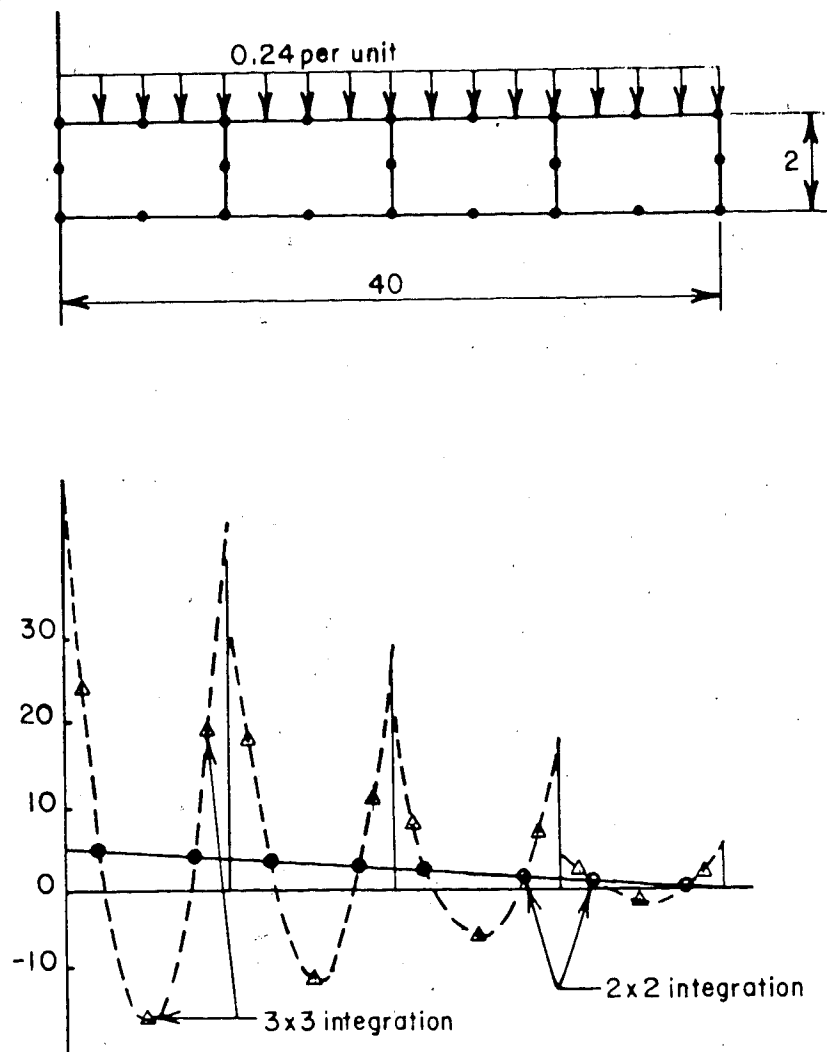


Figure 3.6 Advantage of using Reduced Integration

stress is equal to the sampled average shear stress.

Using reduced integration has become common when conducting a nonlinear analysis because it has the advantage of reducing the amount of storage needed for the strain history of the material at each gauss point. A reduction in the order of integration substantially reduces the cost of a nonlinear analysis, but it affects the rate of convergence as well. The effect of reduced integration when the elements have large aspect ratios is to increase the rate of convergence. However, when the material model used is nonlinear, the progression of the nonlinear effects are more discontinuous with a reduced order of integration. An example of this is shown in Figure 3.7, a single quadratic serendipity element is subjected to a uniform moment field. A quadratic element can represent the displacements under this loading exactly because the theoretical displaced shape is also quadratic. Depending upon the order of the integration used the nonlinear behaviour can change so that the ultimate moment carried changes by over 35 per cent.

#### 3.4.5 Methods of Formulation

Results from a finite element analysis can vary greatly depending upon the material model, its parameters and the formulation method used. The problem being modelled must therefore be understood so that all important features are included in the analysis. To illustrate this a steel plate (Figure 3.8), restrained along two edges against any

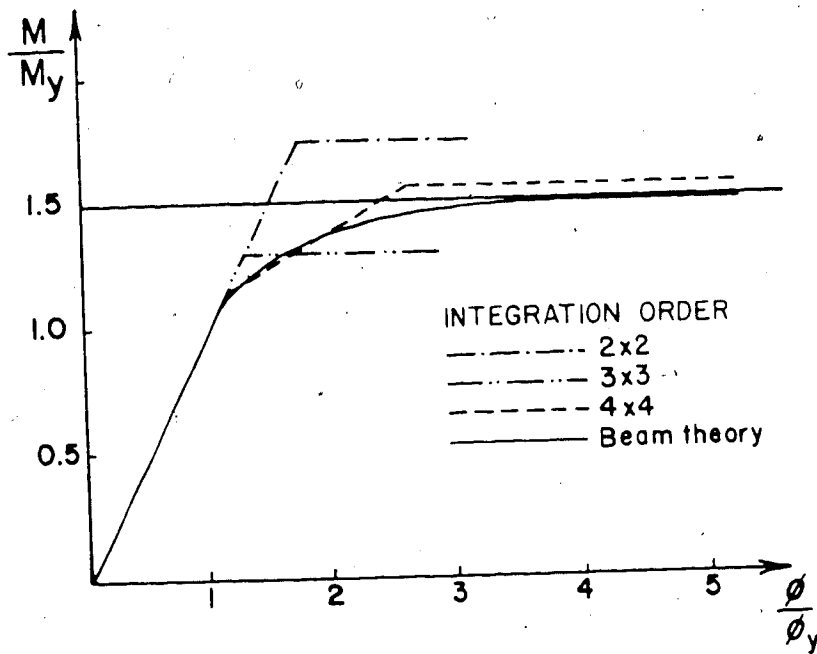
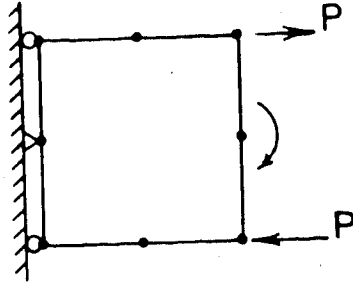


Figure 3.7 Disadvantage of using Reduced Integration

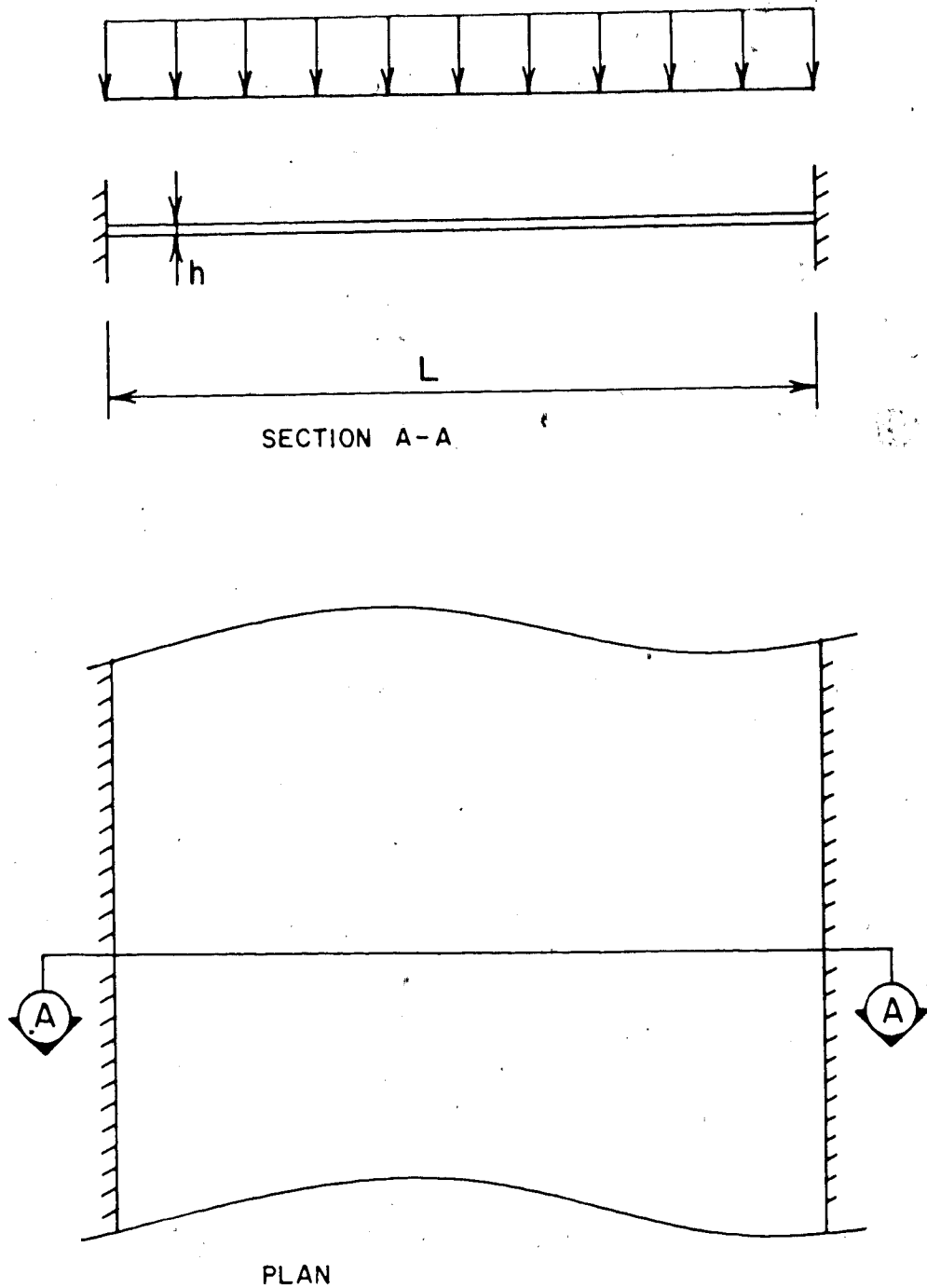


Figure 3.8 A Clamped Continuous Plate



translation and against rotation, infinite in the other direction and subjected to a transverse uniform load (Ratzlaff, Kennedy 1985) [33], was chosen even though it is not a soil structure interaction problem because the changes in behaviour are so dramatic with different assumptions.

Each of the following idealized structures describes the behaviour of the actual problem over a certain range, as shown in Figures 3.9 and 3.10. Each make certain assumptions that allow the analysis to be simplified. The behaviour of each of these structures can be predicted by ADINA when the boundary conditions, material model and formulation are varied or they can be described by a closed form solution.

- B<sub>e</sub> Fixed Elastic Beam  
(Elastic Beam Theory)
  - small deflection
  - linear elastic material
- B<sub>p</sub> Fixed Plastic Beam  
(Plastic Beam Theory)
  - small deflection
  - elasto-plastic material
- M<sub>e</sub> Clamped Elastic Plate  
(Timoshenko)
  - large deflection
  - linear elastic material
- C<sub>e</sub> Elastic Cable
  - large deflection
  - linear elastic material
- C<sub>p</sub> Plastic Cable
  - large deflection
  - elasto-plastic material
  - $\nu = 0.3$
- C'<sub>p</sub> Plastic Cable
  - large deflection
  - elasto-plastic material
  - $\nu = 0.5$

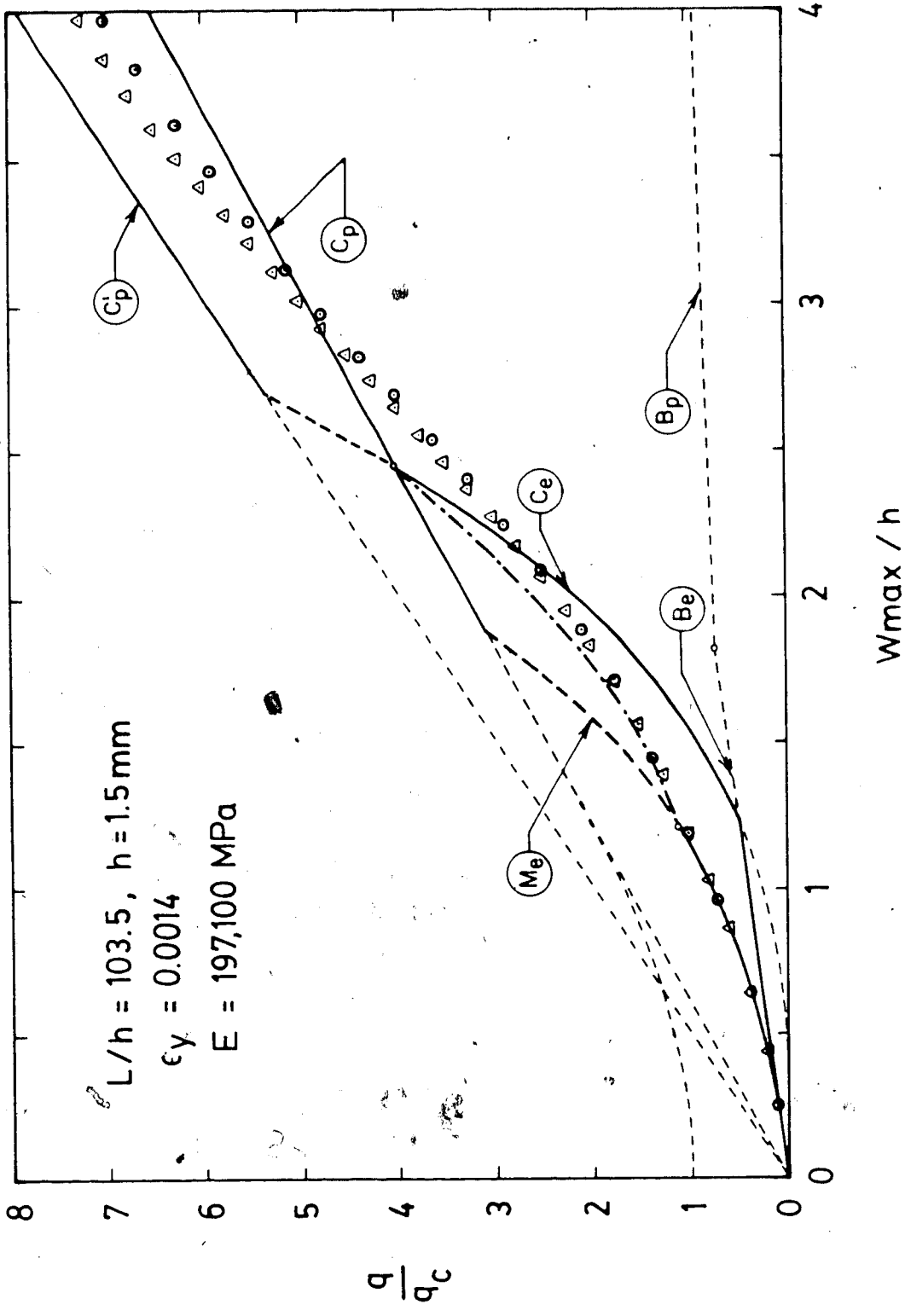


Figure 3.9 Behaviour of a Continuous Plate (detail)

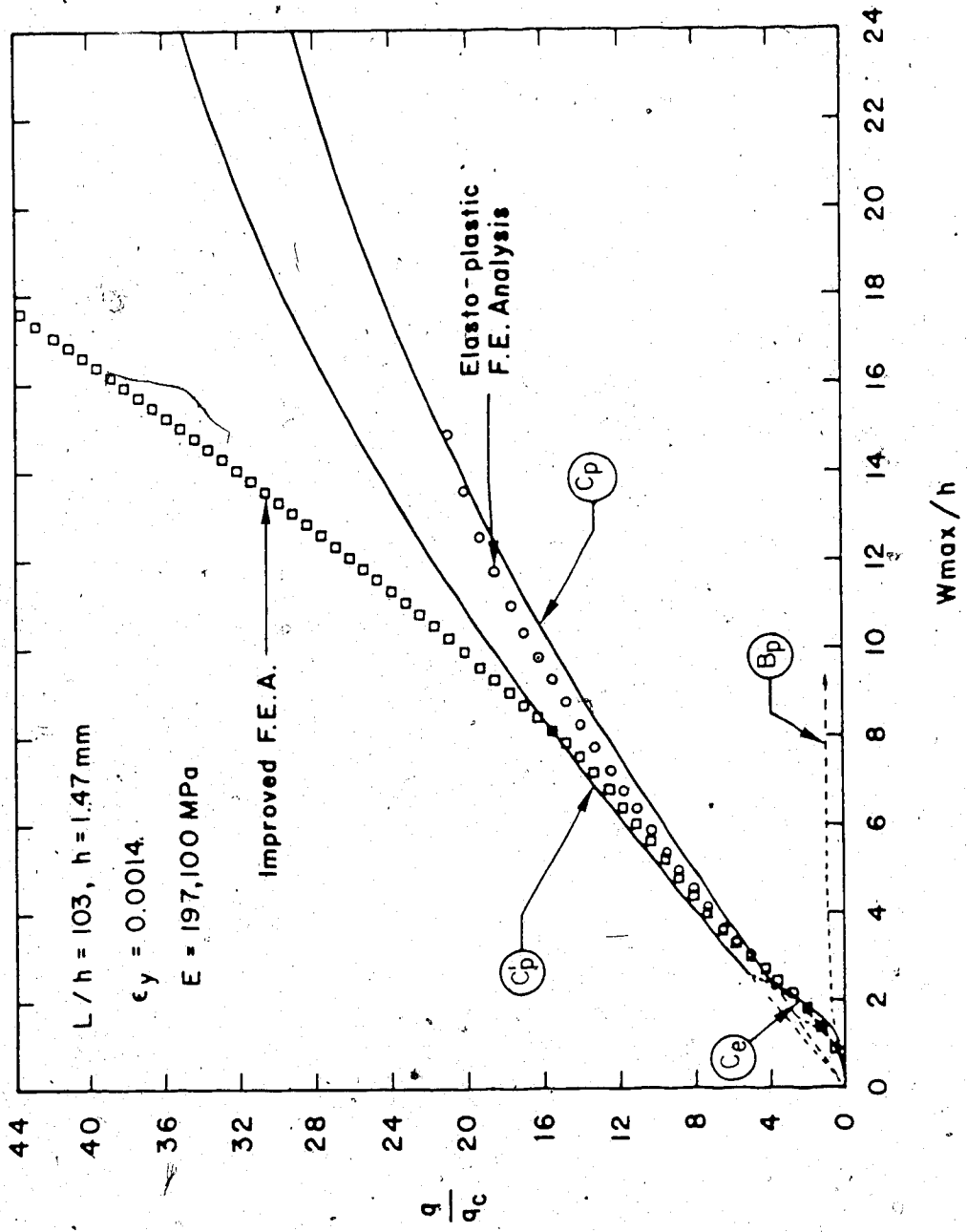


Figure 3.10 Behaviour of a Continuous Plate

Two further sets of assumptions were made and the corresponding curves were generated using ADINA. With these assumptions a closed form solution would be almost impossible to formulate. The only difference between these two sets of assumptions is that the Improved Finite Element Analysis includes strain hardening whereas the Elasto-plastic Finite Element Analysis does not.

#### Elasto-plastic Finite Element Analysis (ADINA)

- large deflection  
(Updated Lagrangian formulation)
- elasto-plastic material  
(Bilinear von Mises Yield criterion)

#### Improved Finite Element Analysis (ADINA)

- large deflection  
(Updated Lagrangian formulation)
- elastic-plastic material  
(Multi-linear von Mises Yield criterion)  
(Isotropic strain hardening)

The results of the analyses for the steel plate depend upon the assumptions made; however each of the analyses is valid within the limitations of the assumptions. The result is that ADINA can model each of the assumptions and the results must be evaluated to check that each of the assumptions is correct. An assumption can be checked by removing the assumption from the analysis using ADINA to see if the results change significantly.

### 3.5 Summary

In this chapter the finite element modelling considerations discussed included those that were used to model the soil-structure interaction problem discussed in Chapters 4 and 5. The procedures used to model construction of this problem can be applied to any analysis where construction must be modelled to arrive at a realistic solution.

Some general finite element considerations were discussed because they were of particular interest when modelling the example problem. The features that are specific to ADINA have been discussed in greater detail than in the ADINA Users Manual [3] to remove the confusion encountered while conducting the analyses.

## 4. ARCH-BEAM CULVERTS

### 4.1 General Description

#### 4.1.1 Description of an Arch-Beam Culvert

Arch-beam culverts are large span, multi-plate, corrugated steel culverts with a concrete shell placed over the upper portion. The soil cover is normally less than allowed in the code requirements for soil-steel culverts. The concrete shell provides resistance to local bending moments caused by individual wheel loads. This concrete shell is reinforced and is bonded to the culvert using shear connectors. The concrete also extends horizontally beyond the culvert to provide its own supports. At the ends of the culvert, end walls are provided to act like diaphragms in a cylindrical shell (Figure 4.1, Figure 4.2).

Arch-beam culverts have a number of advantages over the conventional short span bridges which would otherwise be required. Arch-beam culverts have a completion time of as little as 14 days including earth work. A large portion of this time is required for curing of the concrete. The construction time is less than for conventional bridges that are cast in place because there is little formwork required other than the steel culvert. Once it is constructed, the steel culvert is left in place and with a properly designed stream transition eliminates the scour under the "abutments". They are also more resistant to road salt and

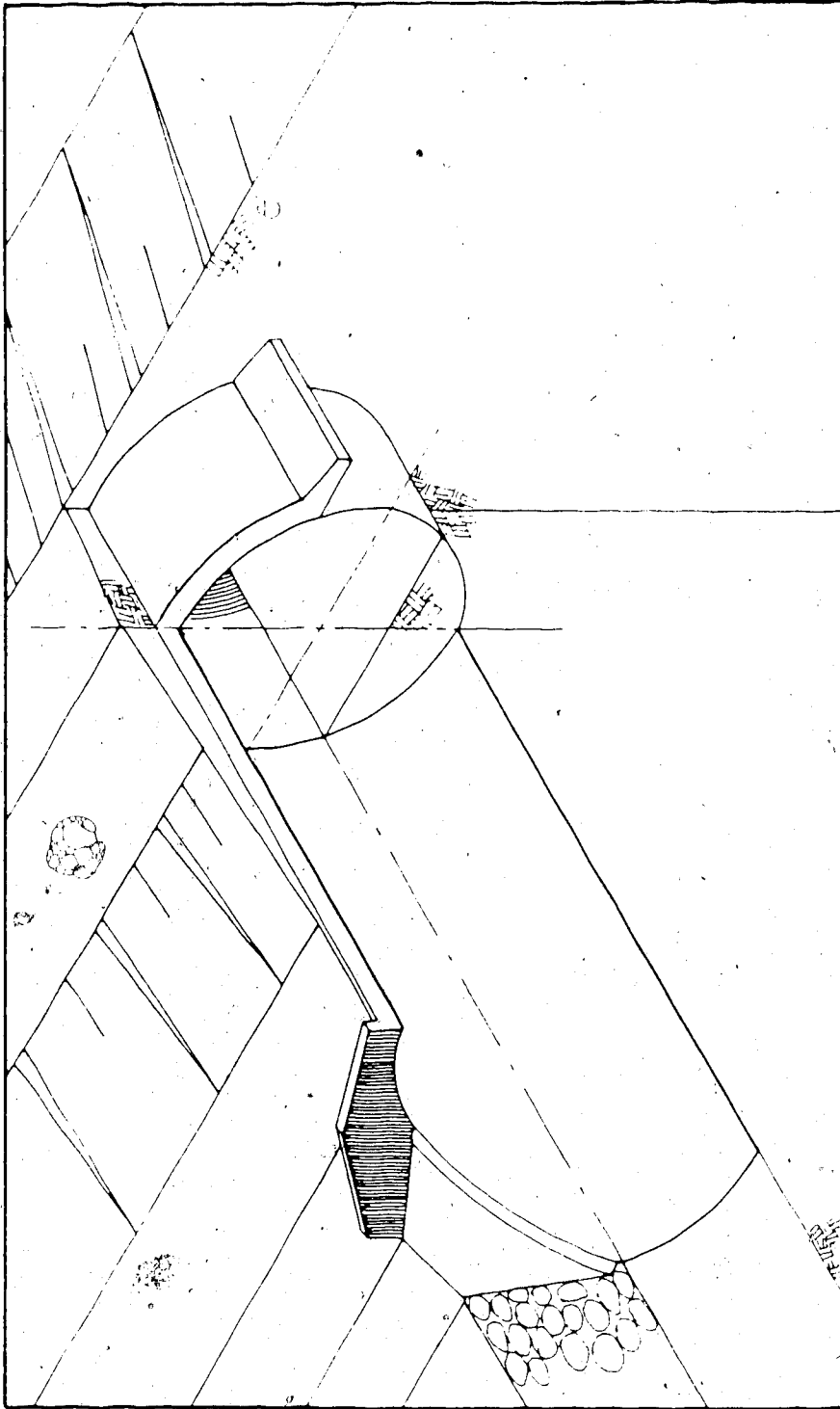


Figure 4.1 Cutaway View of a Circular Arch-Beam Culvert



Figure 4.2 Blairmore Creek Arch-Beam Culvert



Figure 4.3 Compaction Beside the Prototype Arch-Beam Culvert



corrosion because of the soil cover above the concrete. The soil also acts as a temperature damper and reduces the number of freeze-thaw cycles that the structure must withstand. The arch-beam culvert is therefore superior in resisting these three major causes of maintenance problems.

Arch-beam culverts offer a pleasing appearance like that of a stone arch bridge. This type of structure has a very small soil cover compared to conventional soil-steel culverts and reduces the amount of earth work to a minimum. This results in substantial savings as compared to the conventional bridges.

#### 4.1.2 Other Culvert Modifications

The arch-beam culvert is the latest of several modifications to corrugated steel culverts to improve the distribution of applied loads where only a limited soil cover can be used. The first is to place thrust beams along each side of the culvert (Figure 4.4a) [13]. This provides improved abutments for the top arch of the culvert and causes the point loads to be distributed longitudinally. The thrust beams provide the same support to the culvert as the support slab with the arch beam culvert.

The second modification has a horizontal concrete slab cast within the soil (Figure 4.4b) [1]. This slab assists in distributing the wheel loads.

Another modification that is very similar to the arch-beam culvert uses closely spaced transverse steel ribs

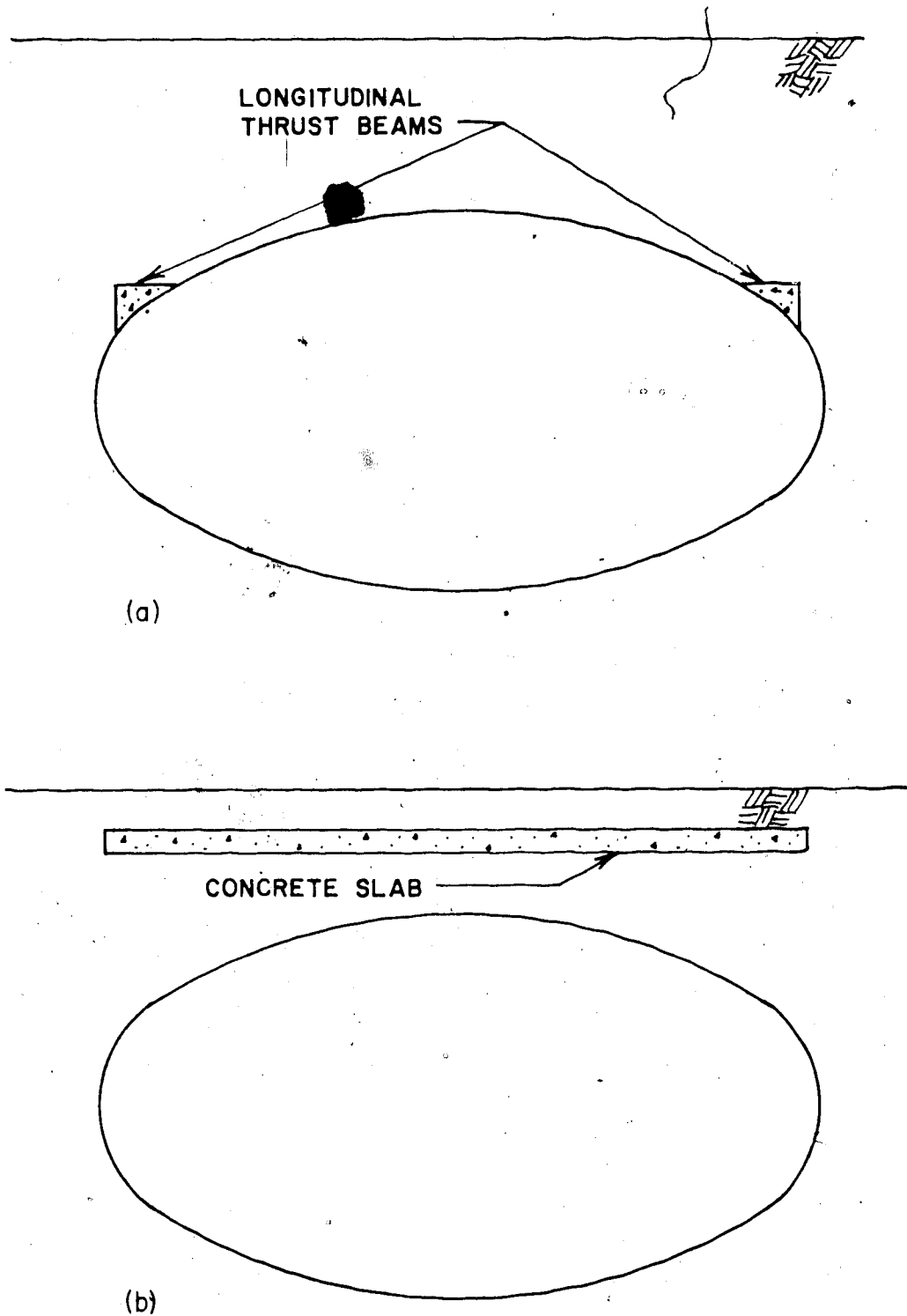


Figure 4.4 Soil Steel Culvert Modifications

and longitudinal thrust beams, instead of the concrete shell and support slabs, to stiffen the steel culvert (Figure 4.5). One such reinforced corrugated steel culvert with a span of 18.0 m was constructed in Wellington County, Ontario [14].

## 4.2 Preliminary Design Considerations

### 4.2.1 Corrugated Steel Culvert Design Considerations

The design procedure for a corrugated steel culvert is to determine its strength as a thin compression ring. The surrounding soil must be capable of providing the required reaction pressures and the culvert cross-section must have sufficient moment resistance to permit handling and installation.

White and Layer [36] outline the assumptions used when designing culverts as compression rings. One assumption is that concentrated loads are not applied directly to the culvert. AASHTO, therefore, requires that the soil cover be at least one sixth of the span. This allows the point load applied at the soil surface to be distributed sufficiently so that it is close to uniform at the culvert. This depth of soil also provides the required confinement to give the culvert its strength.

The axial force in the culvert is assumed to be constant if the friction between the culvert and the soil is neglected. The axial force is calculated as shown in

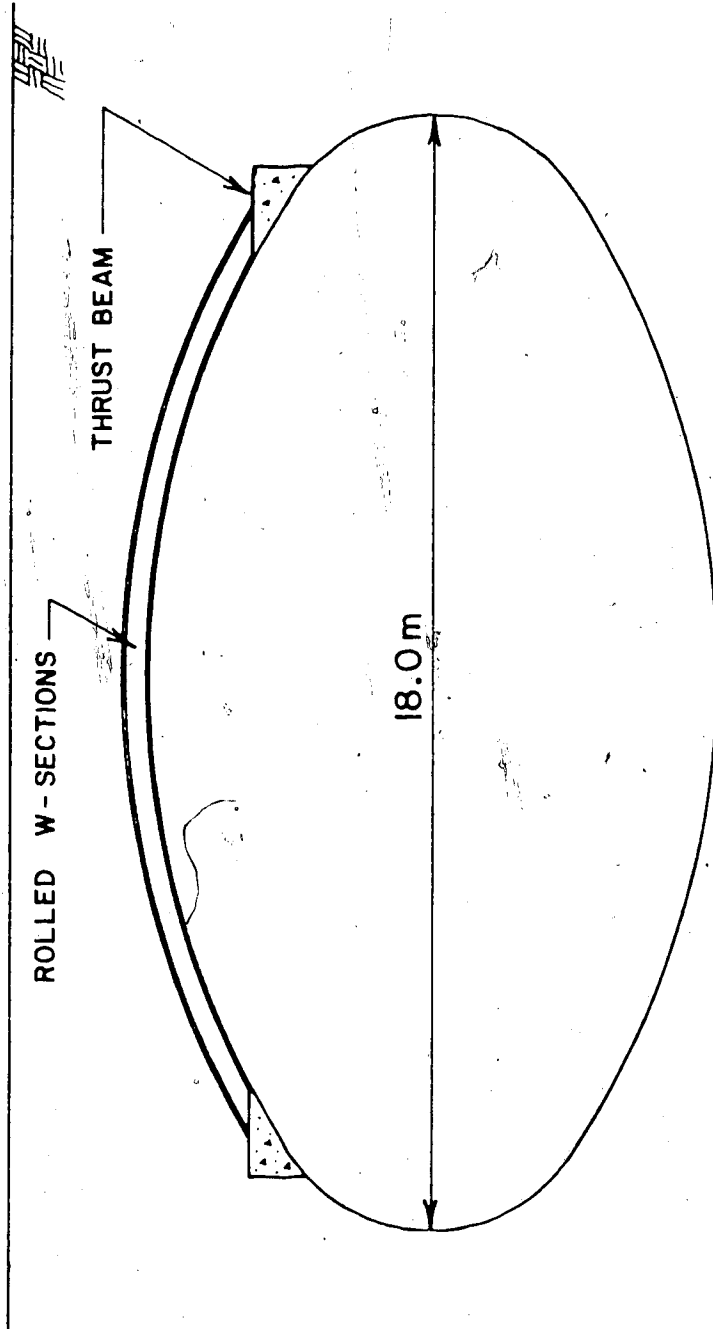


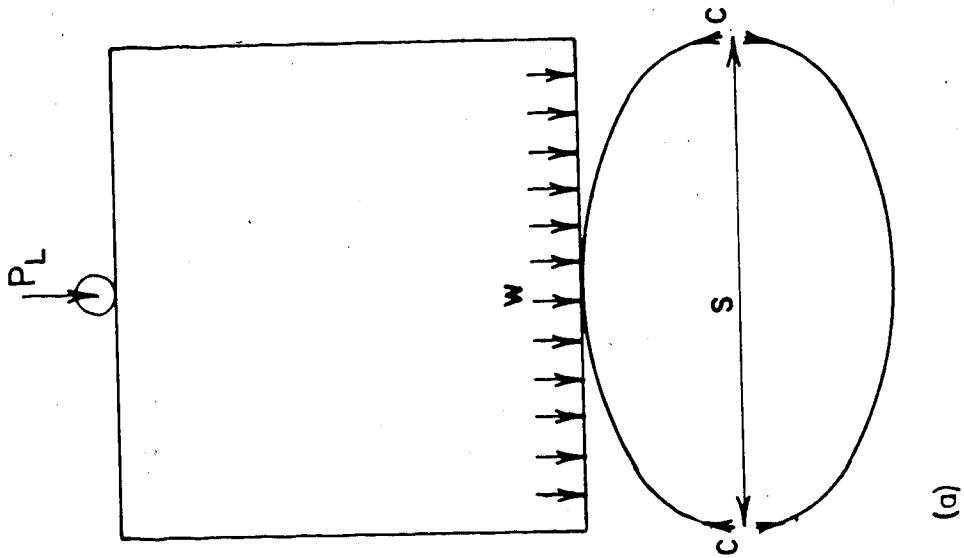
Figure 4.5 Wellington County Culvert

Figure 4.6a. The weight of the soil above the culvert span and the applied live load is assumed to be carried by the culvert. To provide equilibrium in each section of the culvert the radial stress in the soil surrounding the culvert is proportional to the curvature of the culvert (Figure 4.6b).

To reduce the axial force in the culvert, soil archs can be formed during construction. The soil is placed in curved layers above the culvert. As the layers are placed the lower layers carry a portion of the weight by arching to each side of the culvert. To promote this behaviour a soft bedding material is sometimes placed below the culvert. This allows the culvert to settle and have the soil archs carry a larger portion of the load.

#### **4.2.2 Arch-Beam Culvert Design Considerations**

At the time when the prototype culvert was being designed, two principal structural actions were postulated. The first is that the concrete would behave as a cylindrical shell and the horizontal slab would act to provide the horizontal restraint. With this behaviour only a relatively thin concrete section is required since most of the load is carried by an arching action. The second action considers the concrete arch to be sufficiently flat so that the action is primarily that of a one-way slab with the horizontal wings acting as reaction points. This behaviour assumes that the entire load is carried in bending and therefore requires



$$C = (P_L + w \times S) / 2$$

$$P_T = P_B = C / R_T \quad R_T = R_B$$

$$P_S = C / R_S$$

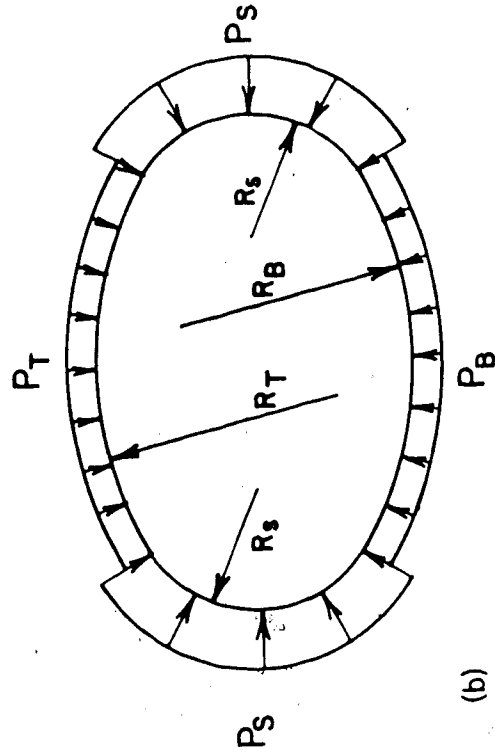


Figure 4.6 Compression Ring Culvert Design

a much thicker concrete foundation.

The importance of the structure and the time constraints imposed by construction required that the more conservative one-way slab action be assumed. The horizontal wings were assumed to provide the required reactions. The distribution of the reactions under the wings were assumed to be uniform for dead load and triangular under live load as shown in Figure 4.7.

An MS30 single axle loading was used in the design. This single axle loading of 240 kN was not reduced for multiple lanes. Impact loading was applied according to section 1.2.12 of the AASHTO Standards Specifications for Highway Bridges. This section allows for a reduction in the impact load from 30% for uncovered culverts down to 0% for culverts with 0.9 m of soil cover. This axle load was applied to the structure as two point loads at 1.8 m spacing each having half the magnitude of the axle load as calculated above. These point loads were then distributed through the soil according to section 1.4.3 of AASHTO. If the depth of fill is 0.61 m or more the concentrated load shall be considered as uniformly distributed over a square, the sides of which are equal to 1.75 times the depth of fill. The dead load due to the soil was assumed to be  $\gamma_s d$  where  $\gamma_s$  is the density of the soil and  $d$  is the height of fill above the structure.

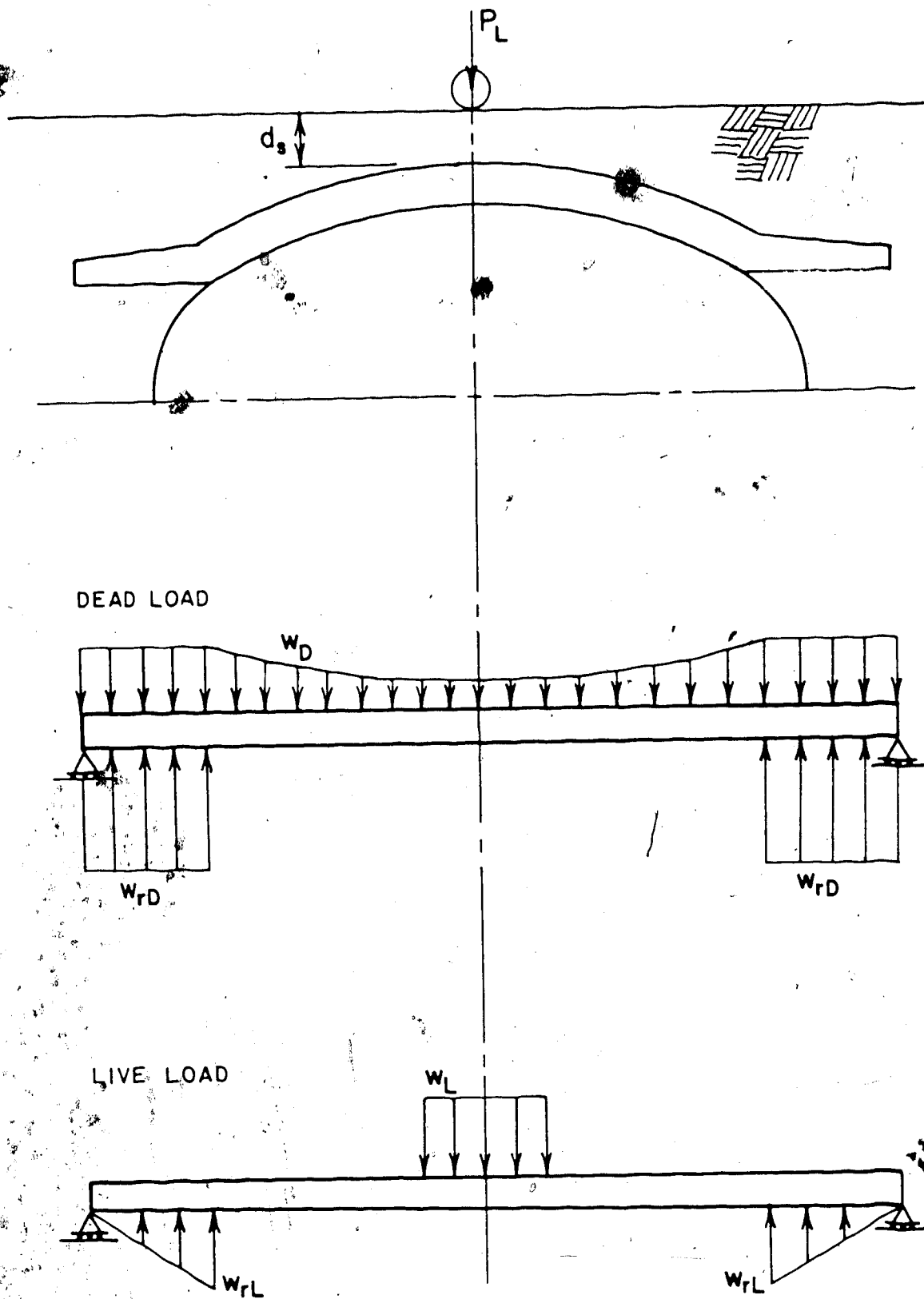


Figure 4.7 Simplified Design Procedure



### 4.3 Prototype Geometry

The prototype structure constructed was a 8.6 m x 4.5 m horizontal ellipse (Figure 4.8) with a crown length of 28.6 m. The culvert material was 5 mm thick corrugated steel with the profile shown in Figure 4.9. The structure had a soil cover that varied between 60 cm and 150 cm under the road surface and as little as 10 cm of soil cover on the shoulders of the road. The nominal thickness of concrete placed was 51 cm. The bottom reinforcement placed was 5 cm above the neutral axis of the corrugated plate, 15M bars at 50 cm longitudinally and 25M bars at 30 cm centers circumferentially. The top reinforcement of 15M bars was placed 8 cm below the surface in the same grid as the bottom reinforcement. A longitudinal cross-section through the concrete slab is shown in Figure 4.10.

### 4.4 Construction of Prototype

The construction begins with the excavation of a stream bed in which to place the structure (Figure 4.11a,b). The bedding surface on which the culvert will be assembled is shaped to the culvert's bottom arc (Figure 4.11c). The culvert plates are assembled starting with the bottom plates and support cables or braces are used to maintain its shape (Figure 4.11d). Backfill material beside the culvert is placed and compacted using hand tamping or light compaction equipment as shown in Figure 4.3. A good quality granular material is required because the culvert is very flexible at

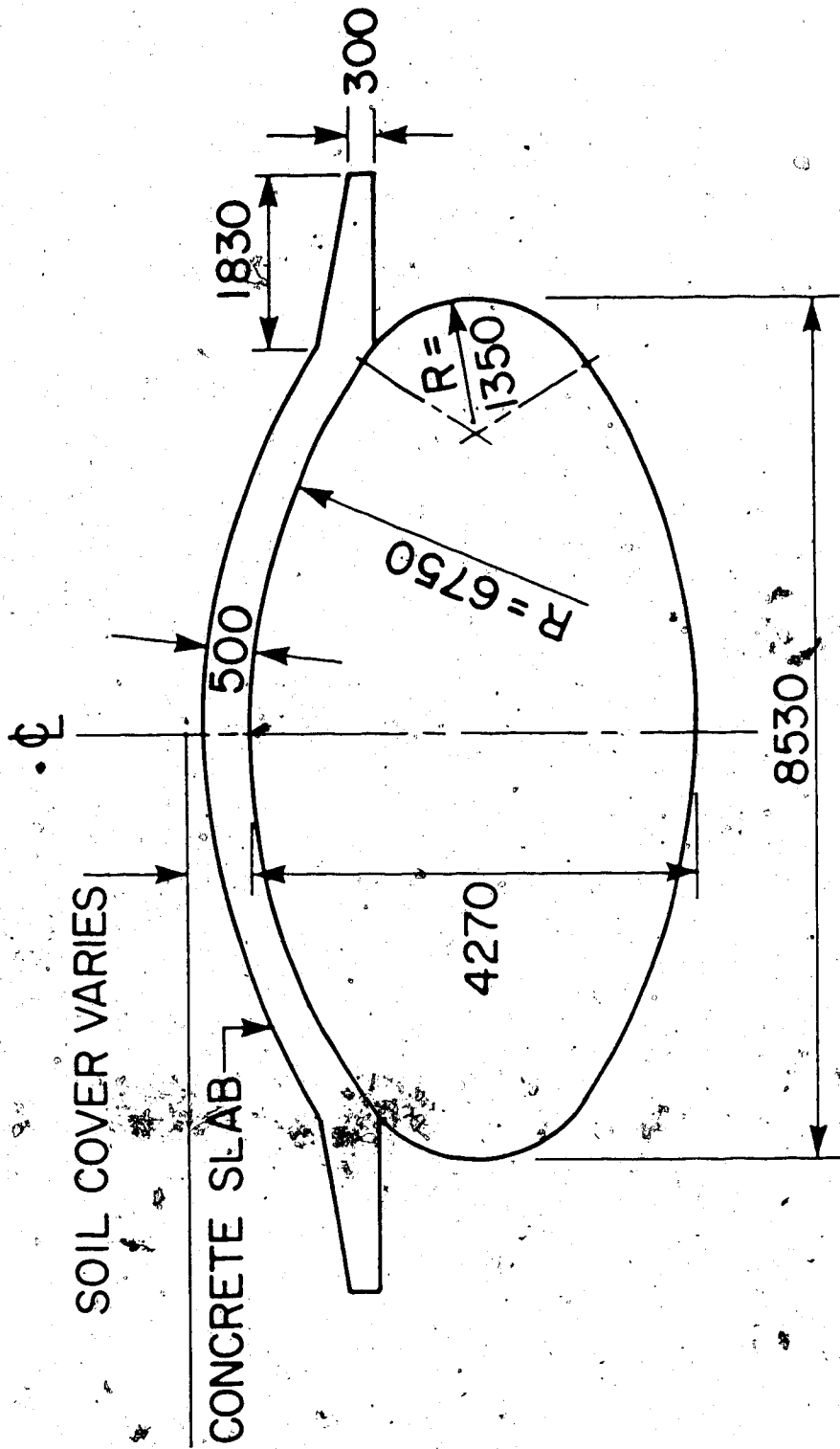


Figure 4.8 Prototype Arch-Beam Culvert Geometry

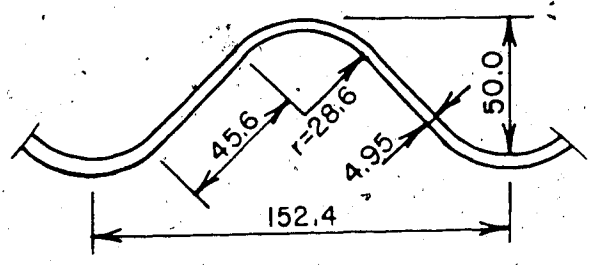


Figure 4.9 Corrugated Culvert Profile

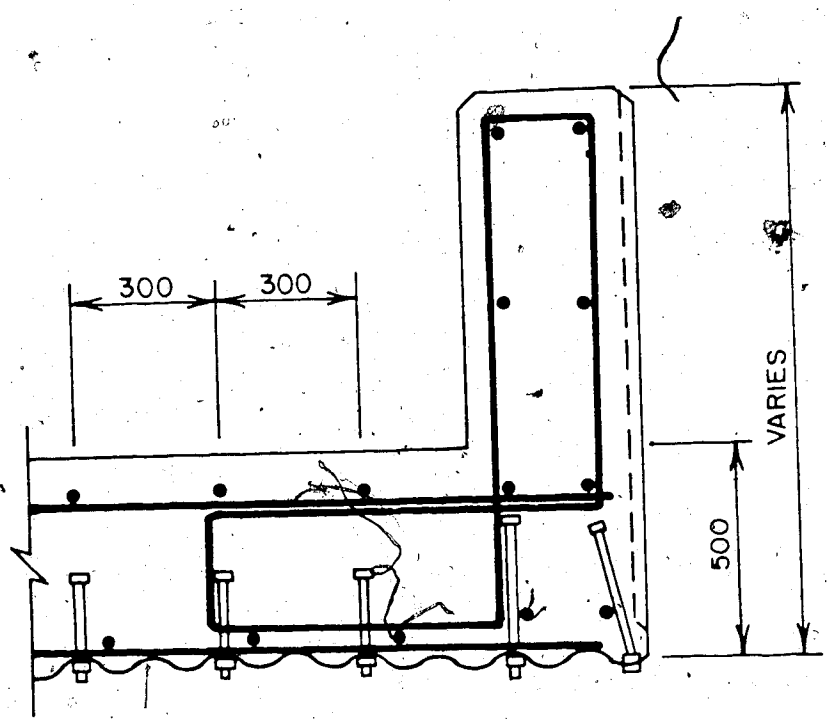


Figure 4.10 Cross-section Through the Composite Culvert

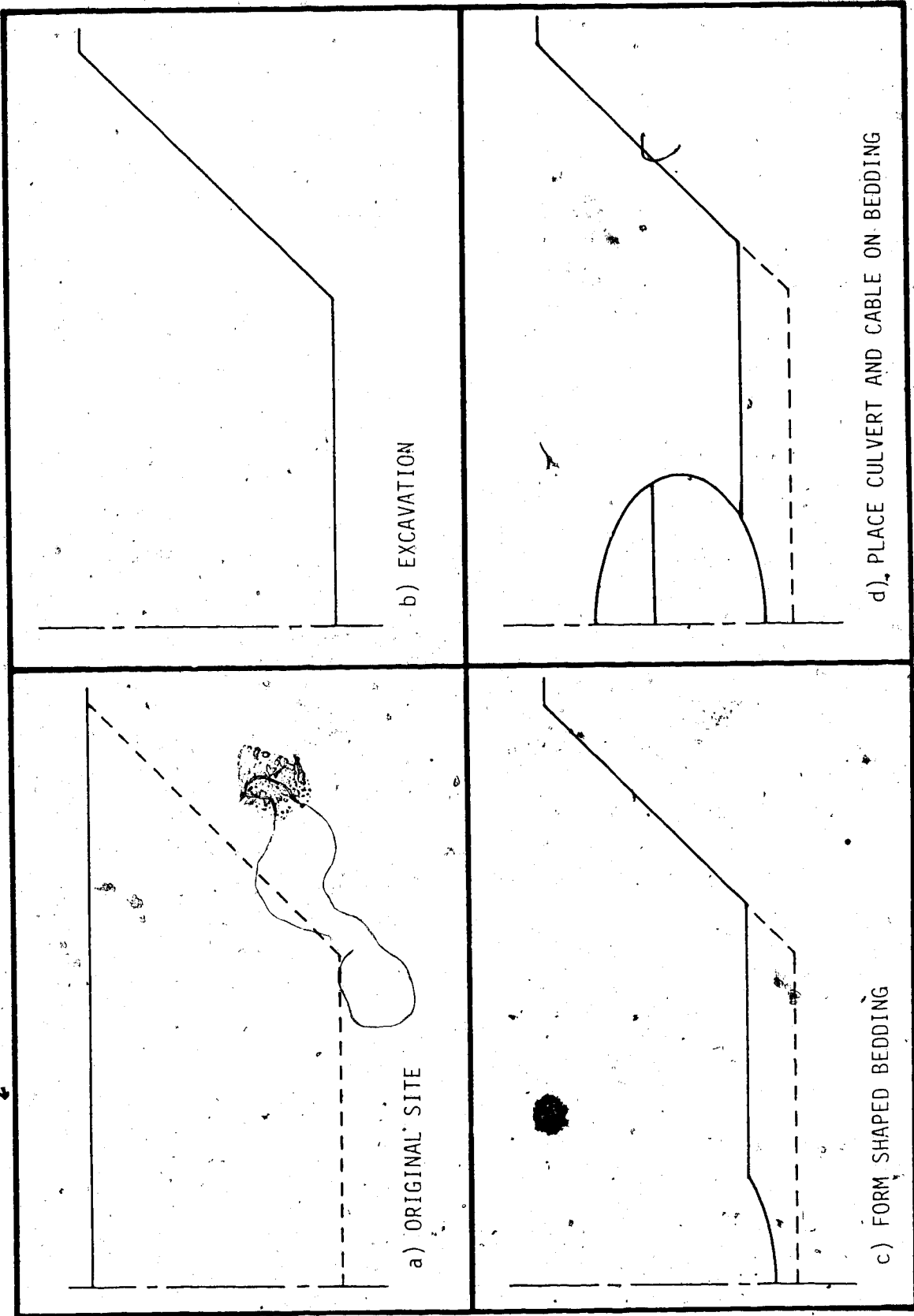


Figure 4.11 Construction Sequence of Prototype

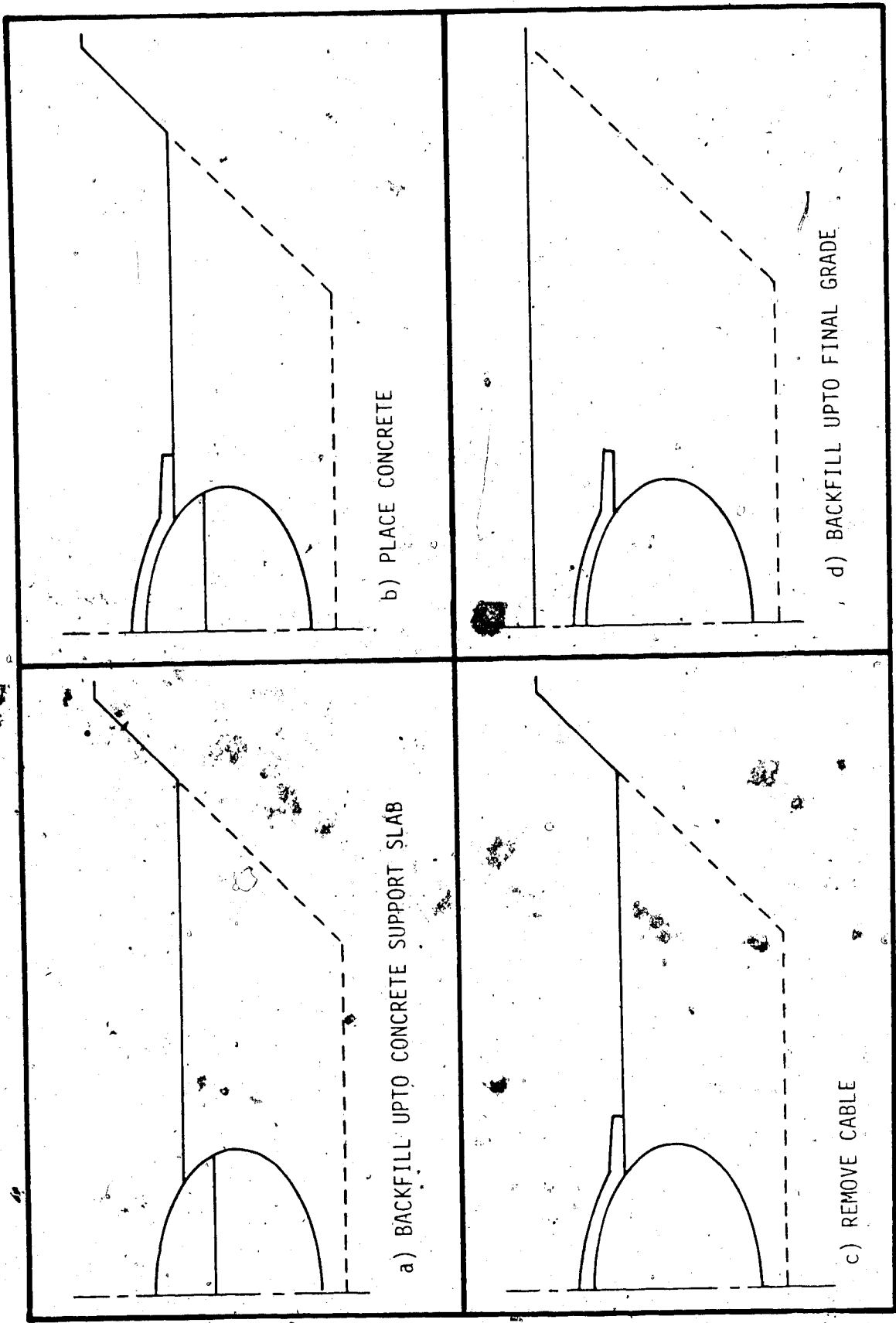


Figure 4.12 Construction Sequence continued

Page 73 omitted in numbering.

#### 4.6 Testing Program

Testing of the structure began during construction. Initial strain and deflection readings were taken when the backfill beside the culvert had been placed to the bottom of the arms. Readings were then taken over the next five days while the reinforcement was installed. Two more sets of readings were taken under dead load, immediately before and after the placement of the concrete.

Two static load test series were conducted after curing of the concrete and the placement of the granular material above the concrete arms. The first test series was conducted seven days after placement of the concrete and with 10 cm of granular material covering the crown. The live load was applied using a self-propelled earthmover straddling cross-section A as shown in Figure 4.13. Strains and deflections were measured under gross axle weights of 311 and 440 kN. At the 440 kN load one wheel of the axle was also positioned directly over cross-section A while readings were taken.

The second test series was carried out 28 days after placing the concrete. The soil cover over the crown of the structure had been increased to 74 cm. This time the load was applied to the structure using two 61 cm by 91 cm H-pile pads at 2.1 m spacing. These H-pile pads were placed straddling cross-section A as it was in the first test series. The steel pads were then loaded using precast concrete bridge deck units. Strains and deflections were

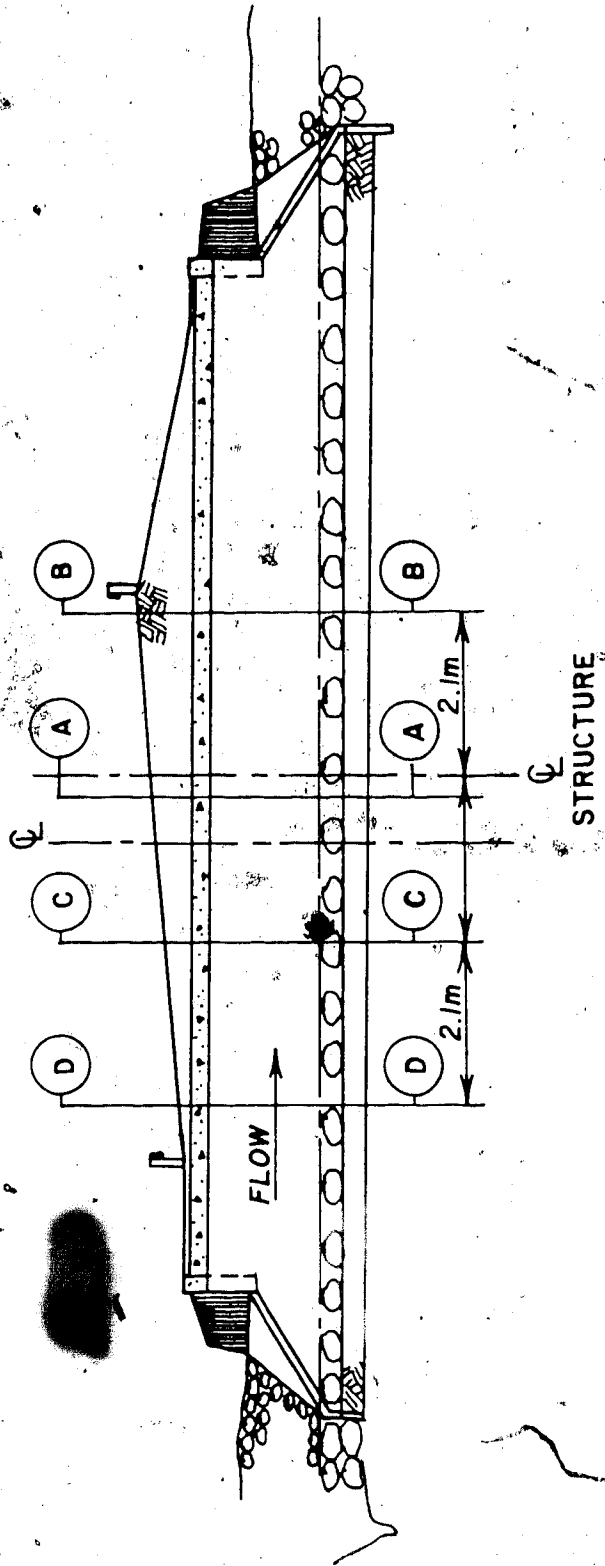


Figure 4.13 Longitudinal Cross-section



measured prior to and after loading as well as at loads of 462, 698, 885 and 1080 kN.

#### 4.7 Summary

The results from these tests are presented in two reports: Blairmore Creek Instrumentation (Summary of Results) [7] and Load-Response Behaviour of Blairmore Creek Arch-Beam Culvert [26]. The first report presents the raw extensometer and load cell readings and the material test information and the second presents the strain gauge reading, relative deflections in the structure and a discussion of the behaviour of the structure.

The interpretation of the results was made difficult because the structure was very stiff resulting in the strains and deflections being very small. The maximum deflection under the applied loads was 1.5 mm downward at the crown of the culvert under the 1080 KN load. The interpretation was further limited because a large number of strain gauges mounted on the corrugated culvert exhibited erratic behaviour or unrealistically large initial strain and were considered to be inoperative.

Where possible a comparison between these test results and the analytical results from ADINA is presented in Chapter 5. For the reasons mentioned above and the limitations of the two-dimensional analysis, the comparison is limited to the general behaviour and the observations during the analysis. As suggested by the Alberta Research

Council Report the effects of reduced soil cover and concrete thickness were also investigated.

## 5. MODELLING OF ARCH-BEAM CULVERTS

### 5.1 Definition of Problem

The analytical modelling of arch beam culverts and the results of these analyses are presented and discussed in this chapter. The behaviour of an arch-beam culvert during construction can be closely approximated by considering a cross-section through the culvert. This permits the structure to be modelled in two dimensions assuming a plane strain condition. The live load applied in the static live load tests on the Blairmore Creek culvert cannot be represented in two dimensions but a series of these loads along the length of the structure can be modelled as a strip load. This strip load is a more severe loading because the load cannot be distributed longitudinally.

Arch beam culverts have two possible principal structural actions in two dimensions, one that it behaves as a one-way slab, and the second that it carries the load in compression as an arch. One of the purposes of the analyses was to determine which of these two structural actions dominate and the possible short term failure mechanisms.

The material features of the structure that were considered to be important in determining the behaviour are the stiffness and nonlinear behaviour of the soil, the cracking of the concrete and the yielding of the steel both in the culvert and in the reinforcement. The geometric considerations that can have a large effect upon the

behaviour are the amount of soil cover, the relative axial and bending stiffnesses of the concrete cross-section and the curvature of the arch.

In this study the shape of the steel culvert was kept constant. Based on the results from the analysis of the prototype structure, constructed at Blairmore, Alberta, it was decided to analyze a second structure with the concrete thickness reduced from 470 mm to 270 mm. The prototype geometry resulted in a very conservative design and a concrete thickness of 270 mm was thought to be the minimum that would be considered for this structure. The amount and location of the reinforcement was changed in the 270 mm section based on the analysis of the prototype structure (Figure 5.1).

With the reduced concrete thickness two crown depths were modelled (Figure 5.2). The first had a crown depth of 1250 mm as in the prototype structure. This permitted a direct comparison between the two structures with only the concrete thickness changed. The second crown depth was 450 mm, which corresponds to a crown soil cover of 150 mm. This would normally be the least soil cover considered in practice.

## 5.2 Structure Nomenclature

The structures described in this chapter can be identified by the following nomenclature. (###C - ####S)

The first number is the thickness of the concrete actually

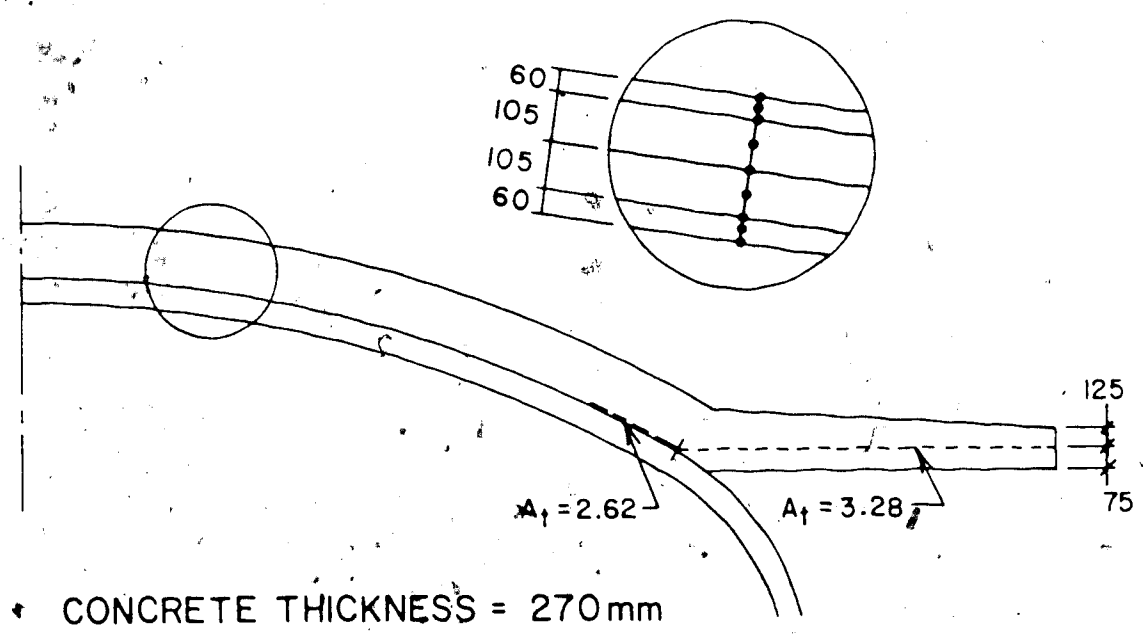
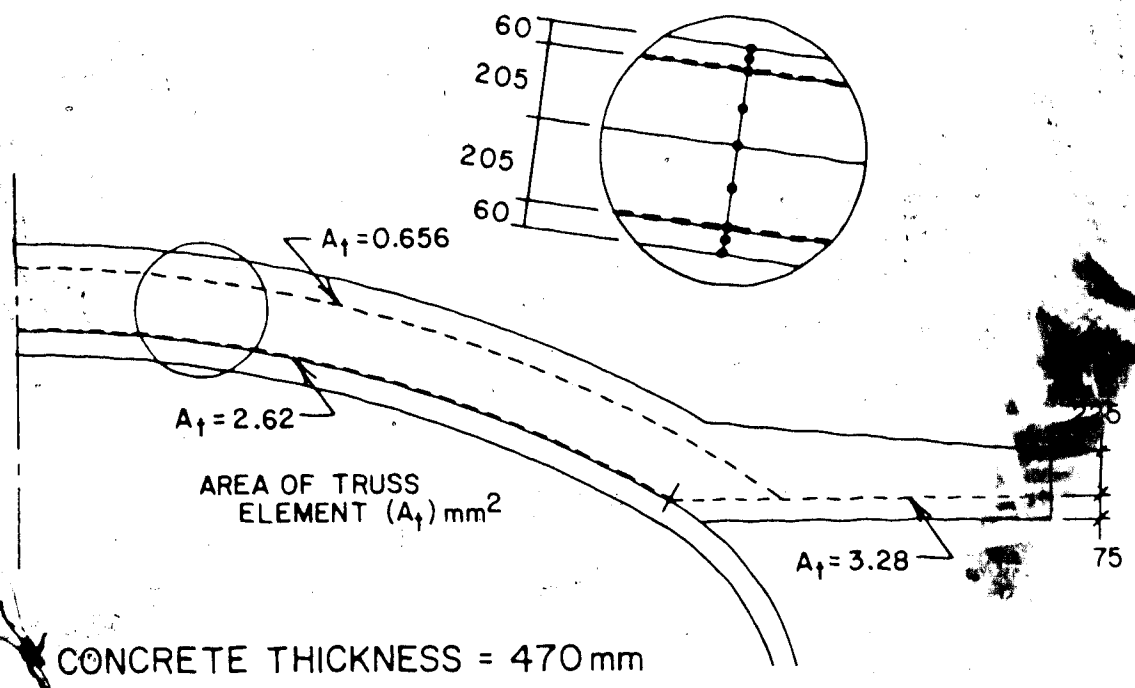


Figure 5.1 Composite Cross-sections used in the Analyses

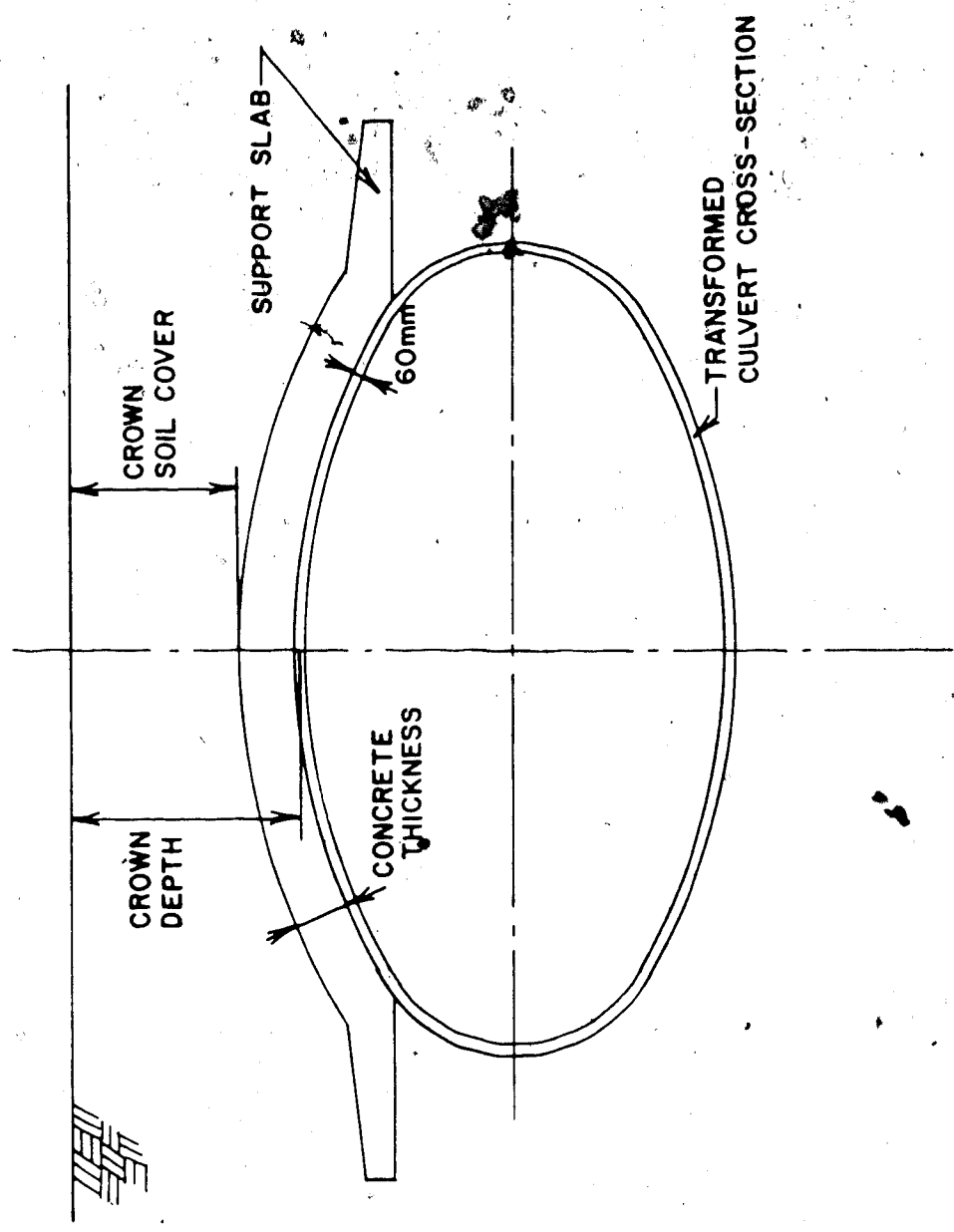


Figure 5.2 Geometry used for Analyses

modelled and the following letter represents the material model used for the concrete: T for Triaxial Concrete Cracking model and D for Drucker Prager yield criterion. The next number is the crown depth as described previously and the letter represents the material model used for the soil: D for the Drucker Prager yield criterion and E for the Linear Elastic model.

For example structure (470D - 1250D) is the prototype structure with the modelled concrete thickness of 470 mm, crown depth of 1250 mm and both the concrete and soil are modelled using the Drucker Prager yield criterion.

### 5.3 Development of the Mesh

The finite element mesh used in all analyses of the prototype geometry is shown in Figure 5.3. To allow for changes in the concrete thickness, the elements representing the concrete in this mesh were reduced in thickness. The thickness of the top two layers of elements were reduced when the crown depth was changed. The final mesh is a result of changes to accommodate various modelling procedures and refinements to the mesh in areas of high stress and where high strain gradients occur. The greatest changes to the mesh were to accommodate the method used to place the soil around the culvert. A previous mesh used layers of soil that followed the contours of the arch. This resulted in slope failures in the soil when the layers of soil were placed. The mesh was then changed to the present one with horizontal

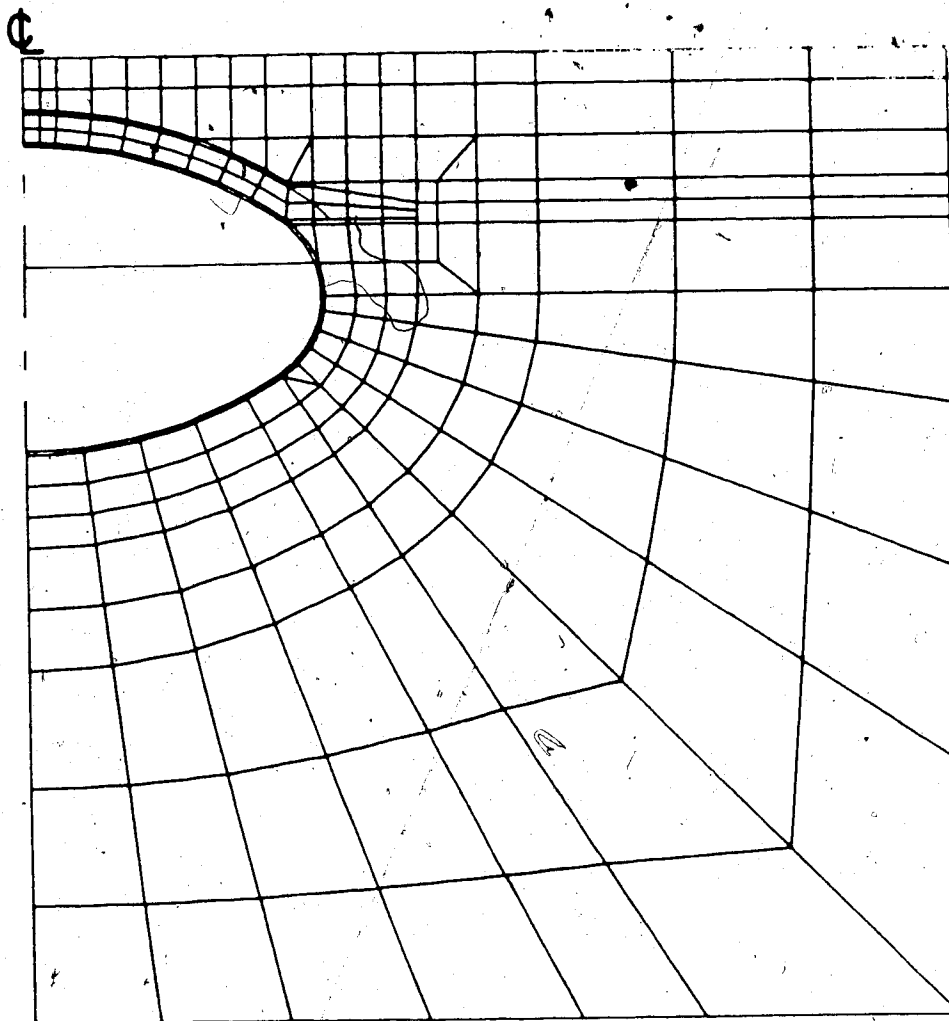


Figure 5.3 A Typical Finite Element Mesh



layers of soil.

In all cases the mesh was two-dimensional and had its stiffness formulated using plane strain constitutive matrices. The soil was modelled using quadratic serendipity elements near the structure and linear two-dimensional solid elements away from the structure. This allowed a large reduction in the number of degrees of freedom required. Compatibility was always maintained within the soil by using transition elements. These elements have some of their nodes and therefore degrees-of-freedom eliminated.

The steel culvert was modelled using 22 quadratic serendipity elements. Some of these elements have aspect ratios as large as 15. A series of auxiliary runs involving single element cantilever beams, with aspect ratios up to 15 and with varied orders of integration, were conducted to determine the error in the elastic response. It was found that if a 2x2 order of integration was used the error is less than 2% even with an aspect ratio equal to 15.

The concrete was modelled as three quadratic elements through the section to allow for progression of cracking and to allow the reinforcement, modelled as quadratic truss elements, to be placed along the boundary between two of the layers of elements. Two areas of discontinuity were introduced into the mesh as shown in Figure 5.4. In the first, the truss elements do not follow the boundary between the two-dimensional elements at the intersection between the arch and the support slab. The second discontinuity is at

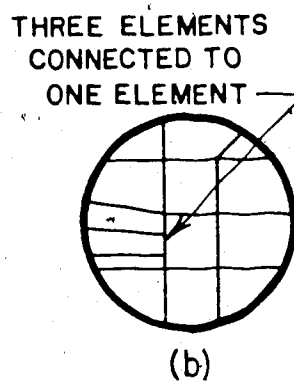
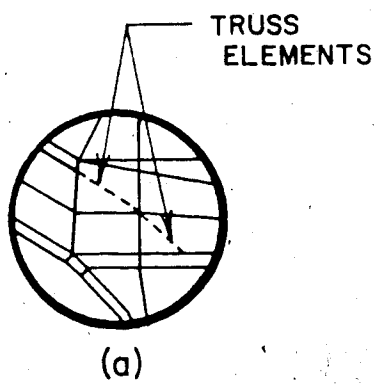
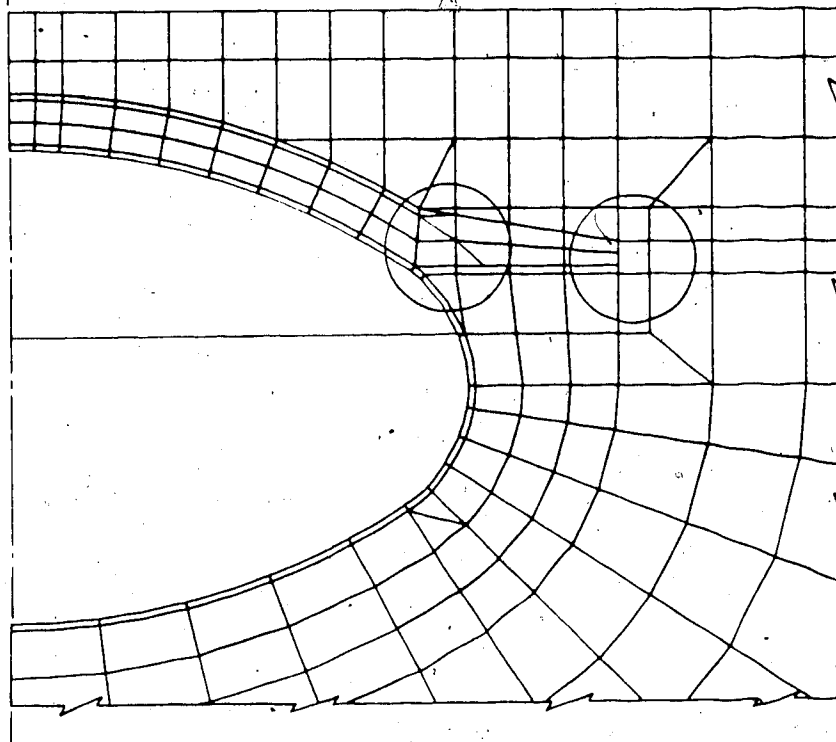


Figure 5.4 Discontinuities in the Finite Element Mesh

the end of the support slab where the three elements in the slab join with one element in the soil. This is to eliminate the need to refine the mesh near the end of the concrete slab.

#### 5.4 Determination of Material Parameters

The units used throughout the analysis were millimeters and newtons with the resulting units of stress of megapascals. The reinforcement was assumed, as in the design of the prototype, to have a yield stress of 300 MPa and a Young's modulus of 200,000 MPa. The area used for the truss element was calculated by taking the area of reinforcement per millimeter because ADINA formulates the stiffness of the plane strain elements on a structure having a unit thickness.

The steel for the corrugated culvert was assumed to have a yield stress of 300 MPa, a Young's Modulus of 200,000 MPa and a Poisson's ratio of 0.3. These material properties were transformed to an equivalent rectangular cross-section because a two-dimensional solid element, with a rectangular cross-section, was used to model the culverts corrugated cross-section. The transformation ensures that the elastic stiffnesses, plastic axial force and first yield moment of the transformed rectangular section are the same as the original corrugated section. The method used is described by the formulae given in Appendix D. The resulting transformed properties are Young's modulus of 20380 MPa,

Poisson's ratio of 0.3, yield stress of 23.85 MPa and a section depth of 60.0 mm.

The soil was the material for which it was the most difficult to determine material properties and the corresponding material model parameters. The only information received from Alberta Transportation on the soil was that the backfill material was a coarse granular backfill with the grain size distribution shown in Figure 5.5. This material was to be compacted to 100% modified proctor; however this degree of compaction could not be obtained near the flexible culvert.

The Curve Description model was not used to model the soil because there was not enough information to determine applicable loading and unloading bulk modulus and shear modulus curves. The nonlinear material model chosen was the Drucker Prager yield criterion. The material parameters required to determine the material behaviour are Young's modulus, Poisson's ratio, the angle of internal friction and the material's cohesion. All of these parameters can be assumed by taking published values for a well compacted granular material. After reviewing many papers in which soil properties were discussed the values were chosen from Bowles [11, 12]. The range of values given by Bowles for a dense granular material were Young's modulus of 80.0 - 200.0 MPa, a Poisson's ratio of 0.2 - 0.4 and an internal angle of friction  $35^{\circ}$  -  $50^{\circ}$ . The values chosen for the soil parameters were, a Young's modulus of 80.0 MPa, a Poisson's

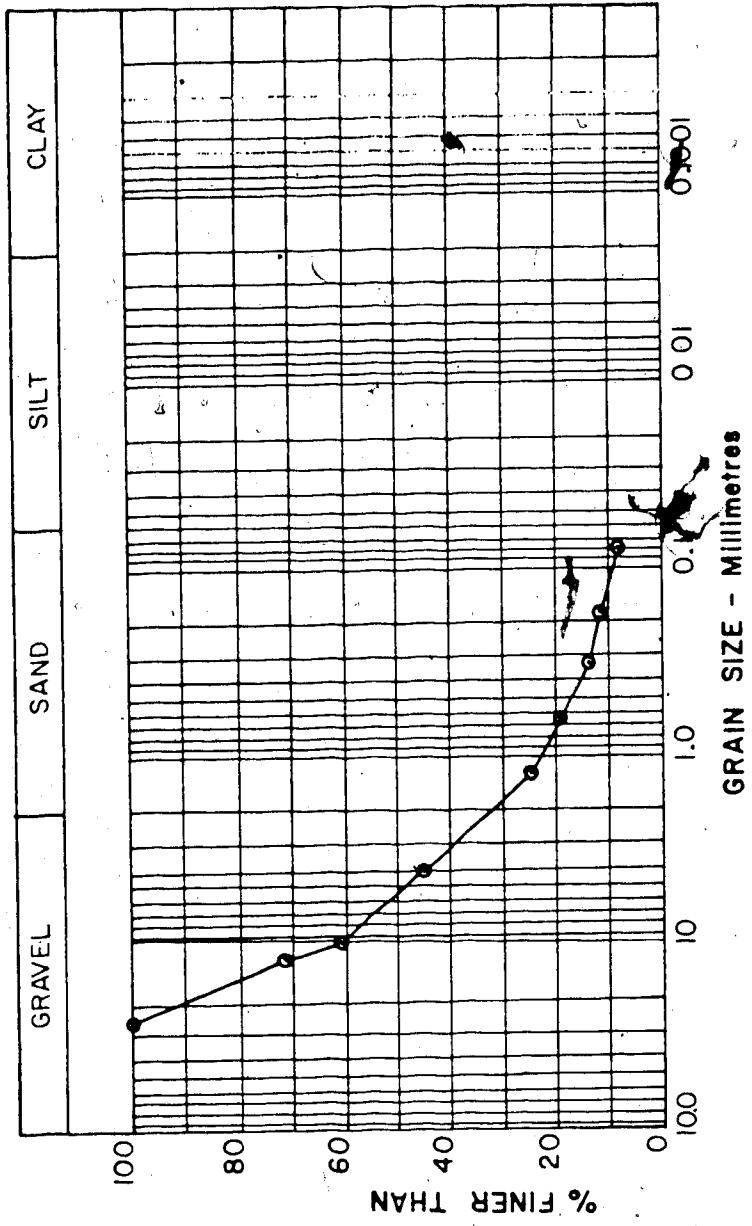


Figure 5.5 Grain Size Distribution for Backfill Material

ratio of 0.3, an internal angle of friction of  $35^\circ$  and a cohesion of 0.015 MPa. The values for the cap hardening parameters, described in Chapter 2, were initially  $\eta = 0.0737$ ,  $D = 0.004 \text{ 1/MPa}$  and  $\sigma_{I_1}^{a'} = 0.0$ .

The cap hardening feature was later eliminated by setting the initial position of the cap at 100 MPa. With the method of modelling used it was not necessary to have the soil remold during construction. The remodeling essentially moves the cap position past where it would have any effect upon the structure after construction. The cap hardening also causes the soil to have a negative effective Poisson's ratio upon initial loading. This is inherent to the model so that the hysteresis effect can be modelled.

The concrete used in the prototype structure was tested at 7 and 14 days to determine its uniaxial compressive strength of 26.3 and 29.7 MPa respectively. This value gives some insight into the strength. However, for the Triaxial Concrete Cracking model the triaxial failure surface and nonlinear stress-strain behaviour must be input. This is more information than would usually be known, therefore values must again be assumed. The initial Young's modulus was assumed to be given by the formula in CAN3-A23.3-M77.

$$\tilde{E}_0 = 5000 \sqrt{f'_c}$$

(5.1)

The maximum stress was assumed to occur at 0.002 strain while the ultimate strain was assumed to be 0.003 and the corresponding stress equal to  $0.85 f'_c$  as suggested by Whitney's stress block. The uniaxial tension stress allowed was calculated using equation 5.2 (CAN3-A23.3-M77).

$$f_r = 0.6 \sqrt{f'_c} \quad (5.2)$$

In addition to the above uniaxial parameters it is necessary to define the triaxial failure surface, values for this were taken from the literature. After reviewing the possible range of results obtained from triaxial tests conducted by Kahn and Saugy-[3] Launay et al [29] and Kupfer et al [28] it was decided that the failure surface determined by Kahn and Saugy (Figure 2.8) was conservative and for lack of specific information represented the best results available.

The other model used for the concrete was the Drucker Prager yield criterion. This model required only the elastic Young's modulus and Poisson's ratio to define the stress-strain behaviour up to failure. The yield surface required the calculation of  $\alpha$  and  $K$ . This calculation was done by taking the discrete points input to the Triaxial Concrete Cracking model and calculating the values of  $\bar{S}$  and  $I_1^a$  then performing a least squares fit to determine the y-intercept  $K$  and the slope  $3\alpha$  (Figure 5.6). The initial cap

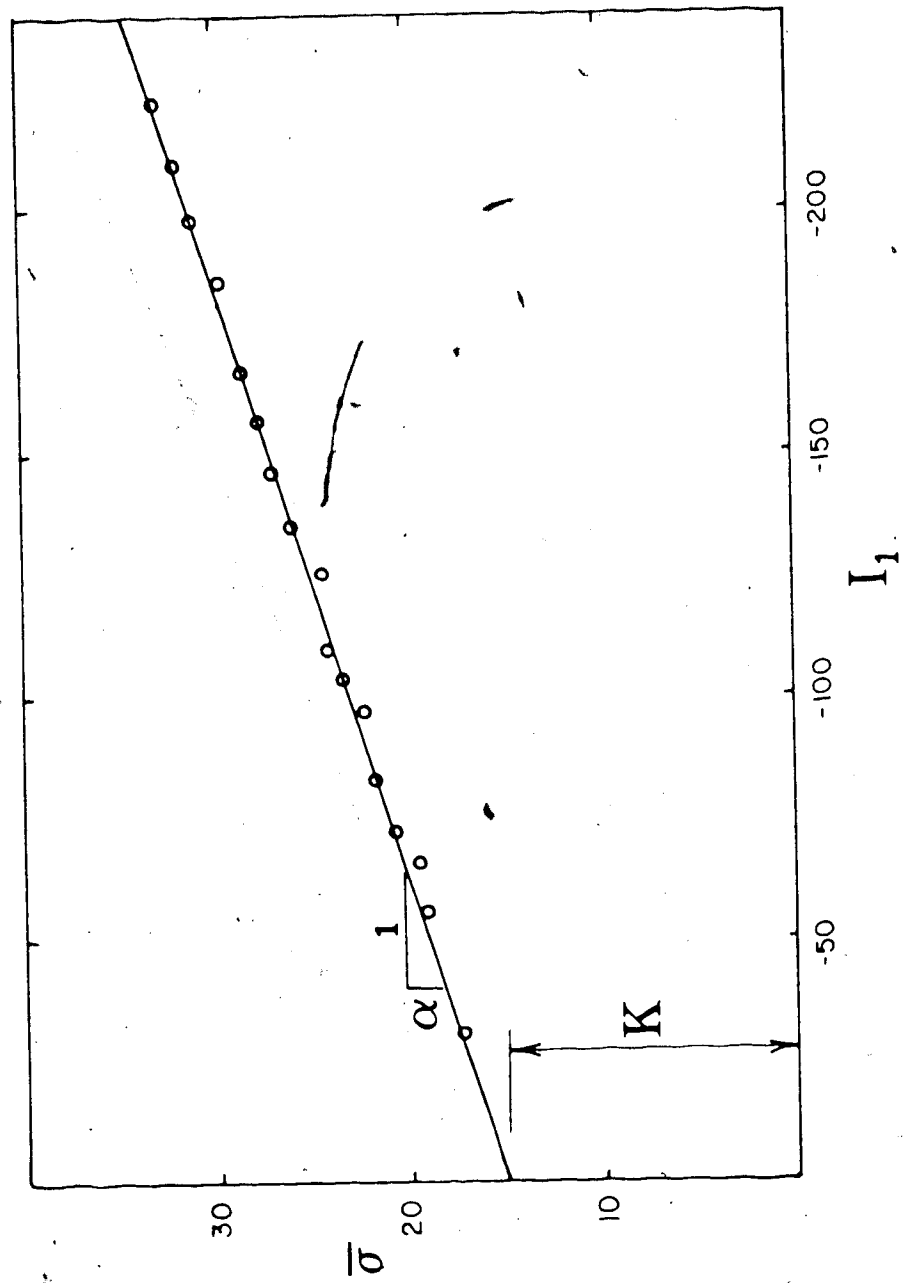


Figure 5.6 Drucker Prager Yield Surface for Concrete



hardening position was set to a large value so that it would have no effect. The tension cut-off stress in this model was set to the same value as in the Concrete Cracking model.

### 5.5 The Triaxial Concrete Cracking Model

The Triaxial Concrete Cracking model had initially been used for the concrete in the analyses but a problem occurred with ADINA formulating a nonpositive definite stiffness matrix. This occurred when the second last layer of soil elements was being formed in the construction modelling. At this point in the analysis all of the material stiffnesses were positive at all of the gauss points within the structure, the order of integration was sufficient and the boundary conditions were sufficient to prevent a rigid body displacement.

The error message given by ADINA at the time is shown below and all of the suggested possible causes listed with the error message were checked.

```
*** STOP STIFFNESS MATRIX IS NOT POSITIVE DEFINITE ***
```

```
NONPOSITIVE PIVOT FOR EQUATION XXX  
PIVOT = -X.XXXXE+XX
```

Depending upon the material model used for the soil and method of construction the equation number and the value of the pivot changed.

A series of runs indicated that the Triaxial Concrete Cracking model was involved. The entire structure was

modelled using the linear elastic material model and no problems were encountered. With only the material model for the concrete changed the nonpositive definite stiffness matrix occurred. This problem could not be reproduced in isolation using a four element mesh. It was concluded that the problem involved the Triaxial Concrete model in combination with another option used to model the construction. The correction for the collapse of rectangular elements to triangular elements could also be involved. When this option was not used in later runs with the reduced concrete thickness a change in the soil material model from Drucker Prager to Linear Elastic eliminated the problem. This phenomenon has never been fully explained.

## **5.6 Method of Analysis**

### **5.6.1 Modelling of Construction**

The method used to model the construction of an arch beam culvert follows closely the construction procedure used in the field. The basic stages in the actual construction are; excavation of the channel to receive the culvert, placing of the culvert with the erection cables, placing of soil beside the culvert up to the level of the support slab, placing of the wet concrete and placing of the soil above the hardened concrete. While following this procedure in the analysis, certain deviations were made to simplify the analysis procedure or to overcome some limitation in the

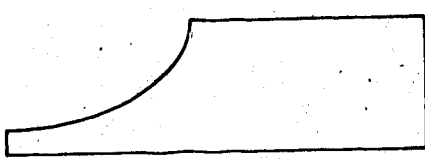
program.

The six mesh configurations used to model the stages of construction are presented in Figure 5.7. To obtain a complete solution for each structure, sixteen time steps were required to model the construction sequence. These steps are summarized in Figure 5.8 and are discussed below.

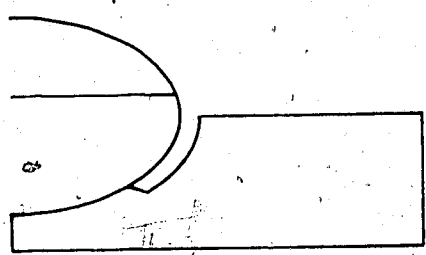
The first deviation from the actual construction procedure was that the excavation of the soil to form the stream bed was not modelled. Instead, the first step was to form the mesh up to the point shown in Figure 5.7a and apply the gravity load so that this soil mass deflected under its own weight. Modelling the excavation procedure would add a large number of degrees of freedom, add a number of time steps to the analysis and have little affect on the final results.

Once the soil mass has deflected the layer of soil below the culvert, the culvert and the support cable are formed and allowed to assume their equilibrium position resting on the bedding. If the elements representing the soil to be placed beside the culvert are just added using the element birth and death option, the soil elements will undergo very large strains because the culvert is very flexible. These strains are sufficient to cause numerical instabilities when using a nonlinear soil model.

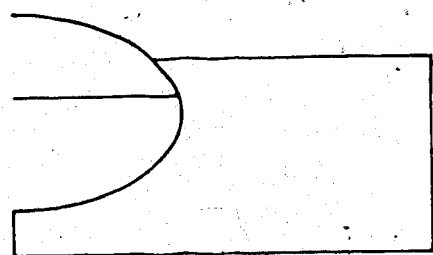
To overcome the numerical problems caused by yielding in the soil, the placing of this soil was modelled using the preload method. With the culvert in place a linearly varying



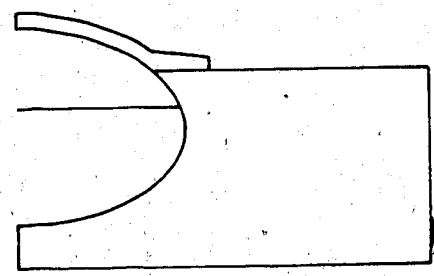
a) FORM SOIL MASS



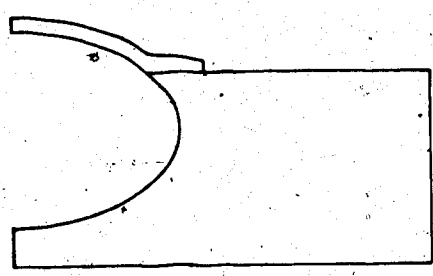
b) PLACE CULVERT AND CABLE ON BEDDING



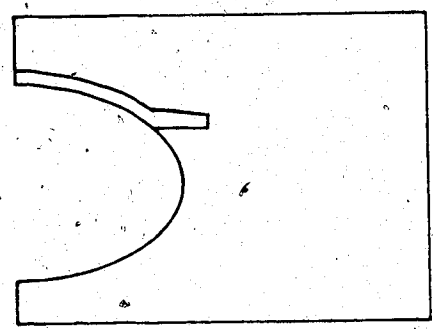
c) FORM SOIL ELEMENTS NEXT TO THE CULVERT



d) PLACE CONCRETE



e) REMOVE CABLE



f) FORM SOIL ELEMENTS UPTO FINAL GRADE

Figure 5.7 Mesh Progression During Costruction

TIME STEP	DESCRIPTION
1.0	Form soil mass with self weight.
2.0	Form culvert with cable and bedding.
3.0	Apply lateral preload used to place the soil next to the culvert
4.0	Form soil elements in the gap beside the culvert and remove that part of the preload.
5.0	Form soil elements upto the support slab and remove the remaining preload.
6.0	Apply a portion of the preload used to place the concrete.
7.0	Apply remaining concrete preload.
8.0	Form hardened concrete elements and remove the preload.
9.0	Remove the erection cable.
10.0	Apply a portion of the preload used to place the soil beside the support slab (layer #1)
11.0	Apply the remaining portion of preload #1
12.0	Form layer #1, Remove preload #1, Apply preload #2
13.0	Form layer #2, Remove preload #2, Apply preload #3
14.0	Form layer #3, Remove preload #3, Apply preload #4
15.0	Form layer #4, Remove preload #4, Apply preload #5
16.0	Form layer #5, Remove preload #5
-	Construction finished

Figure 5.8 Description of the Time Steps used in Modelling

lateral pressure was applied to the culvert as shown in Figure 5.9a. The magnitude of this preload, determined by trial and error, was sufficient to lift the crown slightly above its original position. The resulting preload was approximately 80% of the at-rest lateral pressure of the soil. The next step is to add the elements beside the culvert and remove the preload. The culvert then settles and applies a load to the soil.

To determine the effect of the distribution of the preload used, a second distribution was tried and the two resulting pressure distributions are shown in Figure 5.9. While there are some differences in the final pressure distributions, they both have the same general shape and magnitude. The final distribution of pressure is therefore not sensitive to the initial distribution of the preload.

The next stage in the analysis is to place the concrete in such a way as to have the weight of the cast concrete carried by the culvert in conjunction with the cable and the soil and not by the concrete itself. Once again the preload method was used. The distribution of the preload is equal to the depth of concrete multiplied by the concrete density as shown in Figure 5.10. The preload is then removed and the concrete elements added with their own weight and final stiffness. The result is that the culvert is carrying the concrete and the concrete elements are essentially stress free.

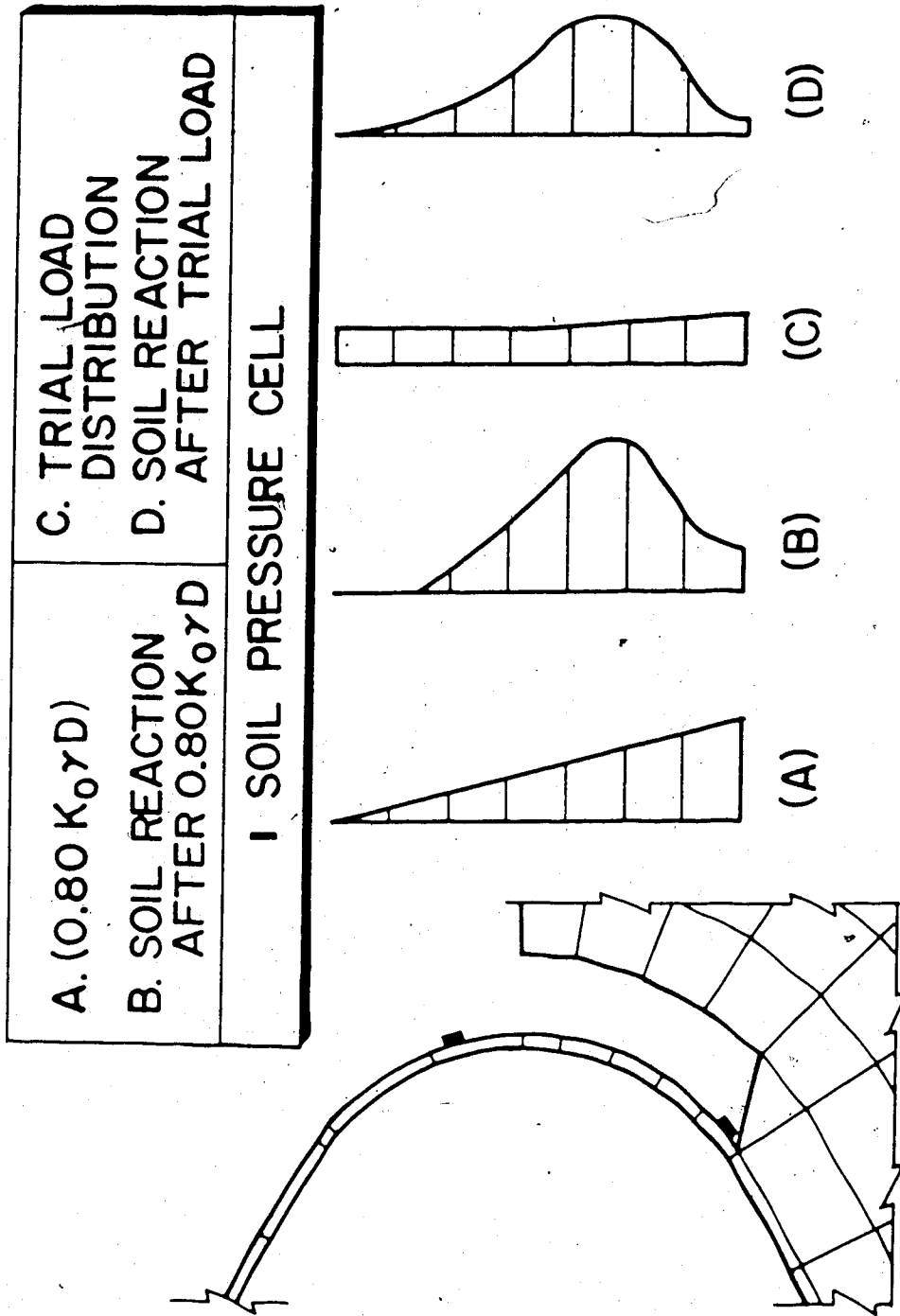


Figure 5.9 Distribution of Lateral Preload Pressure

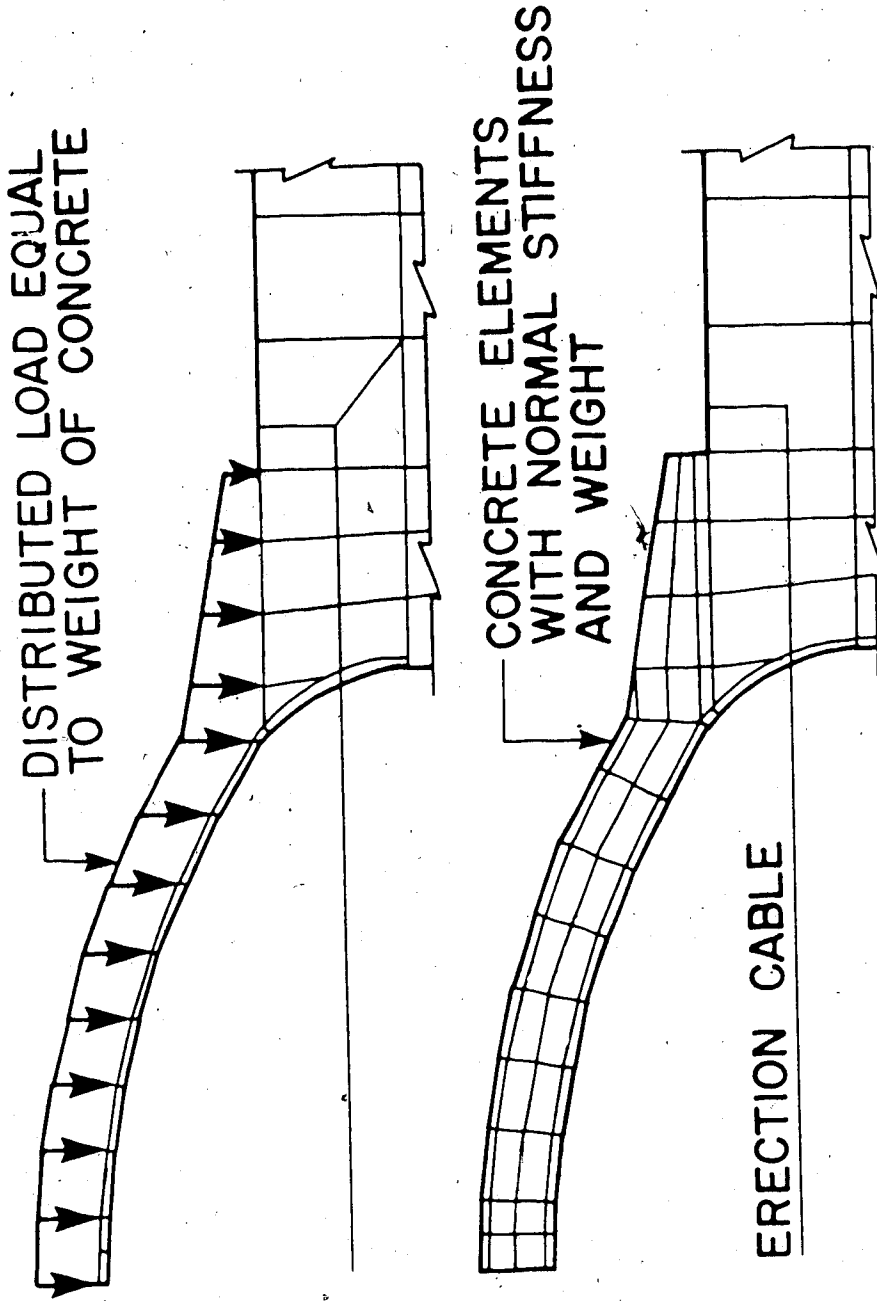


Figure 5.10 Preload used to Place Concrete



The final stage in the construction process is to place the soil above the concrete. The first attempt at modelling was to add all of the elements in a single time step. No numerical problems were encountered but the final stresses in the soil included zones of tension and yielding near the soil surface.

The soil elements were added in layers to simulate the placing of lifts of soil. No problems were encountered placing the first layer beside the support slab but there were zones of tension failure in the soil element adjacent to the concrete. In attempting to add the next layer, ADINA was not able to converge to a solution. This was due to the differential settlements in the underlying layers causing tensile stresses in the top layer of soil elements.

This led to another application of the preload method. The first variation tried involved placing a preload equal to the weight of all the soil to be placed on the structure. The preload is applied to the existing structure and then, as each layer of elements is added the preload is reduced by the weight of this layer and moved to the new surface. This method worked well and the resulting stresses in the soil were reasonable. However, this method forces the dead load of the soil, represented by the preload, to be carried by beam action because the soil was not present to provide the horizontal reaction required for arching.

The next preload method used a preload equal to the weight of the next layer of elements to be added. The

preload is applied in one time step then the next layer of elements is added as the preload is removed. This reduced the effect of the differential settlement but ADINA could not converge to a solution.

This was overcome by using a preload equal to the weight of the next layer of elements but the next preload is placed on the structure at the same time as the preload for the present layer of elements is removed. This kept a net compressive stress in the top layer of elements and increased the stability of the Drucker Prager model used for the soil that included a tension cut-off.

### 5.7 Live Loadings

The AASHTO code [35] provides two types of highway loadings. These loadings are termed M and MS loadings, where the MS loadings are heavier than the M loadings. These two classifications of loadings consist of standard trucks and lane loading which are equivalent to truck trains.

In the design of the prototype an MS30 loading was used. The "30" represents the magnitude of the single axle load  $W$  equal to 300 KN. The resulting point loads for the standard truck are shown in Figure 1.2.5c of the AASHTO code. The lane load considered is a single line load across a traffic lane with a total magnitude equal to  $0.65W$  and a uniform load of  $0.05W$  per meter length of roadway. These loadings are applied to each lane of the highway. The width of a design traffic lane is 3.658 m (12 ft) and the standard

truck or lane loading having a 3.048 m (10 ft) width is placed within the traffic lane to produce the maximum stress.

These loadings are modified to allow for multiple lane loads and impact loading. The load is reduced for multiple lanes by 10% when there are three lanes and by 25% for four or more lanes. Impact load is determined for culverts depending upon the soil cover. The impact load is 30% of the live load when the soil cover is less than 0.305 m (1 ft), 20% when the soil cover is between 0.305 (1 ft) and 0.610 m (2 ft) and 10% for culverts with cover up to 0.889 m (3 ft). When the cover is greater than 0.889 m (3 ft) impact loading is not applied.

The loadings as applied to the analyses included both the design truck and lane loadings. The design truck load was modified to cause a more severe case at the centerline of the structure. The front two axles of the truck were both placed above the centerline as a patch load extending 1.0 m in the direction of the roadway and across the 3.048 m design traffic lane. The resulting pressure on the surface is 0.898 MPa without the impact loading being applied. The impact loading for the crown soil cover in the prototype geometry is 10% while the structure with the reduced soil cover has an impact load of 30%. The resulting load was not modified for multiple lane loads though the two-dimensional analysis caused the structure to act as though the culvert had this load applied along its entire length.

The lane loading was applied in a similar manner with the line load applied on the 1.0 m x 3.048 m patch at the centerline as in the design truck load. The distributed load was applied to the entire surface of the model.

A second load case with the patch load next to the support slab would result in a greater shear force in the concrete and this would also have been a more severe case for the soil supporting the concrete. It was not included in the analyses because it makes the analysis non-symmetric and would require the entire structure to be modelled.

## 5.8 Results of Analysis Using ADINA

### 5.8.1 Elastic Analysis

The first run with every geometry was a preliminary elastic analysis. These runs included modelling of the construction procedure, as it would be done in the inelastic analyses, and the application of some live load. These analyses ensured that the modelling procedure worked as expected and that the preloads and live load were applied correctly.

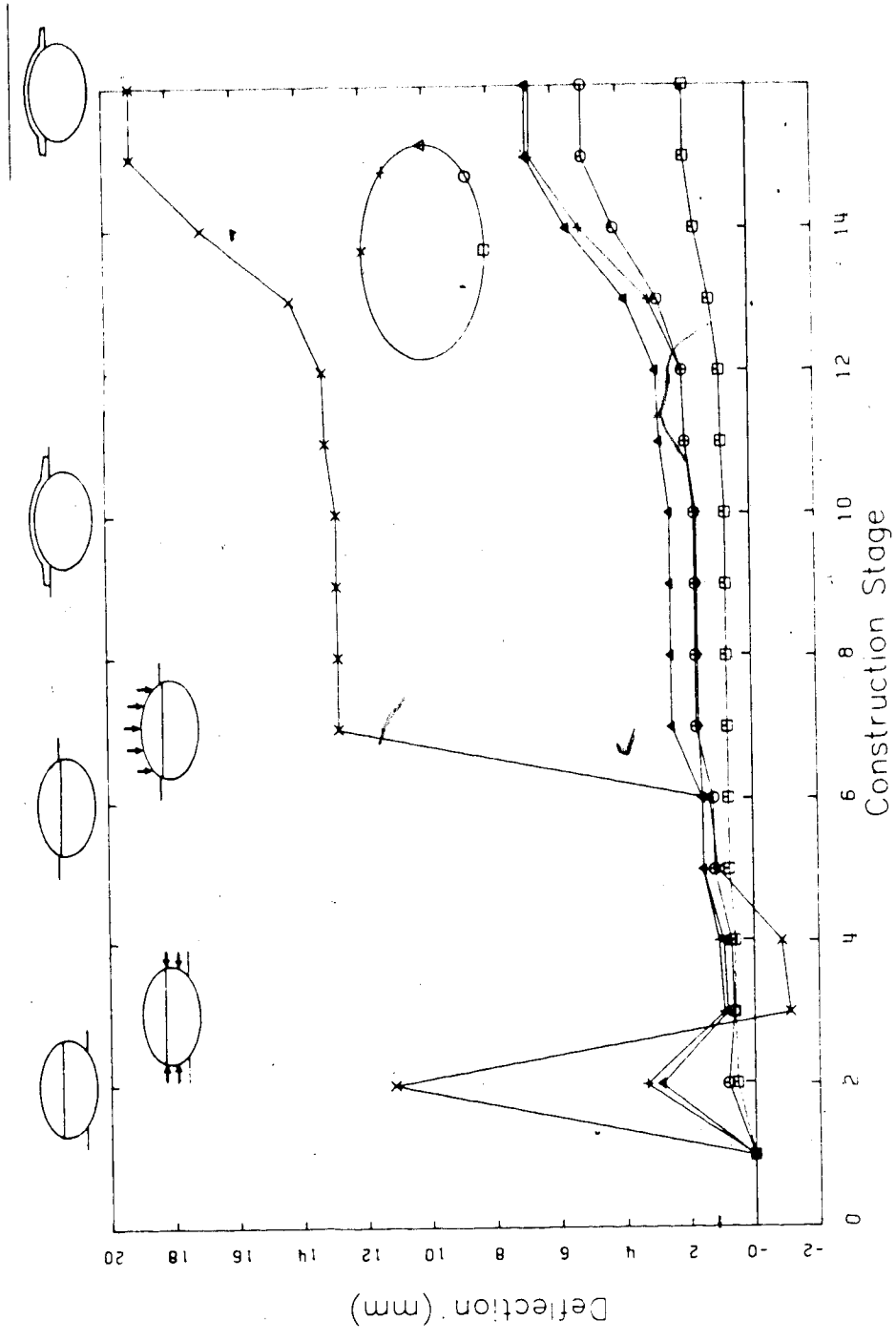
The results from this analysis that are of interest are that only small areas of the soil were in tension at some intermediate construction steps. This indicates that the preload method did eliminate the large areas of yielding and tension that would cause an instability. However, there were tensile stresses in the soil above the support slab when

live load was applied. These stresses would not occur in the actual structure because the soil cannot carry tension. The same is true of the concrete at higher load levels. For these reasons a nonlinear analysis using more realistic material models is required.

### 5.8.2 Nonlinear Analysis

For the prototype structure (470D - 1250D) and the structure with the reduced concrete thickness (270D - 1250D) a material nonlinear analysis was conducted. This included modelling of the construction and the application of both a lane load and the truck load as described in Section 5.7. The material models used were the von Mises yield criterion for the culvert and the reinforcement and the Drucker Prager yield criterion for the soil and concrete, with their appropriate material properties. Initially the Triaxial Concrete Cracking model was used in some analyses but because of the problems described in Section 5.5. it was replaced by the Drucker Prager yield criterion.

With both geometries the construction was modelled as described in Section 5.6.1. The general behaviour of the steel culvert during the construction is illustrated by the deflections at five points on the steel culvert (Figure 5.11). The crown deflection is initially downward but with the application of the preload used to place the soil next to the culvert the crown deflects upward. The magnitude of the preload was chosen so that the crown would



Deflections during Construction

Figure 5.11 Vertical Deflections of Steel Culvert During Construction

be in its original position prior to placing the concrete. This matched the method used in the field because the compaction was controlled so that the culvert had its original geometry prior to placing the concrete.

The axial force and bending moment diagrams for the steel culvert for the construction stages corresponding to the culvert supported on the bedding with the erection cable, prior to placing of the concrete with the soil placed up to the support slabs and after the concrete has been placed are shown in Figure 5.12. These forces in the culvert are of interest when trying to understand the behaviour; however all stresses in the culvert were less than 15% of the yield stress.

During construction, the largest moment in the culvert occurred when the culvert was supporting its own weight. This moment occurred at the point where the soil is no longer supporting the culvert. As construction progressed the position of the maximum moment moved to the new point at which the culvert was no longer in contact with the soil. Placing of the soil beside the culvert increased the axial force in the top arc only slightly because it is still only carrying its own weight. The increase in lateral load is carried by both the lower arc of the culvert and by the soil. The bending moments are reduced at this stage as would be expected because the culvert should be in a position closer to its fabricated geometry.

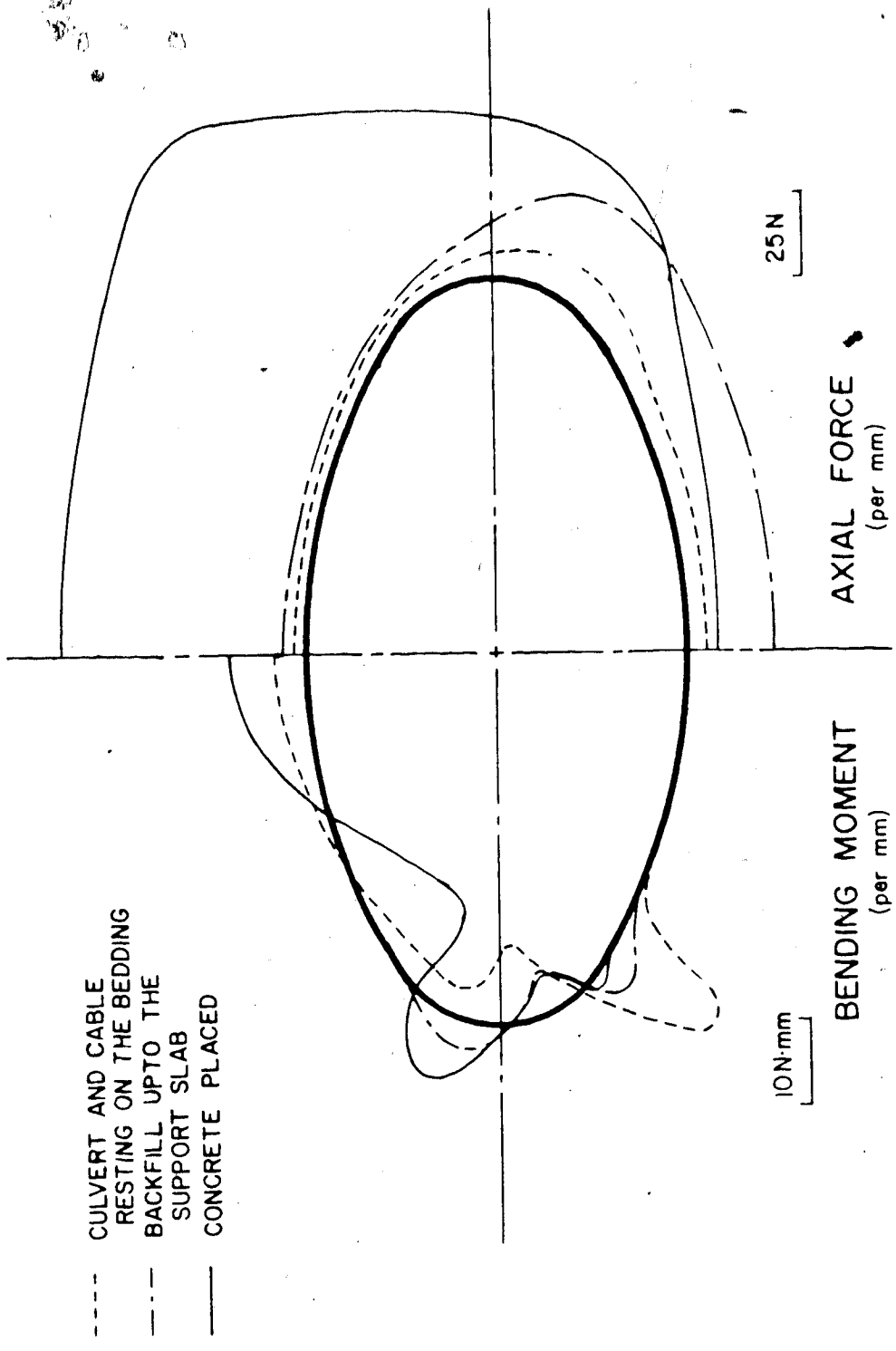


Figure 5.12 Axial Forces and Bending Moments in the Steel Culvert (470D - 1250D)



Placing of the soil beside the culvert resulted in the crown being slightly above its original geometry. This could have been adjusted but the stresses in the culvert were small and the change would have little effect on the final results. The soil pressure on the culvert at this stage of construction was less than the lateral at-rest pressure and therefore the soil beside the culvert must mobilize some of its own strength to carry its weight.

Placing the weight of the concrete onto the culvert caused a large increase of the axial force in the top arc of the culvert. This increased force is removed from the culvert by the soil beside the culvert. This increase in radial stress in the soil causes an outward settlement and the axial force in the bottom arc is reduced. This would not have occurred had it been possible to model the interface between the culvert and soil been model as a friction free surface.

The crown deflection obtained from the analysis under the weight of the cast concrete was less than observed in the field. This was attributed to the fact that the soil modelled at the spring line had initial properties of compacted soil and the soil near the culvert in this region could not be compacted to 100% proctor because the culvert was very flexible. Once the structure has been constructed this soil should have properties close to those given for the rest of the soil. ADINA does not allow the material parameters to be manually changed during an analysis.

Therefore, the assumption was made that the soil was to be initially homogeneous and to use material parameters that model this soil accurately during the live loading stage of the analysis.

The force in the erection cable after the concrete was placed was found to be small and therefore the release of this force had almost no effect on the forces in the culvert. The cable tension was never measured in the field therefore the magnitude of the horizontal force in the cable after placing of the concrete cannot be verified by the field measurement. If the force in the cable was larger, there would be an increase the positive moments in the composite section after the cable is released.

The axial force in the culvert closely follows membrane behaviour when it is not in contact with the soil. The axial force in the culvert was reduced when in contact with the soil because the soil and culvert elements are rigidly connected. The bending moments were also reduced because the soil was attached to the culvert. The soil and culvert were rigidly connected because ADINA does not have an interface element at this time.

With the concrete placed, the axial force and bending moment diagrams for the composite section are shown in Figures 5.13 - 5.16. The initial apparent negative moment is the result of shifting the axis, about which the bending moments are taken, from the neutral axis of the steel to the elastic centroid of the composite cross-section. The steel

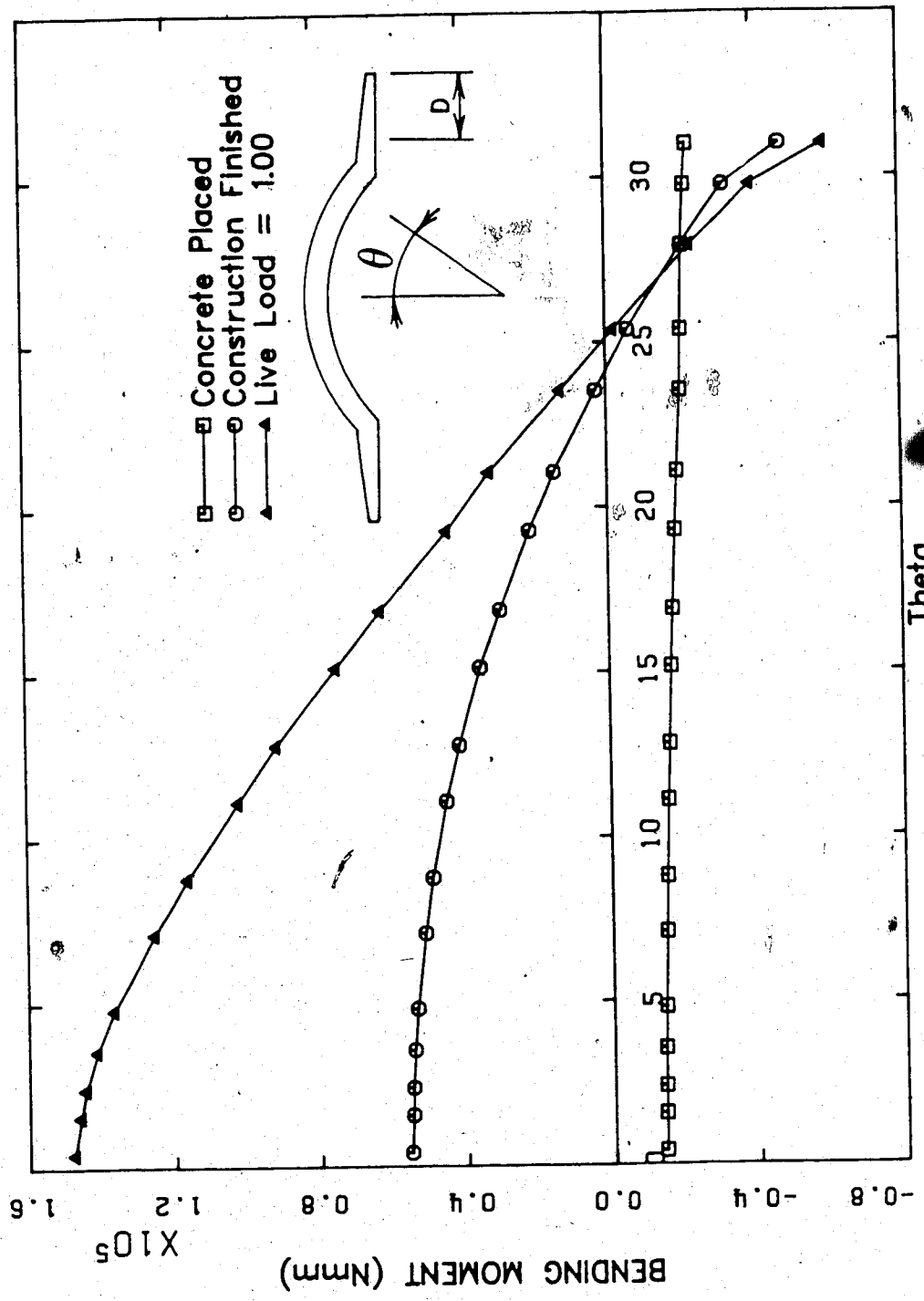
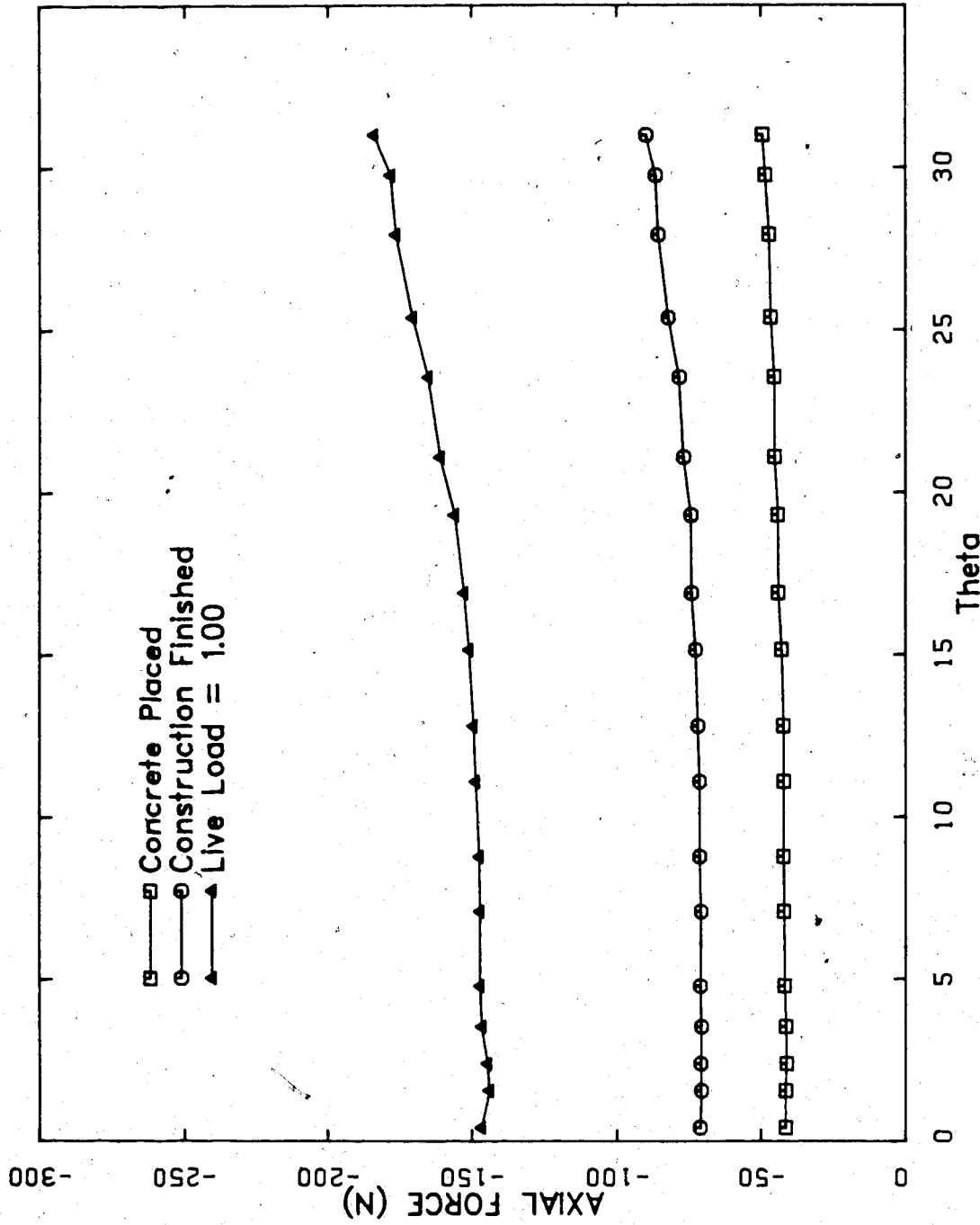
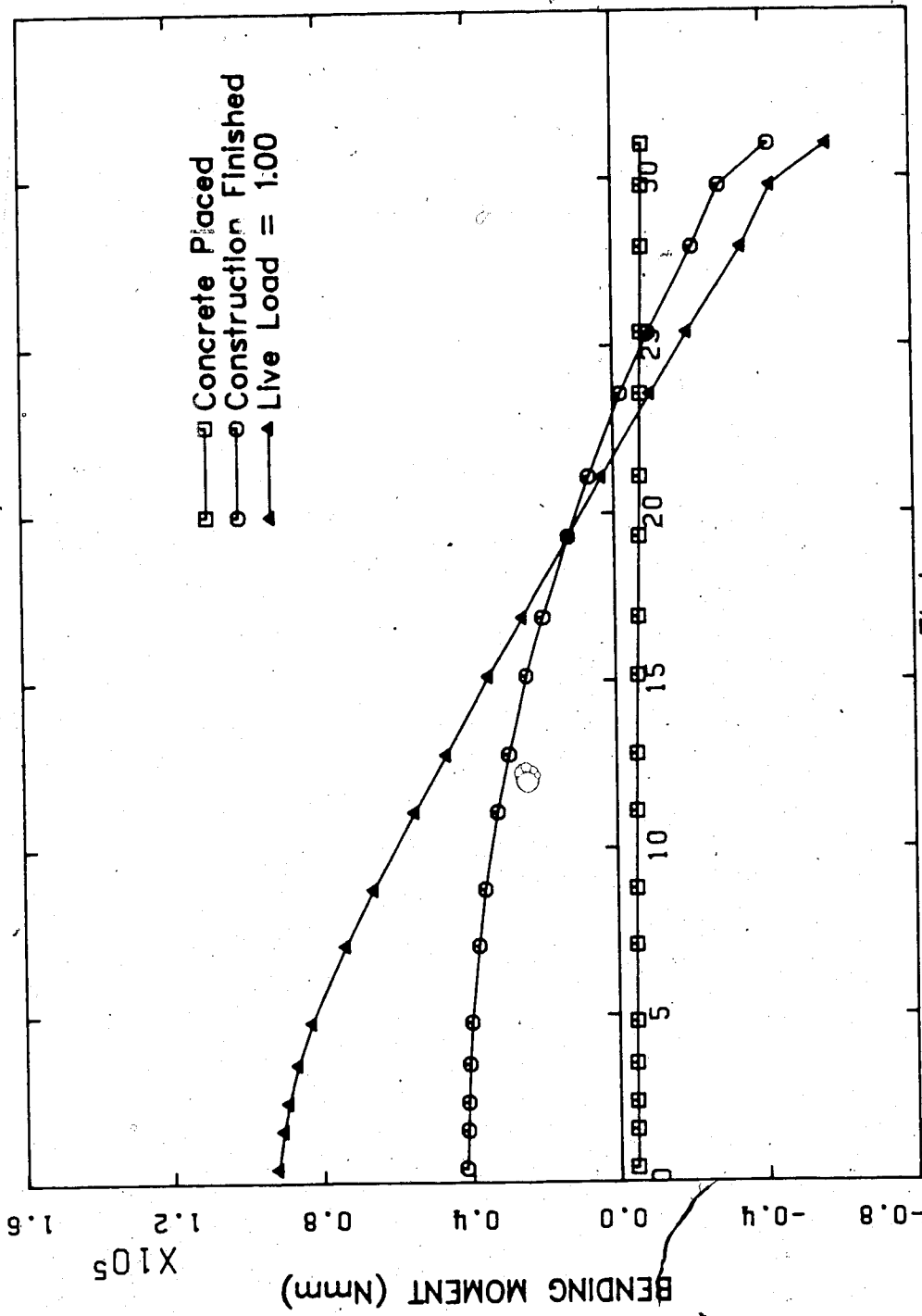


Figure 5.13 Bending Moment Diagram for Mesh 470D - 1250D



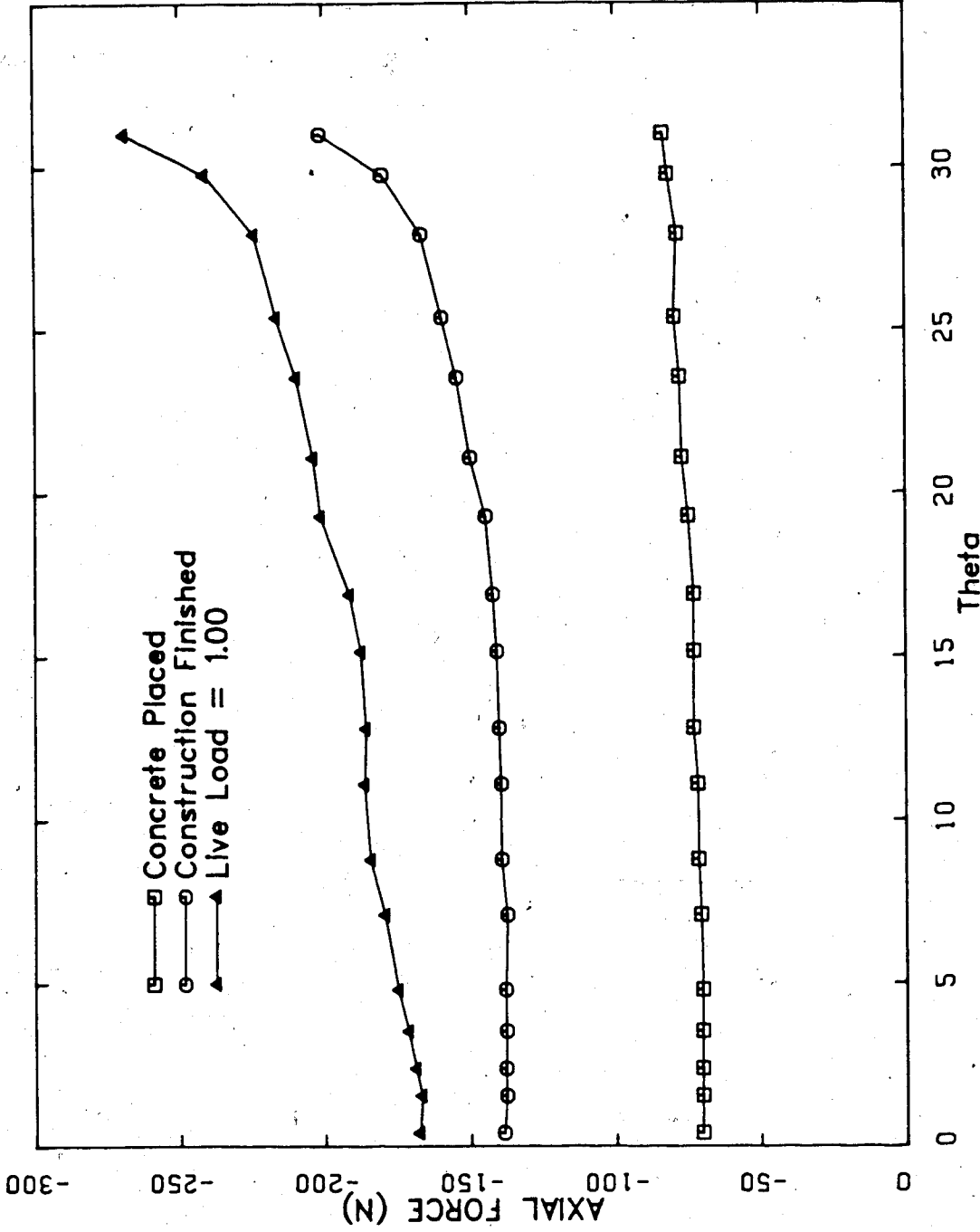
AXIAL FORCE IN COMPOSITE SECTION

Figure 5.14 Axial Force Diagram for Mesh 470D - 1250D



**BENDING MOMENT IN COMPOSITE SECTION**

Figure 5.15 Bending Moment Diagram for Mesh 270D - 1250D



AXIAL FORCE IN COMPOSITE SECTION

Figure 5.16 Axial Force Diagram for Mesh 270D - 1250D

culvert, has a compressive force caused by the weight of the concrete and the concrete is virtually stress free. This results in a net compressive force and a negative bending moment in the composite cross-section.

The bending moments plotted for the composite section were all taken about the initial elastic centroid of the composite section. The elastic centroid was calculated taking into account the effect of Poisson's ratio in the concrete and the culvert steel, while the reinforcement is not affected by Poisson's ratio.

Placing the soil above the concrete in horizontal layers using the preload method resulted in the soil being virtually stress free except for its own weight. The first few layers of soil placed near the support slab caused the crown of the culvert to rise slightly. The rest of the layers being placed resulted in a downward deflection and a positive moment at the crown. The change in the bending moment at the crown, resulting from the placing of the soil above the concrete, was 29% of those given by the simplified design method used for the prototype. This is a result of a portion of the load being carried by arching action as is evident by the increases in the axial force in the composite section.

The vertical stresses on the concrete after construction is completed and with 1.0 times the Service Live Load are shown in Figure 5.17. The distribution of pressures on the top surface of the concrete are close to

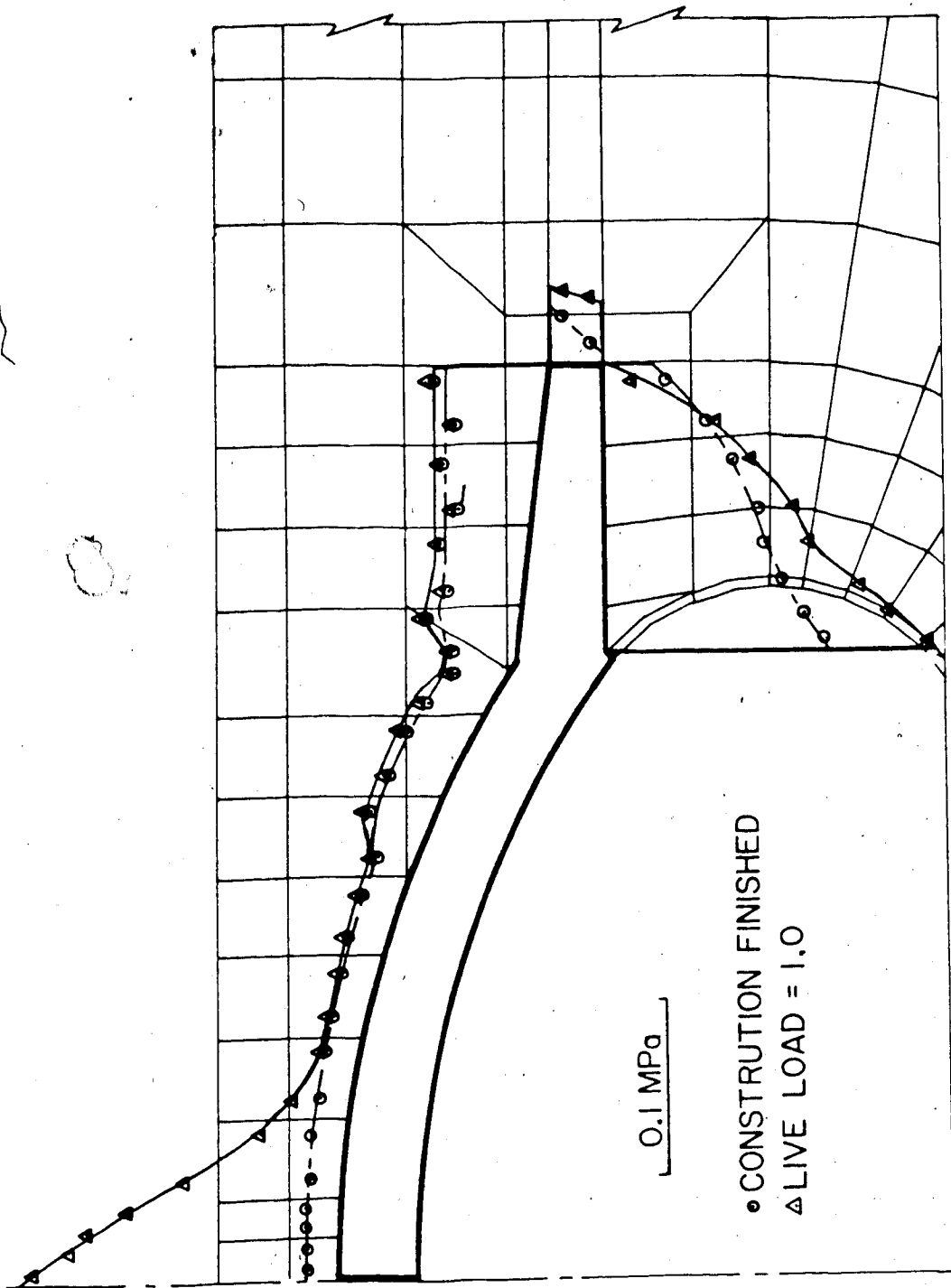


Figure 5.17 Distribution of Vertical Stresses on the Concrete (470D - 1250D)



those assumed in the simplified design procedure (Figure 5.18, Figure 5.19). However, the dead load reaction under the support slab is triangular rather than uniform.

If the dead load reaction used in the simplified design procedure were changed to triangular, the maximum positive moment is reduced and the support slab has negative moments. This would result in closer agreement with the ADINA results.

On the basis of the unmodified simplified design procedure, negative moment reinforcement was not provided in the support slab of the structures analyzed. ADINA allows the concrete to carry some tensile stress and therefore it can have a small negative moment in the support slab but this will be released when the tension cut-off stress has been reached.

The bending moments in the support slab for structure (270T - 1250E) are shown in Figure 5.22. The support slab does not have the apparent initial negative moment that was present in the composite section as a result of the compressive force in the steel culvert. Therefore, the magnitude of the moments at the intersection are not equal but the change in magnitude for any applied load is approximately the same.

The two types of live load were applied to the model of the prototype structure. It was found that the standard truck loading caused the largest mid-span moments. This loading was then used for all of the following analyses. The

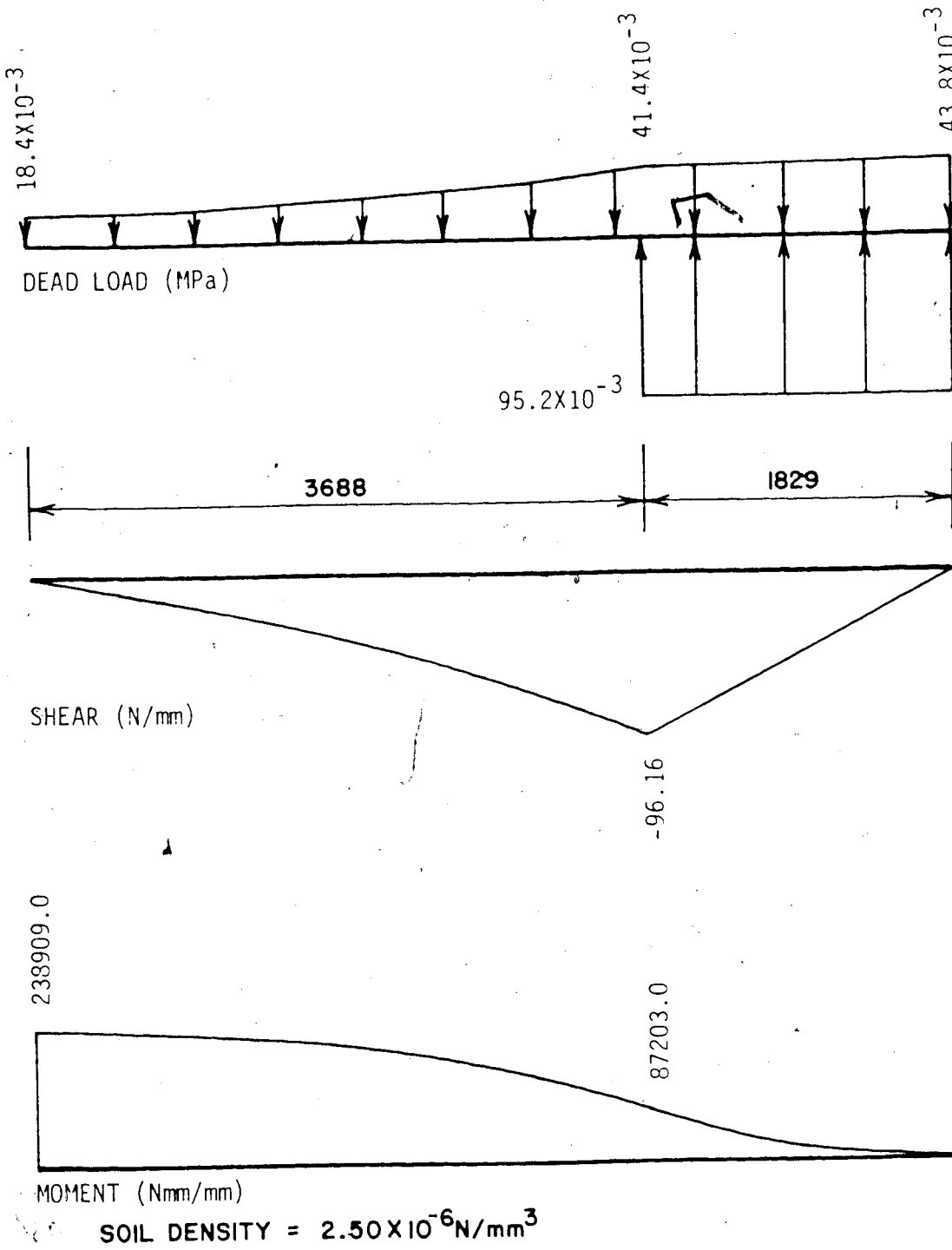


Figure 5.18 Simplified Design Under Dead Load (470 - 1250)

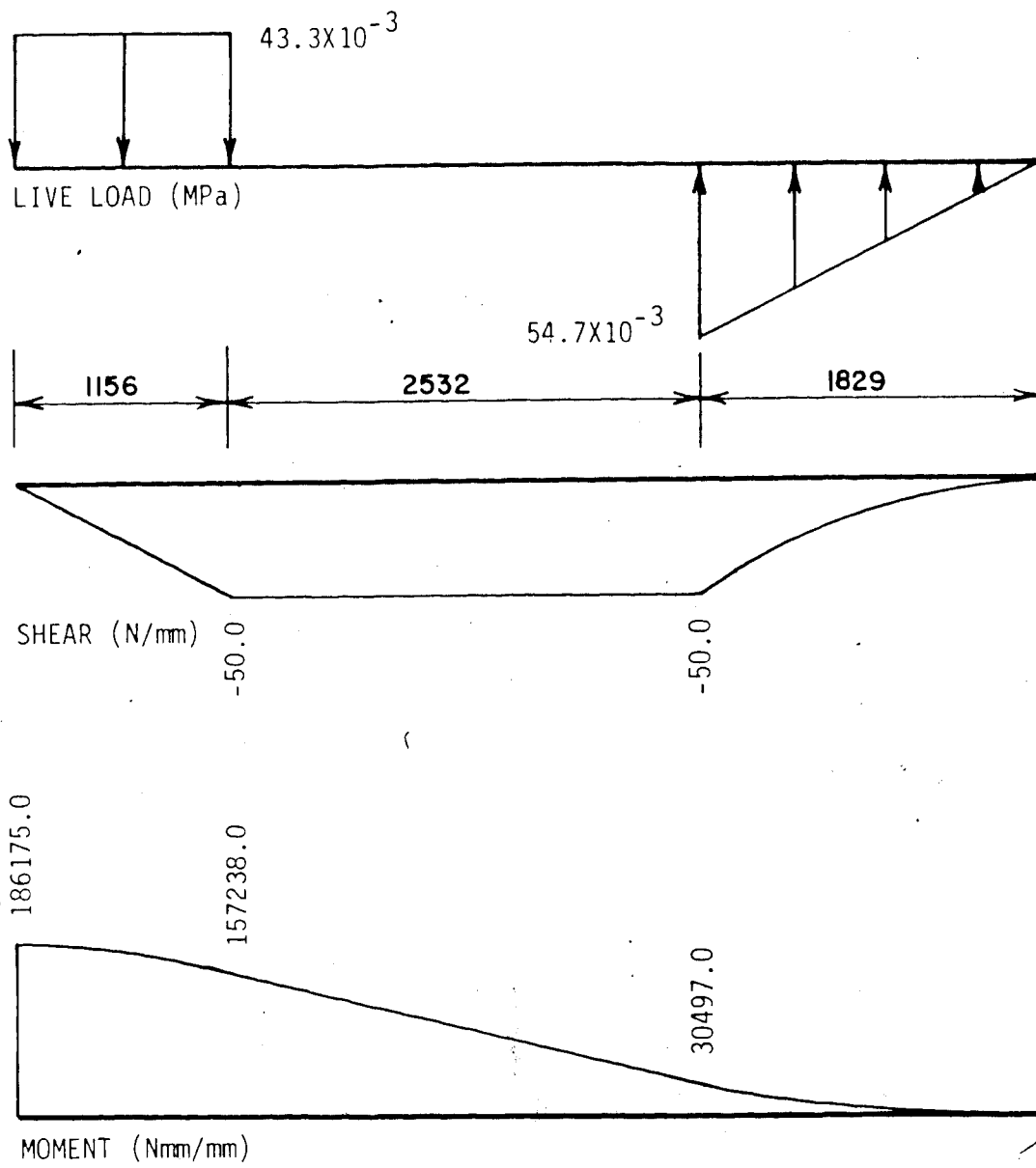
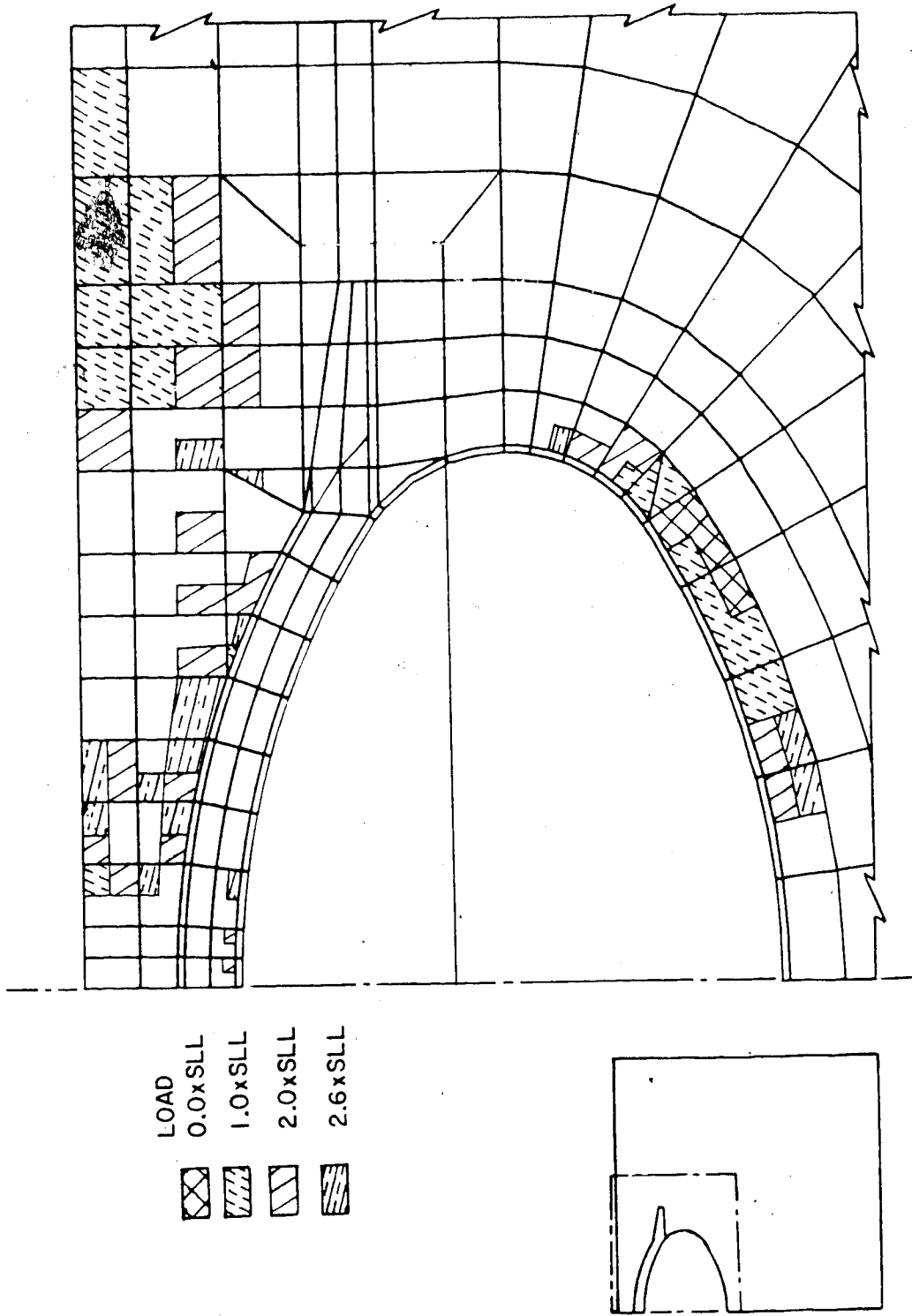


Figure 5.19 Simplified Design Under Live Load (470 - 1250)

magnitude of the loading will be described as a multiple of the MS30 standard truck loading as described earlier.

The live load was applied to the prototype structure (470D - 1250D) in increments of 0.2 times the Service Live Load ( $0.2 \times \text{SLL}$ ). The stiffness matrix was not reformulated between the time steps. This permits a crack to progress through an entire element without causing the element to become unstable. The solution usually converged with 20 modified Newton equilibrium iterations but with a limit of 300 equilibrium iterations, ADINA could not converge when the load was greater than  $2.4 \times \text{SLL}$ . The cracking in the concrete had just proceeded through an entire element and the average stress in the steel was 51.4 MPa at the point of cracking near the crown.

The cause of the instability is thought to have been a localized soil failure in the soil above the concrete support slab. This was confirmed by comparing the incremental deflections in the last time step to previous incremental deflections. It was found that certain deflections were as much as 3000% larger in the last time step than in previous time steps. The yielding in the soil above the concrete support slab can be seen to progress downward as the live load is applied (Figure 5.20). This "failure" was thought to be the result of the coarseness of the mesh and the inability of the Drucker Prager model to resolve the increased rate of strain caused by the cracking in the concrete.



The shape of the bending moment diagram under live load given by the analysis is similar to the bending moment diagram for the dead load. The shape of both of these curves is similar to the bending moment diagram for a pinned circular arch with their respective loadings. The moments are larger in magnitude because the supports were not rigid and have some horizontal settlement. Under both live and dead load the moments were less than those predicted by the simplified design procedure.

This same behaviour was found with the structure having the reduced concrete thickness (270D - 1250D). The equilibrium iteration limit of 300 was reached when the cracking in the concrete progressed through an entire element. The load at this stage was 1.5xSLL. This was less load than that for the prototype structure because the reduced concrete section permitted cracking to occur sooner.

The bending moments due to the live load were 45% less and the axial force was 24% larger in the 270 mm cross-section (270D - 1250D) than in the prototype structure (470D - 1250D). The moment in each of these sections is almost proportional to their relative flexural stiffnesses.

### 5.8.3 Nonlinear Analysis with Elastic Soil

To confirm that the failure was local and to determine the response of the structure at higher loads another run was conducted with the reduced concrete thickness (270T - 1250E). This analysis was conducted in the same

manner as with the Drucker Prager model for the soil with the exception that the load was applied in increments of  $0.5 \times SLL$ . The results through construction were very similar as shown by the bending moment and axial force diagrams in Figure 5.21 and 5.22.

With the elastic model used for the soil the application of live load proceeded until the culvert steel at the crown had yielded in tension. The equilibrium iteration limit was reached when more load was applied. This yielding occurred when the load was  $9.5 \times SLL$ . The resulting load deflection response is shown in Figure 5.23. The response for this structure is almost identical when the soil was modelled elastically as compared to when it was modelled using the Drucker Prager yield criterion up to the load at which the localized failure occurred.

The load deflection plot (Figure 5.23) shows that the structure itself acts almost linearly up until failure. The negative moments at the intersection of the arch and the support slab are reduced as the cracking proceeds through the concrete but the shape of the bending moment and axial force diagrams remain the same. Cracking at the crown causes the stiffness of the cross-section to be reduced and a corresponding increase in the tension stress in the culvert steel.

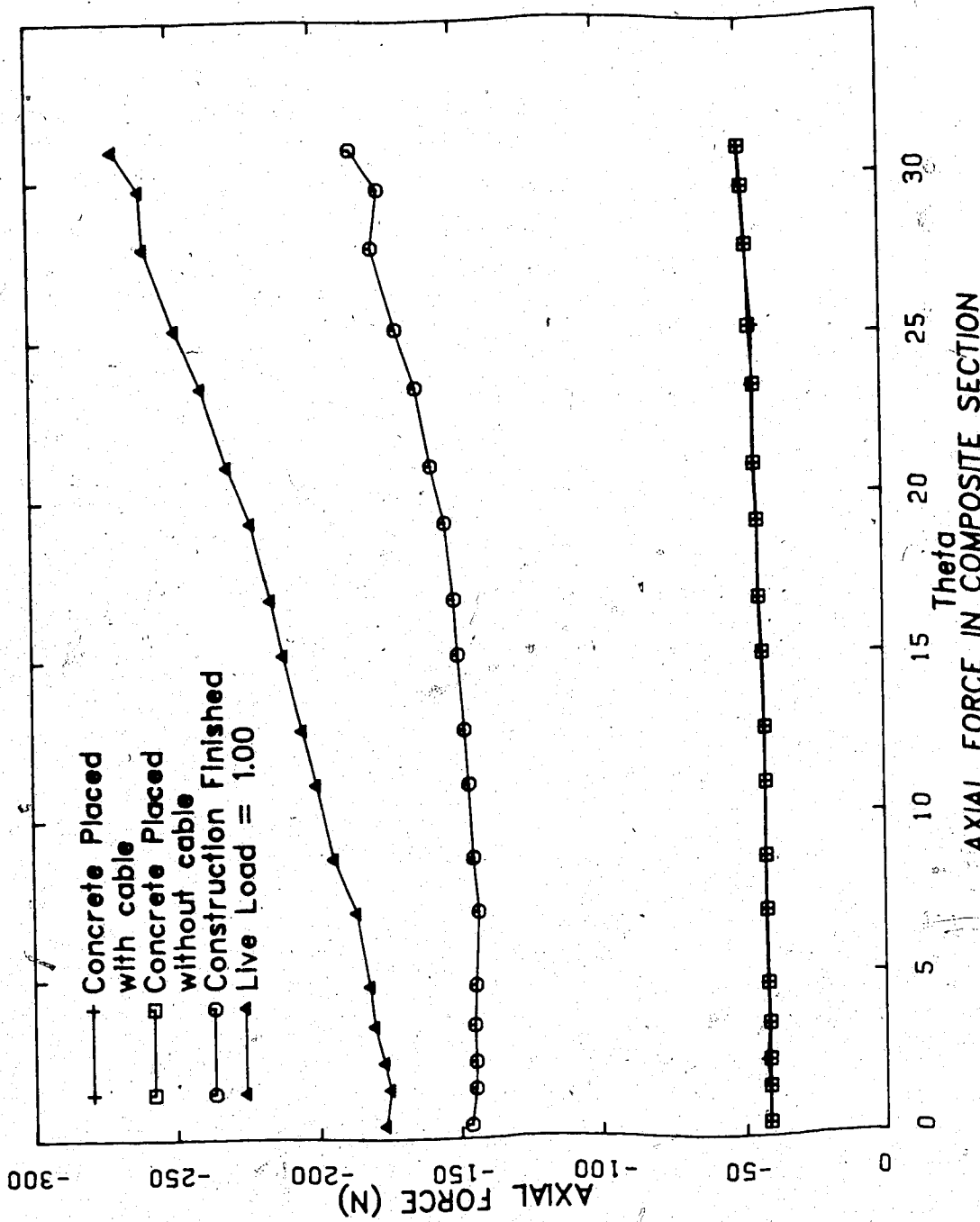


Figure 5.21 Axial Force Diagram for Mesh 270T - 1250E



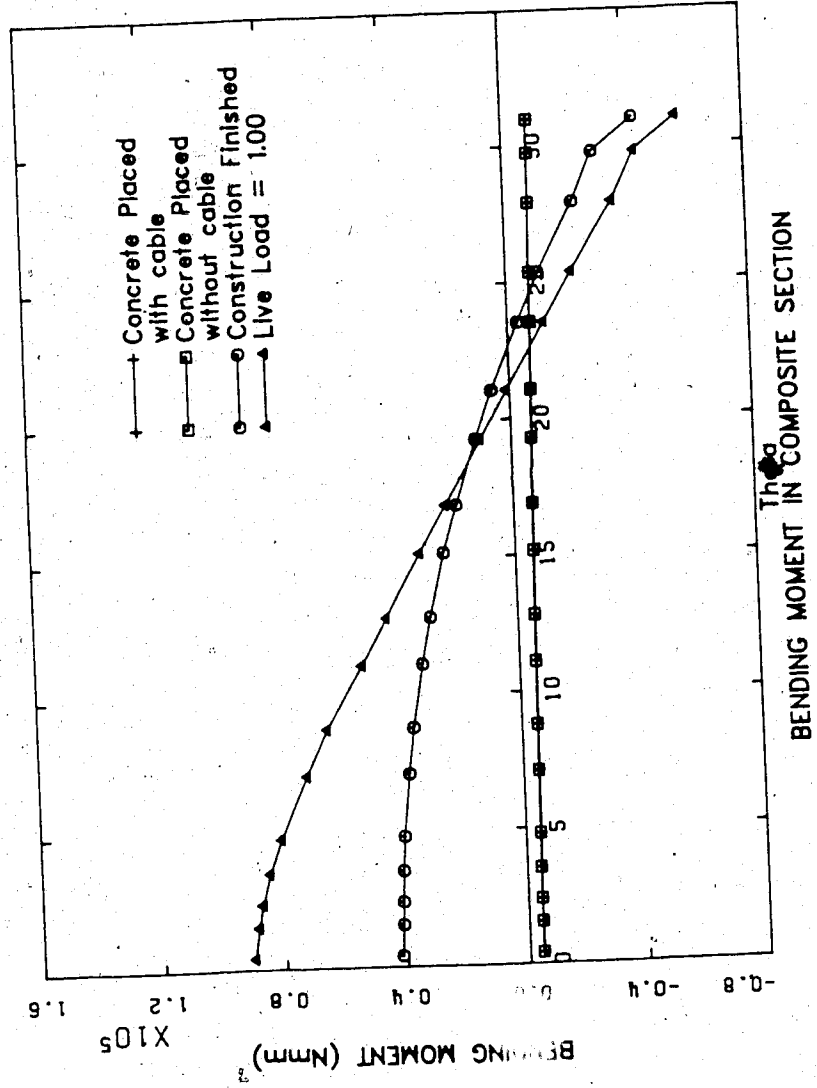
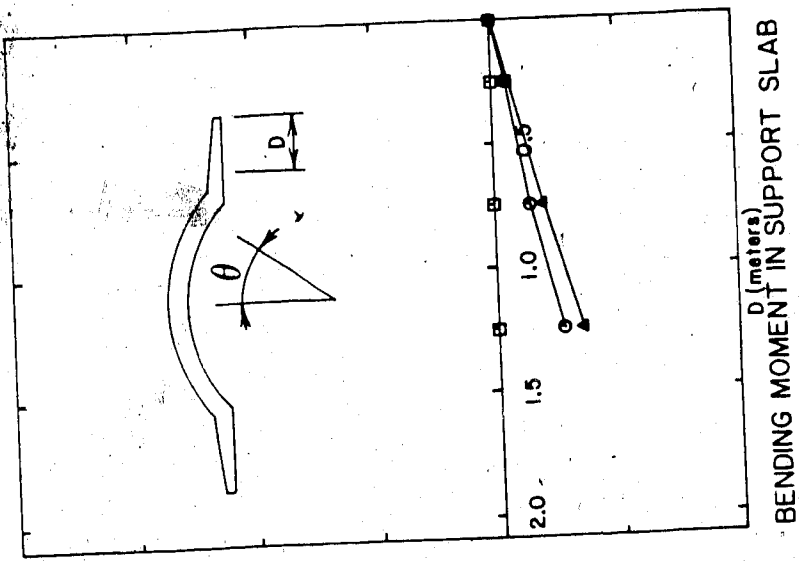


Figure 5.22 Bending Moment Diagram for Mesh 270T - 1250E

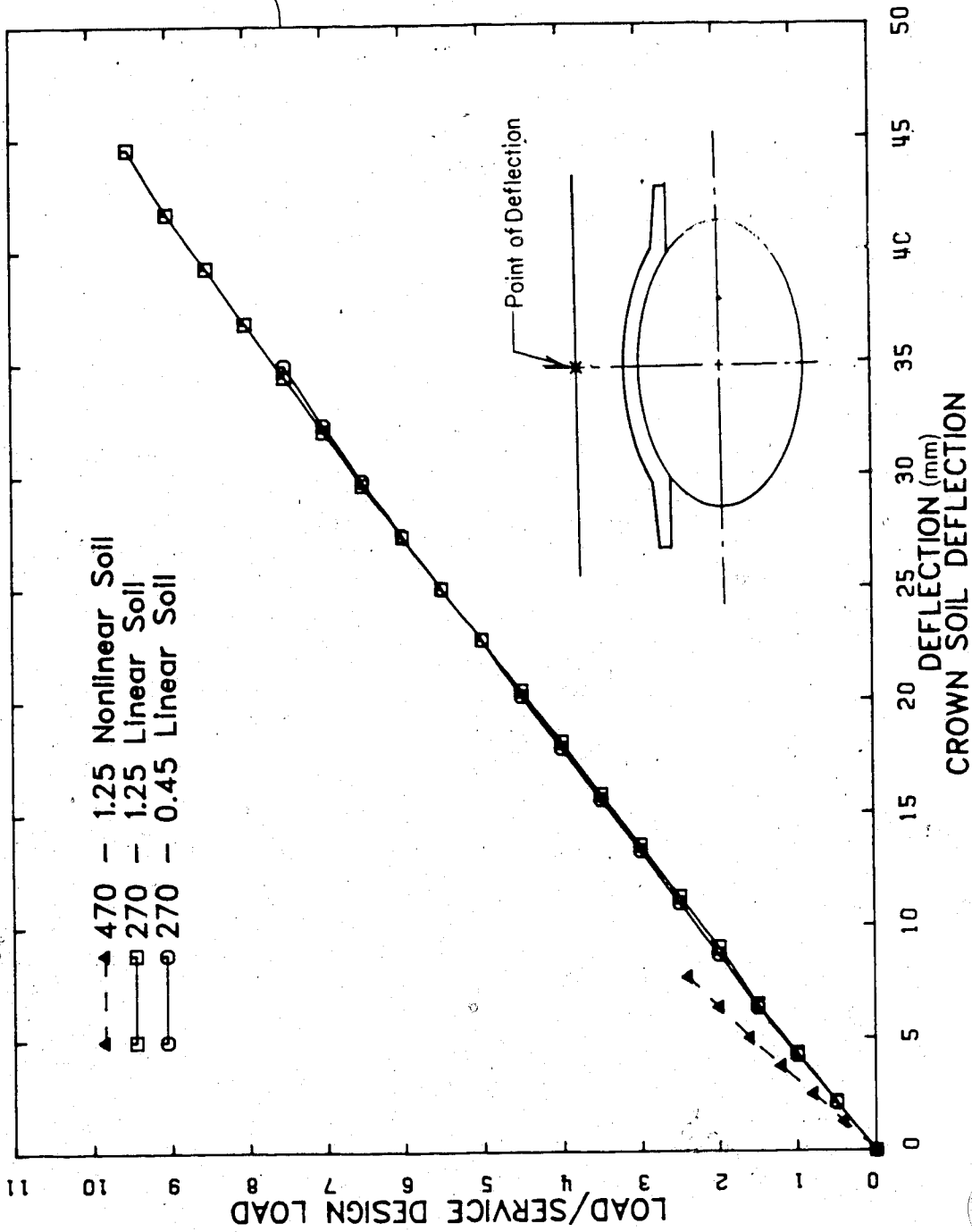


Figure 5.23 Deflection of Soil at the Culvert Crown

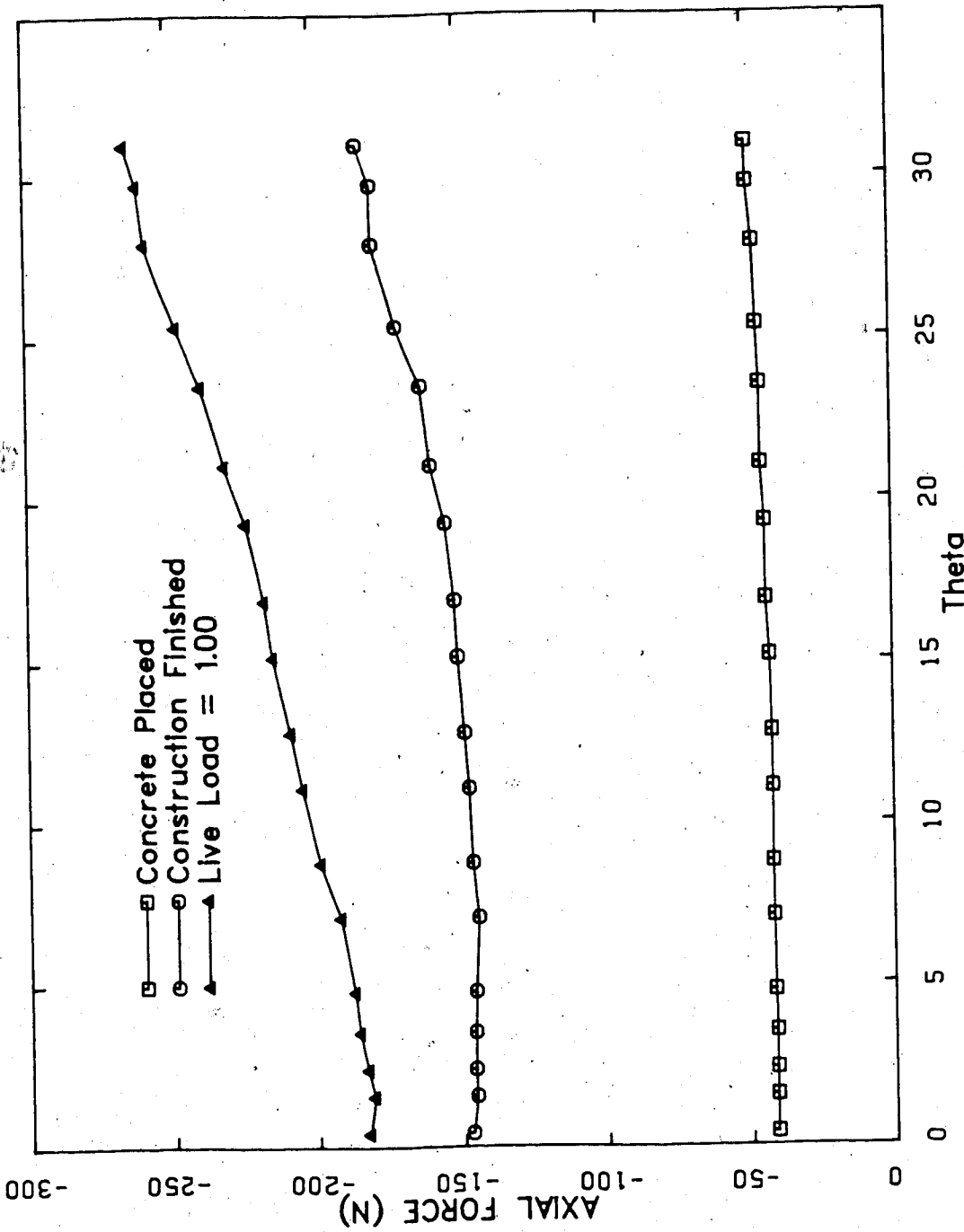
#### 5.8.4 Reduced Soil Cover

Based on the results of the analysis of structure (270T - 1250E) it was decided to model an arch beam culvert with a crown soil cover of 450 mm, structure (270T - 450E). This would show the effect of reducing the soil cover. The construction was modelled using the same procedure used in the previous analyses. The material models were the same as for the Nonlinear Analysis with Elastic Soil.

The results during construction were the same as for the structure having the same concrete section but with the 1250 mm crown depth. As a result of the reduced soil cover, the bending moments and axial forces in the composite section were reduced proportionally (Figure 5.24, Figure 5.25).

The crown soil deflection for structure (270T - 450E) due to the live load was almost the same as for structure (270T - 1250E) having a 1250 mm crown depth (Figure 5.24). The load was applied to the structure until ADINA no longer converged within 300 equilibrium iterations. This occurred when the culvert at the crown had completely yielded and the load was 7.5xSLL. This yield load was less than for the same structure with a crown depth of 1250 mm, even though the moment at the crown was less due to reduced dead load.

The reduced "failure" load for structure (270T - 450E) is because the relative deflection between the concrete crown and the support slab (Figure 5.26) is larger than for structure (270T - 1250E). The change in bending moments and



AXIAL FORCE IN COMPOSITE SECTION

Figure 5.24 Axial Force Diagram for Mesh 270T - 450E

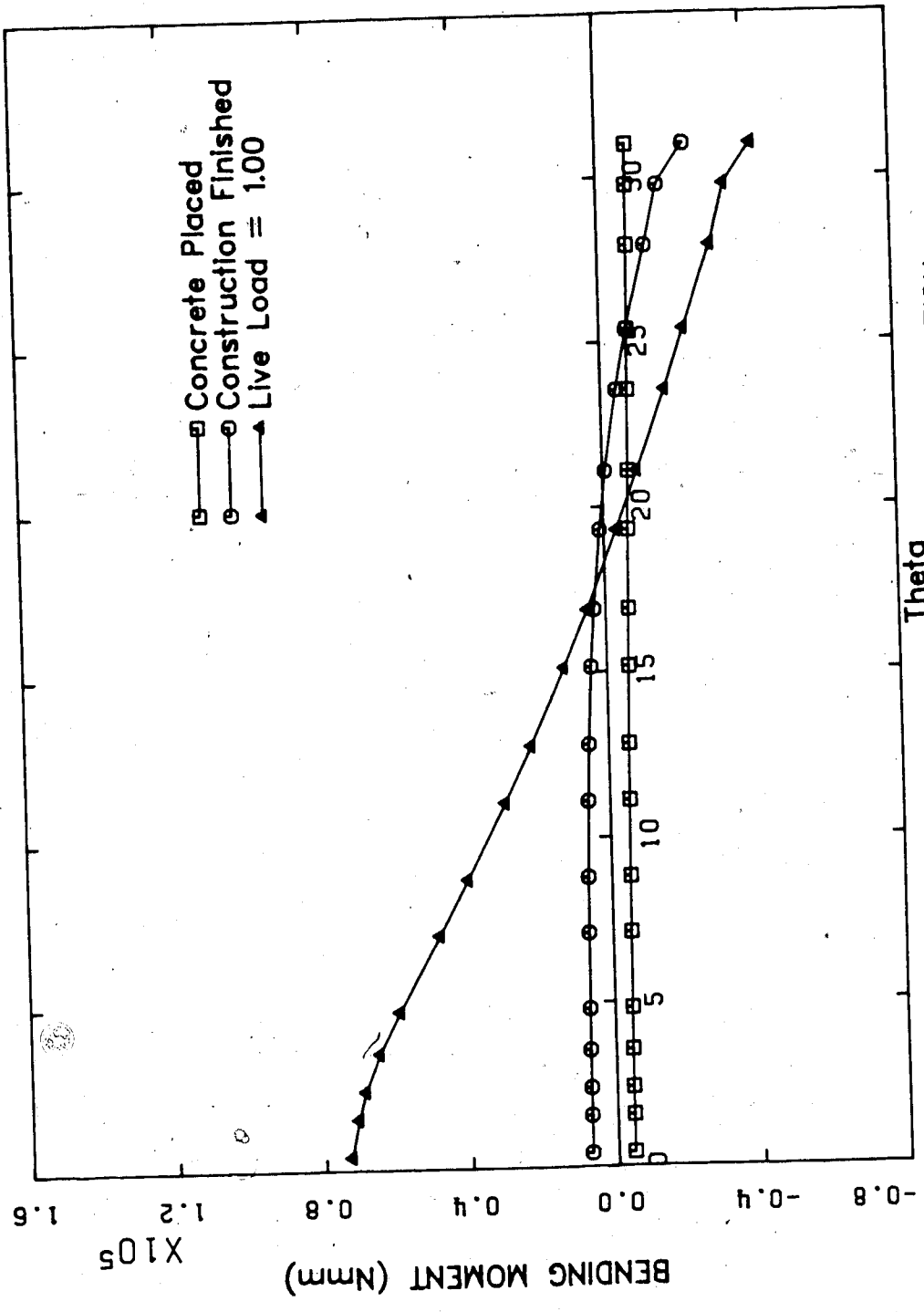


Figure 5.25 Bending Moment Diagram for Mesh 270T - 450E

o

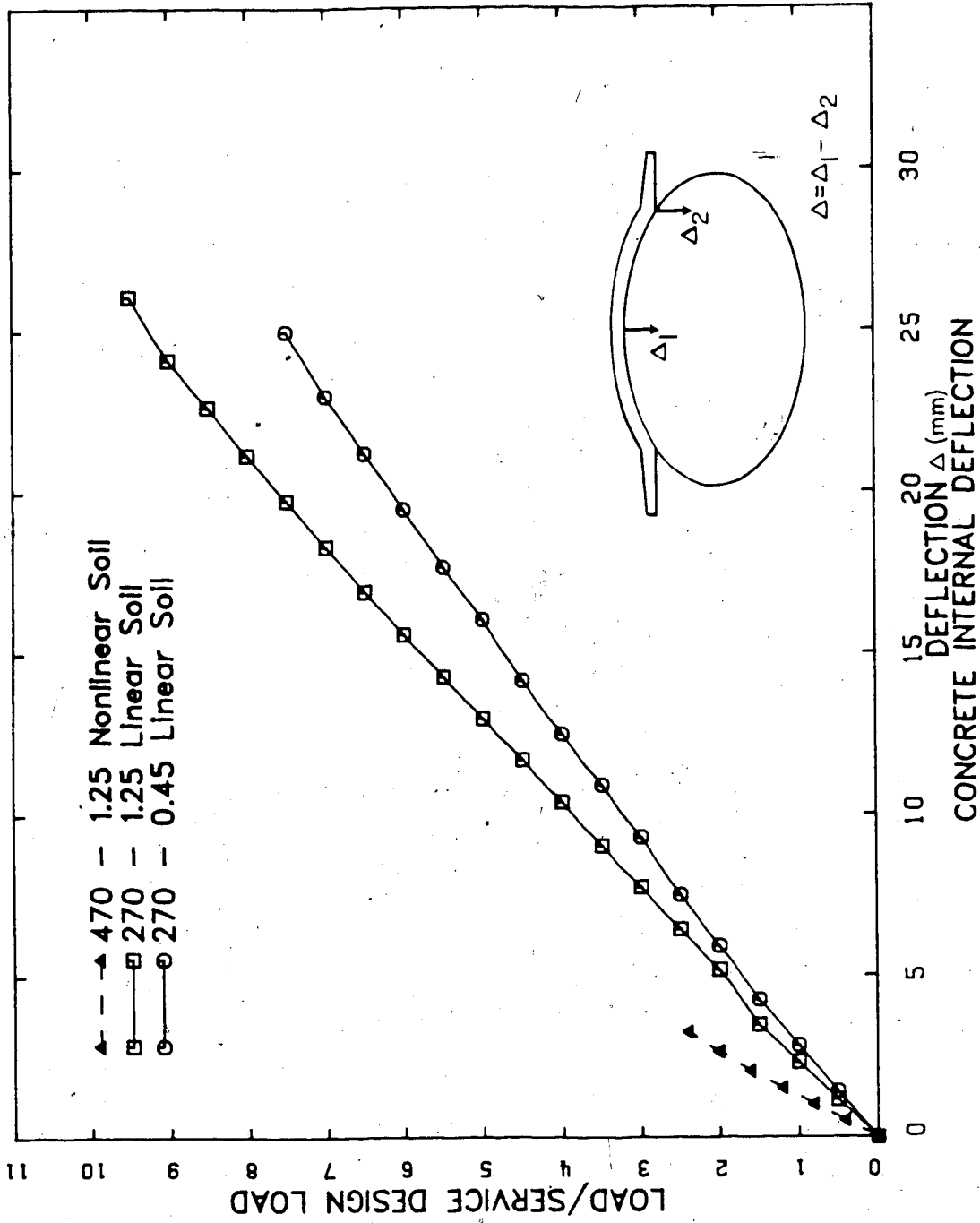


Figure 5.26 Internal Concrete Deflections

axial forces in the composite section, due to the live load (Figure 5.24, Figure 5.25) are proportionally larger as well. The crown soil deflections shown in Figure 5.22 are approximately equal only because the increase in the internal deflection cancelled out the decrease in the deflection within the soil.

#### 5.8.5 Summary of Analyses

A series of analyses of arch-beam culverts showed that the load is carried by a combination of bending and axial forces. The amount of load carried by each of these two actions is dependent on the relative axial and flexural stiffness of the section considered, the loading applied to the structure and the horizontal support provided by the support slab.

The relative axial and flexural stiffnesses are related to the amount of horizontal reaction provided by the support slab because a large portion of the bending moments are caused by the outward movement of the support slab. If the cross-section is sufficiently flexible then the load is carried primarily by arching. However, if the section is very stiff flexurally then the horizontal movement is not sufficient to develop the horizontal force required for arching and more of the load is carried by bending. This occurred when the concrete thickness was reduced from 470 mm to 270 mm.

The distribution of load is a factor in the amount of moment the section must carry because the geometry of an arch is different for each distribution of loading. The "arch" portion of the arch-beam culvert is circular which does not match the shape required for the load to be carried entirely by arch action. Therefore, the cross section of the arch-beam culvert must always be able to carry the corresponding moments.

In general, the more concentrated the load the larger the portion that must be carried by bending. This was confirmed by reducing the soil cover through which the load is distributed. The load on the surface of the structure with the reduced soil cover (270T - 450E) resulted in larger bending moments and a reduced failure load, under the same applied loading.

### 5.9 Effect of not Modelling Construction

Further analyses were conducted in which the various stages of construction were not modelled. The mesh was formed with its final geometry and the live load was applied.

The first analysis attempted was structure (270T - 1250D). With the Drucker Prager yield criterion for the soil, live load could not be applied without large zones of tension failure occurring. However, when the model used for the soil was changed to the linear elastic model (270T - 1250E), live load could be applied. Cracking of the



concrete and yielding of the culvert at the crown occurred at a larger live load than when the construction stage were modelled because the moments due to dead load were reduced.

#### 5.10 Comparison of Analysis and Test Results

The comparison of the analysis results and the test results confirmed that ADINA is able to predict the response of structures such as the Blairmore Creek culvert. The general response is compared because the deflections and strains measured in the field were small and in the order of the experimental error.

The soil pressure cells mounted on the culvert surface were in close agreement with the pressures given by the analysis. These measured pressures, with the crown deflection, were used to determine the magnitude of the preload used to place the soil elements next to the culvert.

The axial force in the steel culvert could not be determined because of the failure of all the strain gauges mounted on the inside surface of the culvert. However, when the wet concrete was placed, the remaining gauges showed a increase in compression similar to the analysis. The deflection in the culvert under this load was larger in the field than in the analysis because the Drucker Prager yield criterion modelled the soil with a Young's modulus that does not depend on the confining pressure. It was noted that the soil beside the culvert could not be fully compacted because of a lack of lateral confinement.

The deflections due to dead load in the structure and those given by the analysis, once the concrete had cured, are of the same sign and order of magnitude. For example, under the weight of the 740 mm of soil placed on the structure the deflection of the crown relative to the invert in the field ranged from 1.9 to 5.9 mm, while the analysis predicted a deflection of 6.1 mm and the range of horizontal movements of the support slab was 1.1 to 2.4 mm and the analysis gave a value of 0.7 mm.

The live load used in the static live load test could not be accurately modelled in a two-dimensional analysis, but the response given by analysis was confirmed by the field measurements. The loading in the field was not uniform along the length of the structure but on a section through the culvert at the point of loading can be compared to the plane strain analysis. The moment at the midspan of the culvert was positive and less than the moment predicted by the simplified design procedure. The moments in the support slab were negative while the simplified design procedure had predicted positive moments. The strain gauge reading also show a net compressive force in the composite section that indicates that some load is carried by arching. All of these are consistent with the response given by the analysis.

The analysis using ADINA was confirmed by the field measurements taken during the test on the Blairmore Creek culvert. With better material information closer agreement could have been achieved.

## 6. CONCLUSIONS, AND RECOMMENDATIONS

### 6.1 Conclusions

#### 6.1.1 Evaluation of ADINA

Through the analyses performed in this study, it has been found that ADINA is capable of accurately modelling soil-structure interaction problems efficiently. In the modelling of these problems, which are often construction dependent and involve more than one material, ADINA's ability to add or remove elements and to combine different material models and different element types proved to be invaluable.

The von Mises yield criterion, used to model the reinforcement and the steel culvert, was found to perform as expected and did not cause any numerical problems.

The Drucker Prager yield criterion was used when the soil was modelled as a nonlinear material. This model worked well but the cap-hardening feature was not used because it caused the effective Poisson's ratio to be negative. The method used for the tension cut-off option caused local failures to occur in the soil. This problem could have been reduced by refining the mesh in the area of the failure. In some cases, had a boundary of interface element been available the failure could have been avoided by reducing the high shear stresses next to the structure. The Drucker Prager yield criterion when used to model the concrete

caused few difficulties.

The Triaxial Concrete Cracking model is a very accurate model, but it requires more material information than would normally be available. It worked well in the test problems which involved only concrete, but when used to model the arch beam culvert a nonpositive definite stiffness matrix was assembled when there was no apparent reason. This problem appears to occur when using the Triaxial Concrete Cracking model in certain combinations with the Drucker Prager yield criterion, the element birth and death option and the correction for the rectangular elements collapsed to triangular elements. The combination of these and possibly other factors that causes the nonpositive definite stiffness matrix has not been isolated.

Modelling the construction using just the element birth option to add the concrete and soil elements resulted in unrealistic stresses. This problem was overcome by using the preload method in combination with the element birth option. This method allowed the concrete to be placed with the steel culvert carrying the weight of the concrete and it also reduced the high shear stresses at the interface between the soil and the structure, which were caused by modelling the interface without allowing slip to take place. If a better soil model and boundary or interface element were available the preload method may not be needed to place the soil but it would still be required to model the placing of the concrete.

### 6.1.2 Recommendations for Arch-beam Culverts

ADINA was able to predict the behaviour of the Blairmore Creek culvert which is a very complex soil structure interaction problem. The predicted behaviour was confirmed by the response given by the field tests. The predictions could be improved if a soil model such as the hyperbolic soil model [20,21] or if a boundary element were made available.

The behaviour confirmed by the field test is a combination of arching and bending actions. The amount of each is dependent upon the amount of horizontal reaction provided by the support slab, the relative bending and axial stiffnesses and the loading on the structure.

It was found that the simplified design procedure, which considers the concrete to act as a simply supported beam, does not accurately predict the elastic bending moments in the concrete. The bending moments at midspan are significantly smaller than predicted and there are negative moments in the support slab that are not predicted by the simplified design procedure. It is therefore recommended that future design procedures use a triangular dead load reaction rather than one that is uniform and the axial force in the concrete be taken into account.

The design should either provide negative moment reinforcement in the support slab or allow for a plastic redistribution of moments. The possibility of a shear failure in the concrete should be evaluated with the loading

modified to cause a more severe shear force than when the live load was applied at midspan.

If further analyses are to be conducted in conjunction with field tests the following should be given consideration. To permit a better comparison of behaviour, more complete material property information is required. The field instrumentation should include the measurement of the forces in the temporary supports used during construction. More measurements taken at different intervals during construction would allow a better comparison to be made during this critical stage.

Under live load either a three-dimensional analysis must be done or the test live load must be modified to allow it to be modelled in two dimensions. A destructive test would be useful in confirming the behaviour past the linear region.

## 6.2 Recommendations for Ancillary Programs

ADINA, like all nonlinear finite element programs is very large and complex. The time required to learn how to use such a program is a major portion of any nonlinear finite element analysis. ADINA addresses this problem by making the program's input modular. This allows the users to concern themselves only with the sections that are related to their problem.

The largest amount of time spent during an analysis is used in the manual operations of preparing the input and

evaluating the output. It is therefore strongly recommended that the preprocessor ADINA-IN be acquired before any further major analyses be conducted using ADINA. ADINA-Plot should also be improved to make the evaluation of the output more automated. At this time ADINA-Plot has no form of command replication and is without a facility to resolve stresses into directions other than the global axes. At the present time users must create their own post-processing programs.

## BIBLIOGRAPHY

- [1] Abdel-Sayed G. and Baidar Bakht, "*Soil-Steel Structure Design by the Ontario Code: Part 2, Structural Considerations*", Canadian Journal of Civil Engineering, Vol 8, 1981, pp. 331-341.
- [2] Abel, John F., Robert Mark and Rowland Richards, "*Stresses Around Flexible Elliptic Pipes*", Journal of the Soil Mechanics and Foundation Division, ASCE, No. SM7, July 1973, pp 509-526.
- [3] "*ADINA Users Manual*", ADINA Engineering Inc. Report AE81-1, Watertown, Mass., 1981.
- [4] "*ADINA - IN*", ADINA Engineering Inc. Report AE83-6, Watertown, Mass., December 1983.
- [5] "*ADINA -oPlot*", ADINA Engineering Inc. Report AE82-3, Watertown, Mass., March 1982.
- [6] "*ADINAT*", ADINA Engineering Inc. Report AE81-2, Watertown, Mass., September 1981.
- [7] "*Blairmore Creek Instrumentation (Summary of Results)*", Alberta Transportation, June 26 1983.



- [8] Bathe, Klaus-Jurgen, *"Finite Element Procedures in Engineering Analysis"*, Prentice-Hall, Inc., Englewood Cliffs, New Jersey, 1982.
- [9] Bathe, Klaus-Jurgen and Seshadri Ramswamy, *"On Three-dimensional Nonlinear Behaviour of Concrete Structures"*, Nuclear Engineering and Design, Vol. 52, 1979, pp. 385-409.
- [10] Bathe, Klaus-Jurgen, Mark D. Snyder, Arther P. Cimento and W. Donald Rolph, *"On Some Current Procedures and Difficulties in Finite Element Analysis of Elastic-Plastic Responce"*, Computers and Structures, Vol. 12, 1980, pp. 607-624.
- [11] Bowles, Joseph E., *"Foundation Analysis and Design"*, McGraw-Hill, New York, New York, 1977.
- [12] Bowles, Joseph E., *"Physical and Geotechnical Properties of Soils"*, McGraw-Hill, New York, New York, 1979.
- [13] *"Canadian Civil Engineer, Wellington County Culvert"*, Vol 2, No. 1, January 1985, pp. 3.

- [14] Chen, W. F., *"Plasticity in Reinforced Concrete"*, McGraw-Hill, New York, New York, 1982.
- [15] *"Code for the Design of Concrete Structures for Buildings"*, (CAN3-S23.3-M77), Canadian Standards Association, 1977.
- [16] *"Design of Highway Bridges"*, (CAN3-S6-M78), Canadian Standards Association, 1978.
- [17] DiMaggio, Frank L. and Ivan S. Sandler, *"Material Model For Granular Soils"*, Journal of the Engineering Mechanics Division, ASCE, No. EM3, June 1971, pp. 935-950.
- [18] Drucker, D. C. and W. Prager, *"Soil Mechanics and Plastic Analysis or Limit Design"*, Quarterly of Applied Mathematics, Vol. 10, No. 2, 1952, pp. 157-165.
- [19] Duncan, James M., *"Behaviour and Design of Long-Span Metal Culverts"*, Journal of the Geotechnical Engineering Division, ASCE, Vol. 105, No. GT3, March 1979, pp. 399-418.

- [20] Duncan, J. M., P. Byrne, K. S. Wong and P. Makry, "Strength, Stress-strain and bulk Modulus Parameters for Finite Element Analyses and Movements in Soil Masses", Report UCB/GT/80-01, University of California, Berkely, 1980.
- [21] Duncan, J. M. and C. V. Chang, "Nonlinear Analysis of Stress and Strain in Soils", Journal of the Soil Mechanics and Foundation Division, ASCE, Vol. 96, 1970 pp. 1629-1653.
- [22] Hafez, Hisham and George Abdel-Sayed, "Finite Element Analysis of Soil-Steel Structures", Canadian Journal of Civil Engineering, Vol 10, 1983, pp. 287-294.
- [23] Hafez, Hisham and George Abdel-Sayed, "Finite Element Analysis of Soil-Steel Structures", Canadian Journal of Civil Engineering, Vol 10, 1983, pp. 287-294.
- [24] Hafez, Hisham and George Abdel-Sayed, "Soil Failure in Shallow Covers Above Flexible Conduits", Canadian Journal of Civil Engineering, Vol 10, 1983, pp. 654-661.

- [25] Huiskamp, W. J. and J. T. Christison, "*Load-Response Behaviour of Blairmore Creek Arch-Beam Culvert*", Civil Engineering Department, Alberta Research Council, Report HTE 83/04, November 1983.
- [26] Jaeger, J.C., "*Elasticity, Fracture and Flow*", Halsted Press, New York, New York, 1978.
- [27] Kupfer, H., H. K. Hilsdorf and H. Rusch, "*Behaviour of Concrete under Biaxial Stresses*", Journal of the Am. Concrete Inst., Vol. 66, No 8, August 1969, pp. 656-666.
- [28] Launay, P. and H. Gachon, "*Ultimate Strength of Concrete Under Triaxial Stress*", Am. Concrete Inst., Special Publication 34, paper 13, 1972.
- [29] Mirza, Cameran and Baidar Bakht, "*Soil-Steel Structure Design by the Ontario Code: Part 1, General and Geotechnical Considerations*", Canadian Journal of Civil Engineering, Vol 8, 1981, pp. 317-330.
- [30] Meyerhof G. G., "*Problems in the Design of Shallow-Buried Steel Structures*", Canadian Structural Engineering Conference, 1968.

- [31] Peterson, C. W., "ABC Structural System - Outline of the Concept and It's Applications", Canadian Society of Civil Engineering, Western Region Seminar, Edmonton, March 1985.
- [32] Playdon, David K. and Sidney H. Simmonds, "Finite Element Modelling of Buried Structures", Research in Structures and Dynamics Symposium, Washington, D.C., NASA Conference Publication 2335, October 22-25 1984.
- [33] Ratzlaff, K. P. and D. J. L. Kennedy, "Behaviour and Ultimate Strength of Continuous Steel Plates Subjected to Uniform Transverse Loads", Proceedings: Canadian Society of Civil Engineering Annual Conference, Saskatoon, Saskatchewan, June 1985.
- [34] Sandler, Ivan S., Frank L. DiMaggio and George Y. Baladi, "Generalized Cap Model For Geological Materials", Journal of the Geotechnical Engineering Division, ASCE, No. GT7, July 1976, pp. 683-699.
- [35] "Standard Specifications for Highway Bridges", The American Association of State Highway and Transportation Officials, Twelfth Edition, 1977.

- [36] White H. L. and J. P. Layer, "*The Corrugated Metal Conduit as a Compression Ring*", Armco Drainage and Metal Products, January 1960.

## APPENDIX A

Abstracts for the ancillary programs to ADINA. These abstracts were taken directly from the User Manuals for each program [4,5,6].

### *ADINA-Plot*

"ADINA-PLOT can directly be used in conjunction with the ADINA program to display input and output data. The porthole file created by an ADINA run is used to load a specially designed database. ADINA-PLOT can be run in batch or interactively and a command language is used to request plotting, listing or scanning operations. Lay-out options are available so that plots and tables can be produced ready for insertion in a report. Examples of plot capabilities are meshes (deformed or undeformed), modeshapes, time histories, line variations and principal stresses. The operations may be applied to the whole model or a selected part. Resultants such as total displacements, effective stresses or radial displacements, may be calculated by userdefined formulas written in a Fortran like manner. The scanning operations include identification of a requested number of extreme values or of results exceeding a specified value."

### ADINA-IN

The pre-processor ADINA-IN is designed for effective generation of input data to the ADINA program. ADINA-IN can be run in batch or interactive operation. The user input consists of command, parameters and data lines, which define the ADINA variables and generate element meshes, nodal coordinates, loads and so on. Plotting and listing facilities enable the user to check the ADINA model. Data is stored in a specially designed database. A complete ADINA input file can be generated. Nodal points can be numbered in any order since ADINA-IN can reduce the bandwidth and profile of the ADINA stiffness and mass matrices by optimization of the equation numbering. The numbering of the nodal points are not affected by the optimization of the equations numbering.



### ADINAT

"The program ADINAT (a Finite Element Program for Automatic Dynamic Incremental Nonlinear Analysis of Temperatures) is currently available on the MTS system at the University of Alberta. Although the terminology is that of heat transfer problems, ADINAT can be used to model other field problems, such as seepage, Torsion, and electrical conductivity. ADINAT employs one-, two-, and three-dimensional elements, and three basic material models : Isotropic constant conductivity, Orthotropic constant conductivity, and nonlinear temperature dependant isotropic conductivity. Both steady-state and transient analyses may be performed. A new version of ADINAT is now available (ADINAT81) which adds some new capabilities such as phase changes and distribution heat flux loading.

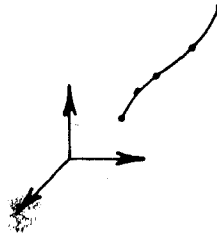
## APPENDIX B

### List of Element Types and Corresponding Material Models

[3].

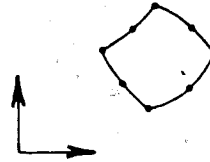
#### TRUSS ELEMENT

- a. Linear Elastic
- b. Nonlinear Elastic
- c. Thermo-Elastic
- d. Elastic-Plastic
- e. Thermo-Elastic-Plastic and Creep



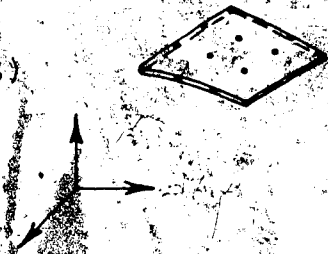
#### TWO-DIMENSIONAL PLANE STRESS, PLANE STRAIN AND AXISYMMETRIC ELEMENTS

- a. Isotropic Linear Elastic
- b. Ortotropic Linear Elastic
- c. Isotropic Thermo-Elastic
- d. Curve Description Nonlinear Model for Analysis of Geological Materials
- e. Concrete Model
- f. Isothermal Plasticity Models, Von Mises Yield Condition or Drucker-Prager Yield Condition with Cap
- g. Thermo-Elastic-Plastic and Creep, Von Mises Yield Condition
- h. Isotropic Nonlinear Elastic, Incompressible (Mooney-Rivlin Material) (plane stress only)



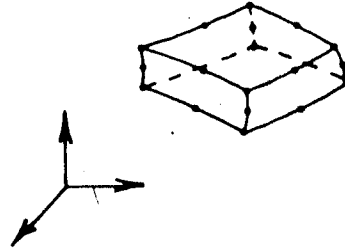
#### THIN SHELL ELEMENT (VARIABLE-NUMBER-NODES)

- a. Isotropic Linear Elastic
- b. Isothermal Plasticity, Von Mises Yield Condition



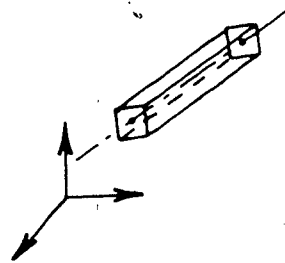
## THREE-DIMENSIONAL SOLID AND THICK SHELL ELEMENT

- a. Isotropic Linear Elastic
- b. Ortotropic Linear Elastic
- c. Isotropic Thermo-Elastic
- d. Curve Description Nonlinear Model for Analysis of Geological Materials
- e. Concrete Model
- f. Isothermal Plasticity Models, Von Mises Yield Condition or Drucker-Prager Yield Condition with Cap
- g. Thermo-Elastic-Plastic and Creep, Von Mises Yield Condition



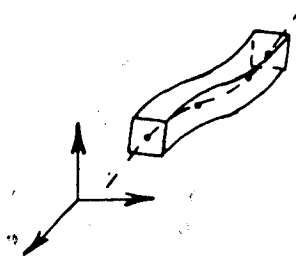
## TWO-NODE THREE-DIMENSIONAL BEAM ELEMENT

- a. Isotropic Linear Elastic
- b. Elastic-Plastic Von Mises Yield Condition



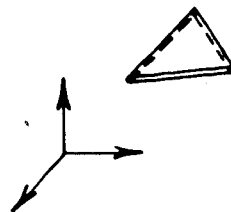
## ISOPARAMETRIC BEAM ELEMENT

- a. Isotropic Linear Elastic
- b. Isothermal Plasticity, Von Mises Yield Condition



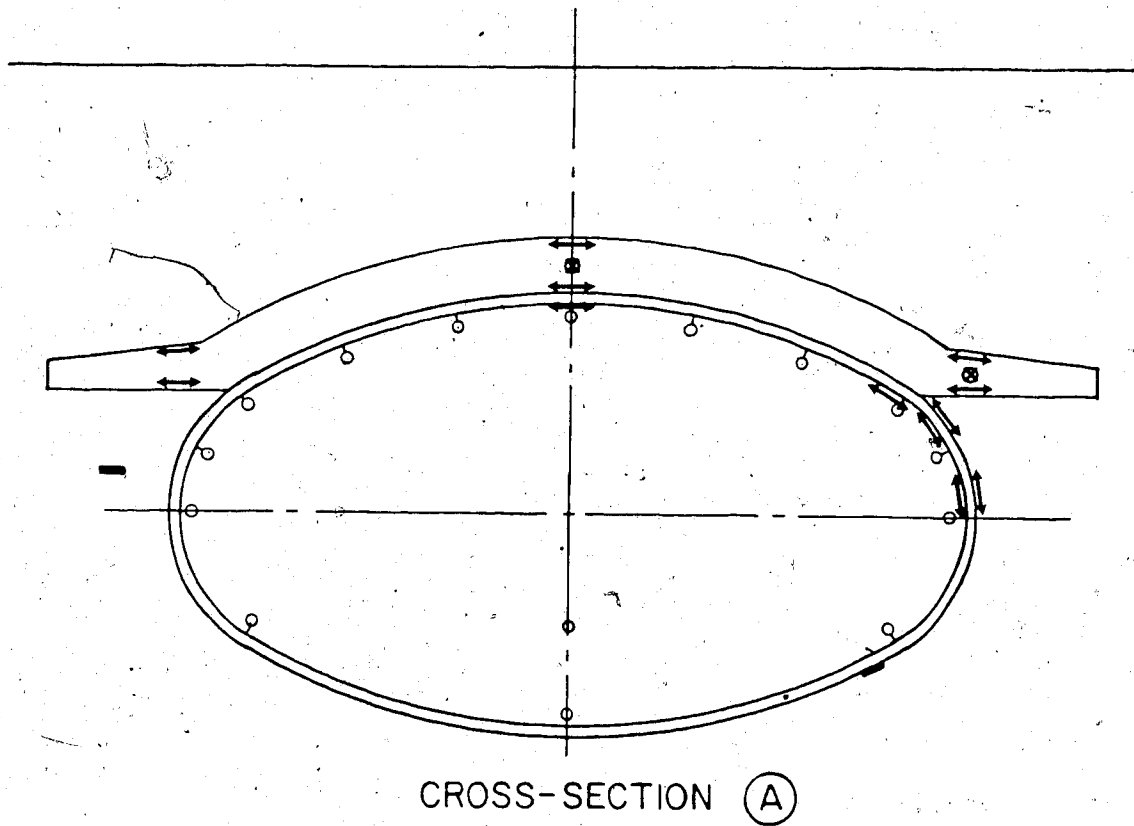
## THREE-NODE PLATE/SHELL ELEMENT




- a. Isotropic Linear Elastic
- b. Isothermal Plasticity, Ilyushin Yield Condition



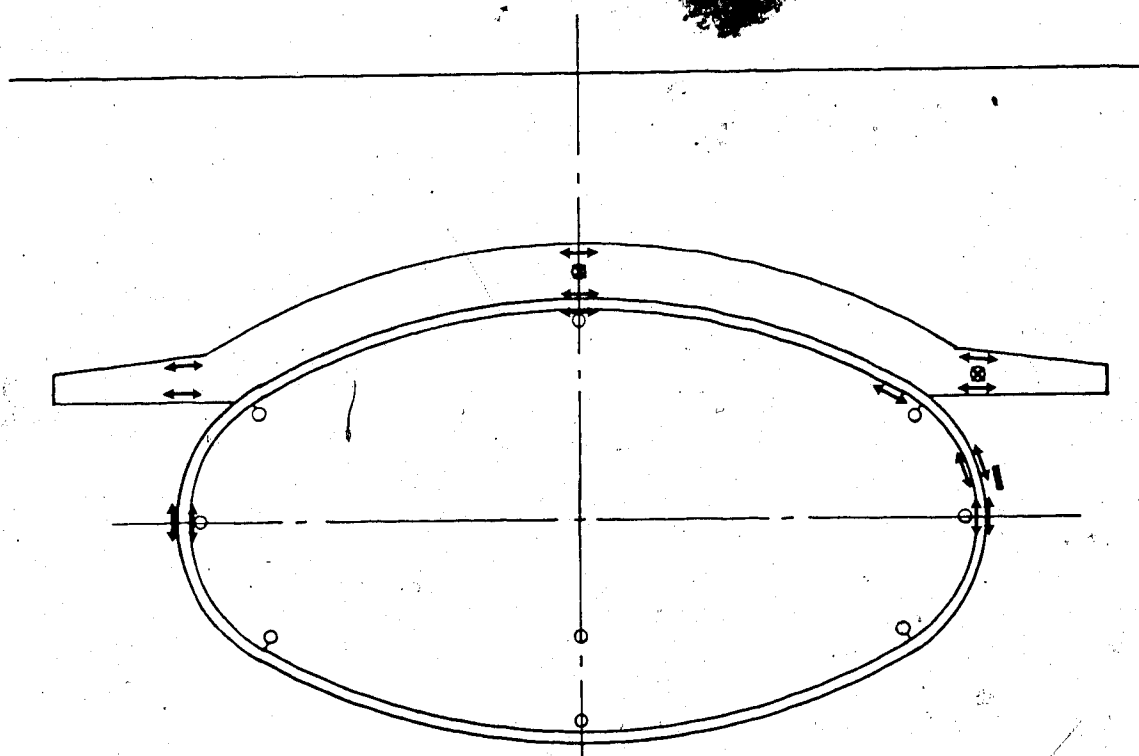
## APPENDIX C

Instrumentation of the Arch-Beam Culvert at Blairmore, Alberta. The locations of the cross-sections are shown in Figure 4.13.



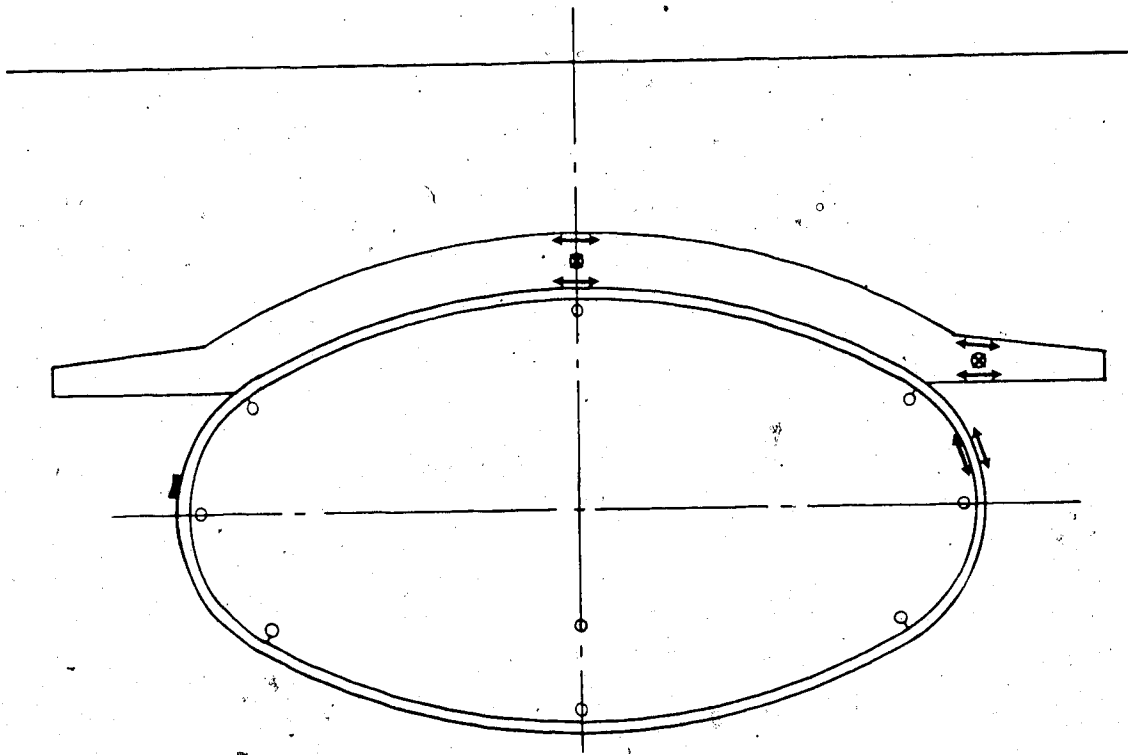
-  DEFLECTION CONTROL POINT
-  CIRCUMFERENTIAL STRAIN GAUGE
-  LONGITUDINAL STRAIN GAUGE

Instrumentation on Cross-Section A



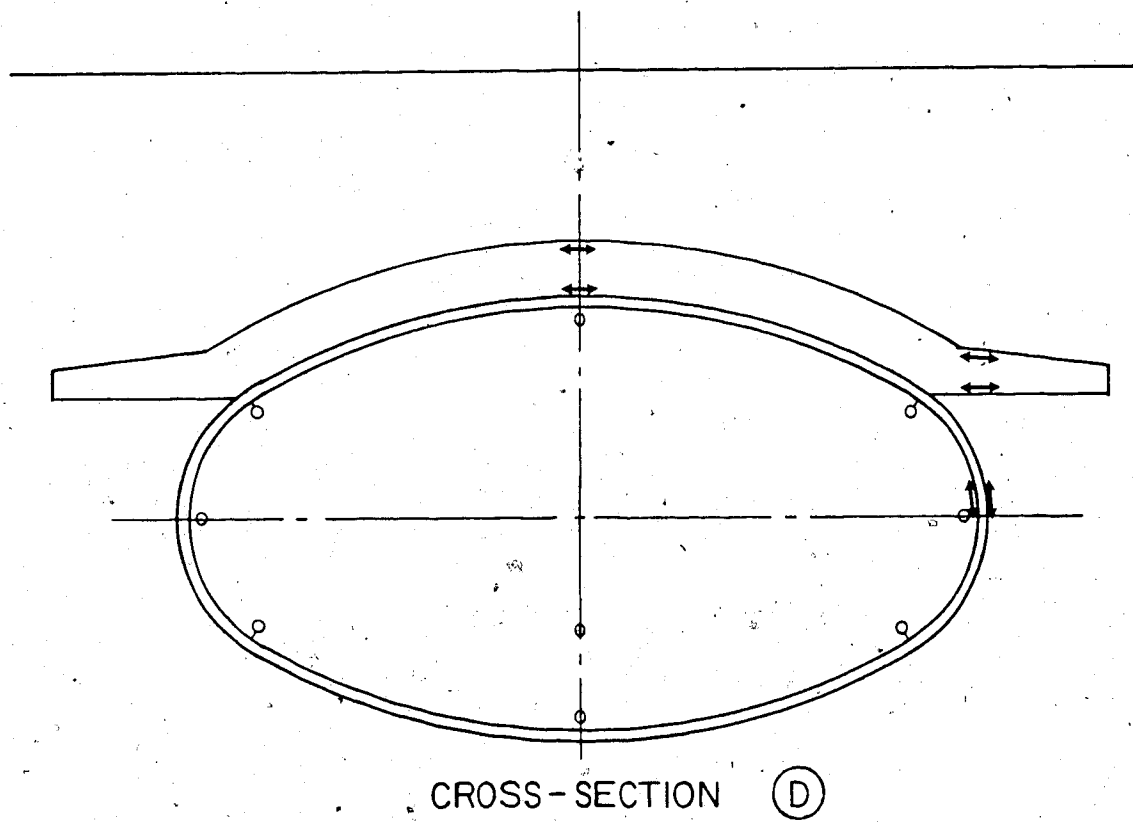
CROSS SECTION (B)

Instrumentation on Cross-Section B



CROSS-SECTION (C)

Instrumentation on Cross-Section C



Instrumentation on Cross-Section D

## APPENDIX D

Transformation of the elastic stiffness properties from the corrugated steel culvert cross-section to an equivalent rectangular section.

$$EA = E^* bh$$

$$EI = E^* \frac{bh^3}{12}$$

ASSUME  $b=1$

$$E^* = \frac{EA}{h}$$

$$EI = \frac{EA}{h} \frac{h^3}{12}$$

$$h = \left[ 12 \frac{I}{A} \right]^{\frac{1}{2}}$$

	Actual	Model
A	6.150 mm <sup>2</sup>	60.36 mm <sup>2</sup>
I	1867 mm <sup>4</sup>	18325 mm <sup>4</sup>
E	200,000 MPa	20378 MPa
AE	1.23 X 10 <sup>6</sup> mm <sup>2</sup> N/mm <sup>2</sup>	1.23 X 10 <sup>6</sup> mm <sup>2</sup> N/mm <sup>2</sup>
EI	373.4 X 10 <sup>6</sup> mm <sup>4</sup> N/mm <sup>2</sup>	373.4 X 10 <sup>6</sup> mm <sup>4</sup> N/mm <sup>2</sup>

Note - The depth of the actual section is 55 mm and this transformation does not account for the concrete displaced.